1989

A Spectroscopic Study of Charge Distribution in Transition Metal Bridging Hydride Complexes

Shixiong Chen

Eastern Illinois University

This research is a product of the graduate program in Chemistry at Eastern Illinois University. Find out more about the program.

THESIS REPRODUCTION CERTIFICATE

TO: Graduate Degree Candidates who have written formal theses.

SUBJECT: Permission to reproduce theses.

The University Library is receiving a number of requests from other institutions asking permission to reproduce dissertations for inclusion in their library holdings. Although no copyright laws are involved, we feel that professional courtesy demands that permission be obtained from the author before we allow theses to be copied.

Please sign one of the following statements:

Booth Library of Eastern Illinois University has my permission to lend my thesis to a reputable college or university for the purpose of copying it for inclusion in that institution's library or research holdings.

Sep 14, 89

_____   _____
        Date   Author

I respectfully request Booth Library of Eastern Illinois University not allow my thesis be reproduced because _____ _____

_____

_____

_____   _____
        Date   Author

m

A Spectroscopic Study of Charge Distribution in

Transition Metal Bridging Hydride Complexes

(TITLE)

BY

Shixiong Chen

THESIS

SUBMITTED IN PARTIAL FULFILLMENT OF THE REQUIREMENTS
FOR THE DEGREE OF

Master of Science in Chemistry

IN THE GRADUATE SCHOOL, EASTERN ILLINOIS UNIVERSITY
CHARLESTON, ILLINOIS

1989

YEAR

I HEREBY RECOMMEND THIS THESIS BE ACCEPTED AS FULFILLING
THIS PART OF THE GRADUATE DEGREE CITED ABOVE

9/13/89

DATE

ADVISER

9/ / /

DATE

DEPARTMENT HEAD

A Spectroscopic Study of Charge Distribution in

Transition Metal Bridging Hydride Complexes

Thesis Approved

Dr. E. A. Keiter

9-13-89
Date

Dr. R. L. Keiter

9-13-89
Date

Dr. D. W. Ebdon

9-13-89
Date

Dr. B. E. Miller

9-14-89
Date

ABSTRACT

Title of Thesis: A Spectroscopic Study of Charge Distribution in

Transition Metal Bridging Hydride Complexes

Name: Shixiong Chen

Thesis directed by: Dr. Ellen A. Keiter

A series of transition metal bridging hydrides of general for-
mula $C[\mu-HM_2(CO)_{10}]$ (C = tetraethylammonium, Et_4N^+; tetraphenyl-
phosphonium, Ph_4P^+; of bis(triphenylphosphine)iminium, PPN^+; M =
Cr or W) were synthesized from $M(CO)_6$ and $NaBH_4$ bt known methods.
As a means of obtaining information about the charge distribution
in these complexes, they were allowed to interact in solution and
the solid state with triphenylphosphine oxide (TPPO) on the premise
that this electron donor could identify sites of relative electron
deficiency. Evidence for interaction was sought via solution and
solid state infrared (IR) spectroscopy and solution ^1H nuclear
magnetic resonance (NMR) spectroscopy.

Solution IR spectra for mixtures of TPPO and complexes in a
number of ratios were examined for changes in the bands associated
with CO stretching, PO stretching, and MCO bending motions. For
comparison, spectra of mixtures of TPPO with Ph_4PCl and Et_4NBr were
also collected. Spectral alterations suggest that TPPO associates
with both the cation and anion in $[Ph_4P][\mu-HM_2(CO)_{10}]$ (M = Cr, W).
Evidence is presented that more than one site on the anion in
these complexes is involved and that one of these is the carbon
atom of an equatorial CO ligand. This result supports proposed
mechanisms for reactions of transition metal carbonylates that are
catalyzed by TPPO. In contrast, spectra for mixtures with $[Et_4N]-$
$[\mu-HW_2(CO)_{10}]$ suggest that there is little or no association with
TPPO in these samples. This is interpreted as arising because
interactions with TPPO are inhibited by substantial ion pairing
for this cation-anion combination. All of the spectra show
conclusively that TPPO does not associate with a metal atom in

I

any of the mixtures studied. The solution IR spectra provided
no direct information regarding interaction of TPPO with the
bridging hydrogen atom. The solid state IR spectra of mixtures
of the complexes and TPPO inseveral ratios show no evidence
for adduct formation.

In ^{1}H NMR spectra of the mixtures, the chemical shifts of
the bridging hydrogen atoms are altered only slightly from their
values in the pure complexes. In view of the presumed low
sensitivity of this parameter to weak interactions involving a
bridging hydrogen, this result is regarded as neither strongly
supporting nor ruling out an association of TPPO with the bridging
atom.

ACKNOWLEDGMENT

I would like to thank my adviser Dr. E. Keiter for her great patience and help during this study.

Thanks also to those who gave me supports in many respects during my staying at EIU.

TABLE OF CONTENTS

LIST OF TABLES

LIST OF FIGURES

VIII

X

Chapter I
Introduction

Compounds with hydrogen ligands on transition metals are called transition metal hydrides, whether or not they display any hydridic behavior. Transition metal hydrides of the type $[\mu\text{-}HM_2(CO)_{10}]^-$ which contain only one M-H-M bond are known as dinuclear transition metal complexes with a single bridging hydride ligand, where M can be either the same or different transition metals. This study concentrates on complexes in which the two M's are the same metal.

Compounds with the anion $[HM_2(CO)_{10}]^-$ ($= [\mu\text{-}HM_2(CO)_{10}]^-$) were first prepared by Behrens about thirty years ago.[1] More convenient synthesis methods for the $[HM_2(CO)_{10}]^-$ series of anions later developed by Hayter[2] and some others[3,4] have made these metal carbonyl hydrides more accessible. Extensive structural investigation has been thus permitted and has established the presence of an unusual unsupported M-H-M three-center two-electron (3c-2e) bond. The bond is unsupported in the sense that there is no formal M-M bond joining the two $M(CO)_5$ units. These complexes are of interest also because of their potential importance as catalysts and their use as reagents for the synthesis of organometallic derivatives.[5,6]

The purpose of this study was to investigate, via various spectroscopic methods, the nature of the M-H-M bond in bridging transition metal hydrides, with special emphasis on obtaining information regarding charge distribution. The compounds chosen for study were a series containing the anions $[HM_2(CO)_{10}]^-$ (M-Cr,W). These complexes

1

have been well-characterized crystallographically by X-ray and neutron diffraction.[7-26] The structural studies have revealed a particularly interesting feature of the M-H-M bond: There is considerable variation in the M-H-M bond angle, even among compounds involving the same metal atoms. For example, the anion $[HW_2(CO)_{10}]^-$ displays different angles in the W-H-W bond depending on the positive ion with which it is crystallized.

The apparent flexibility of the M-H-M moiety raises the question: What alterations in electron distribution accompany the bond angle changes? One goal of this study was to answer this question through nuclear quadrupole double resonance (NQDR) spectroscopy of the deuterated forms of a series of hydrides which show the angular variation of interest. The measured quantities obtained from an NQDR spectrum for a given nucleus (in this case D) are the nuclear quadrupole coupling constant and asymmetry parameter. These quantities are directly related to the distribution of charge in the immediate vicinity of the nucleus.[27] Thus the method provides access to detailed information about electronic participation in chemical bonds--information that is not readily accessible by other means. Whereas there have been no previous NQDR studies reported for the complexes chosen here, there has been one report of deuterium nuclear quadrupole parameters obtained by solid state deuterium NMR for the bridging deuteride in $[(\eta^5-C_5H_5)_2ZrD_2]$.[28] In addition, a theoretical study on the [Na-D-Na]+ model system has predicted the effect of changes in the Na-D-Na angle on the quadrupole coupling constant and asymmetry parameter of the bridging atom.[29] There has thus far been no experimental confirmation of these predictions.

A second approach to obtaining information regarding the charge distribution in the complexes of interest was to examine, via IR and NMR spectroscopy, their interactions with an electron donor. Extensive spectroscopic studies have been carried out on the tendencies of a variety of hydridic compounds, including the complexes of this study and related monometallic species, to associate in solution with various cations.[30] These studies have shown a considerable variation not only in whether an association exists but also in the specific site to which an electropositive center binds. However, there have been essentially no systematic studies of the interactions of transition metal hydrides with electron donors. The electron donor chosen for this investigation was triphenylphosphine oxide (TPPO), a compound known to form adducts, both in solution and in solid state, with a wide variety of organic and inorganic proton donors.[31,32] It was expected that information obtained from this portion of the study would have potential relevance to the reactivities of the complexes of interest as well as the charge distribution in the M-H-M bond.

Chapter II
Background

A. Crystal structures of $[HM_2(CO)_{10}]^-$ complexes

The crystal structures of $[HM_2(CO)_{10}]^-$ complexes have been mainly studied by X-ray and neutron diffraction. There have been several structural reviews on these transition metal hydrides.[7-11] The structures of these anions may be classified according to the $(OC)_{ax}M$---$M(CO)_{ax}$ "backbone" (linear or bent) and the relative orientation of equatorial carbonyls on each metal center (eclipsed or staggered). Models of the two most common combinations---linear, eclipsed (**1**) and bent, staggered (**2**) are shown:

       1   **2**
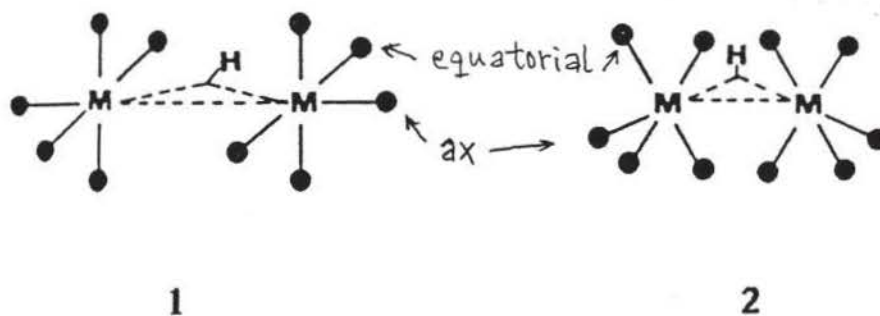
The first bridging complex of the type $[(CO)_5M-H-M(CO)_5]^-$ ever examined using X-ray diffraction was $[Et_4N^+][HCr_2(CO)_{10}^-]$.[12] Initially it was found that the nonhydrogen portion of the anion had D_{4h} symmetry, with a linear backbone and eclipsed equatorial carbonyl groups. Since the scattering of X-rays is roughly proportional in amplitude to the number of electrons in an atom, it is difficult to get accurate coordinates of H atoms bonded to heavy metals and more difficult in the case of bridging hydrides. Thus early attempts to locate H atoms with X-ray data

were indirect: The "missing" hydrogen positions were deduced by examining the geometry of the rest of the molecule. The high symmetry of the anion and the unusually long Cr-Cr distance (3.41(1) A, compared with 2.97(1) A in $[Cr_2(CO)_{10}^{2-}]$), led to the hypothesis that the Cr-H-Cr bond in this complex is linear and symmetric (see **3**).[12,13] However, further detailed X-ray and neutron diffraction studies showed that the Cr-H-Cr angle is not 180 degrees but 158.9 degrees.[14] The M-H-M bond angles are now believed to be not only nonlinear (see **4**) but also to depend to

M —H— M   M —H— M
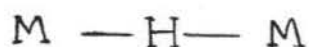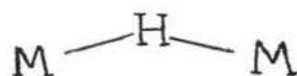
3   **4**

a large extent on the type of cation bound to the $[HM_2(CO)_{10}^-]$ anion in the crystal lattice.[7,14-26] Some of these results are summarized in Table 1.

Molecular structures for two bridging hydrides, $[Et_4N^+][HCr_2(CO)_{10}^-]$ and $[Ph_4P^+][HW_2(CO)_{10}^-]$, based on neutron diffraction data are shown in Figs. 1-4.[14,26] Neutron diffraction has played a unique role in these structural determinations. It has an advantage over the X-ray method because of the fact that the neutron coherent scattering lengths (scattering factors) for most elements are roughly within the same order of magnitude, although the two techniques and the theory of the two scattering experiments are very similar. It is thus more possible to detect the exact coordinates of the H positions with neutron diffraction.

5

Table 1 Summary of configurations of some M-H-M bridged compounds

Compound	Conformation	M-H, Å	M-H-M, deg	M-M, Å	Displacement*	Ref	Temperature
$[Et_4N][HCr_2(CO)_{10}]$	eclipsed	1.707(21) 1.737(19)	158.9(6)	3.386(6)	0.3	14	room T.
$[PPN][HCr_2(CO)_{10}]$	eclipsed	1.675		3.349(13)		19,20	room T.
$[PPN][DCr_2(CO)_{10}]$	eclipsed	1.718(9) 1.729(1) 1.737(9) 1.750(8)	157.6(7) 153.9(10)	3.390(3)	0.3	22	
$[Et_4N][HW_2(CO)_{10}]$	eclipsed	1.718(12) 2.070(12)	137.0(10)	3.528(2)	0.71(1)	7	14 K
$[PPN][HW_2(CO)_{10}]$	staggered	...	(150)	3.391(1)		17	
$[Ph_4P][HW_2(CO)_{10}]$	staggered	1.897(5)	123.4(5)	3.340(5)	0.899(5)	26	40 K
α-$HW_2(CO)_9(NO)$	staggered	1.875(4) 1.876(4)	125.0(2)	3.328(3)	0.866(4)	16	
β-$HW_2(CO)_9(NO)$	staggered	1.870(4)	125.9(4)	3.330(3)	0.850(4)	16	
$[PPN][HMo_2(CO)_{10}]$	staggered	1.76(5)	136(3)	3.422	0.69	24	
$[K(crypt-222)]$ $[HCr_2(CO)_{10}]$	intermediate	1.723(5) 1.734(5)	145.2(3)	3.300(4)	0.52	23	

* Distance of H atom from the mid-point between two M metals, in Å.

Figure 1. Geometry of the [HCr$_2$(CO)$_{10}{}^-$] in [Et$_4$N$^+$] salt[14]

Approximate D$_{4h}$ geometry of the metal carbonyl framework and two centrosymmetrically related (half-weighted) sites of the bridging hydrogen atom in the bent Cr-H-Cr fragment were observed.

7
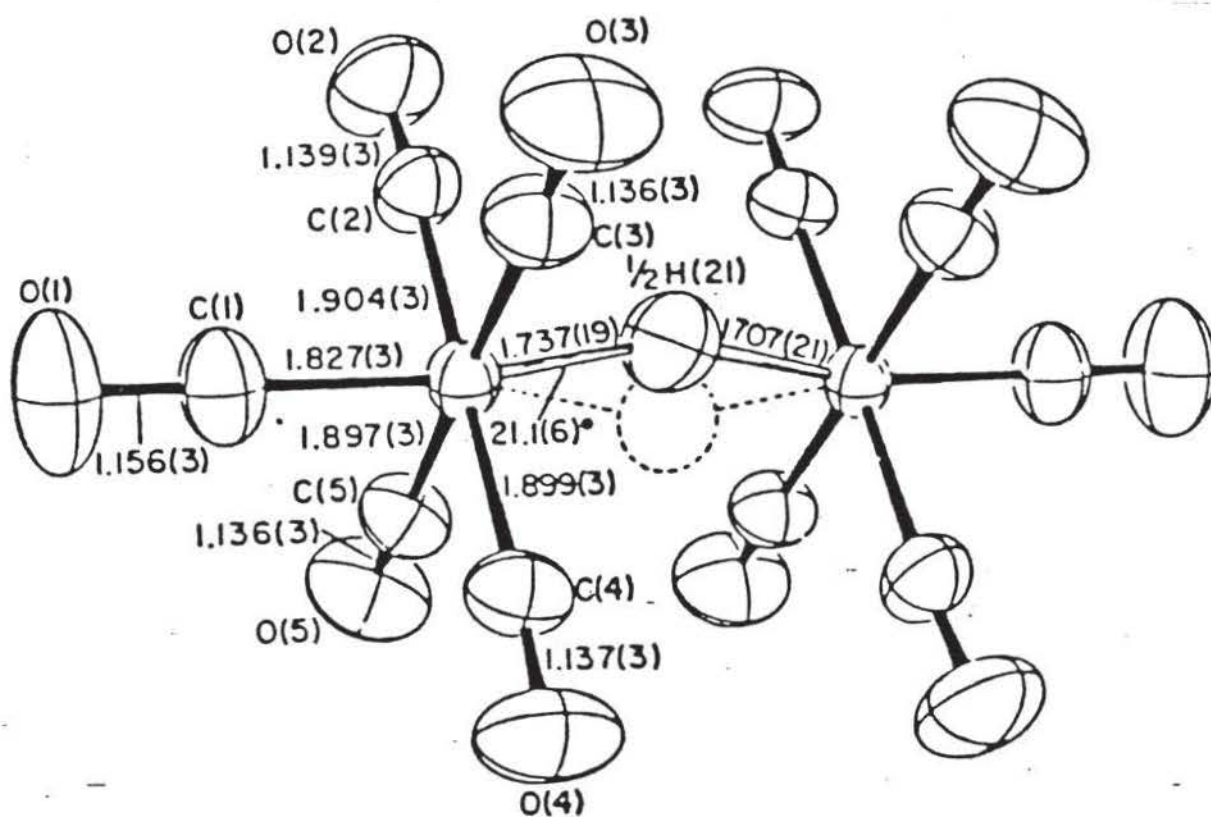
Figure 2. Another view of the geometry of the $[HCr_2(CO)_{10}^-]$ in $[Et_4N^+]$ salt[14]

The two centrosymmetrically disordered, half-weighted hydrogen sites are staggered relative to the eclipsed arrangement of the two sets of equatorial carbonyl ligands.
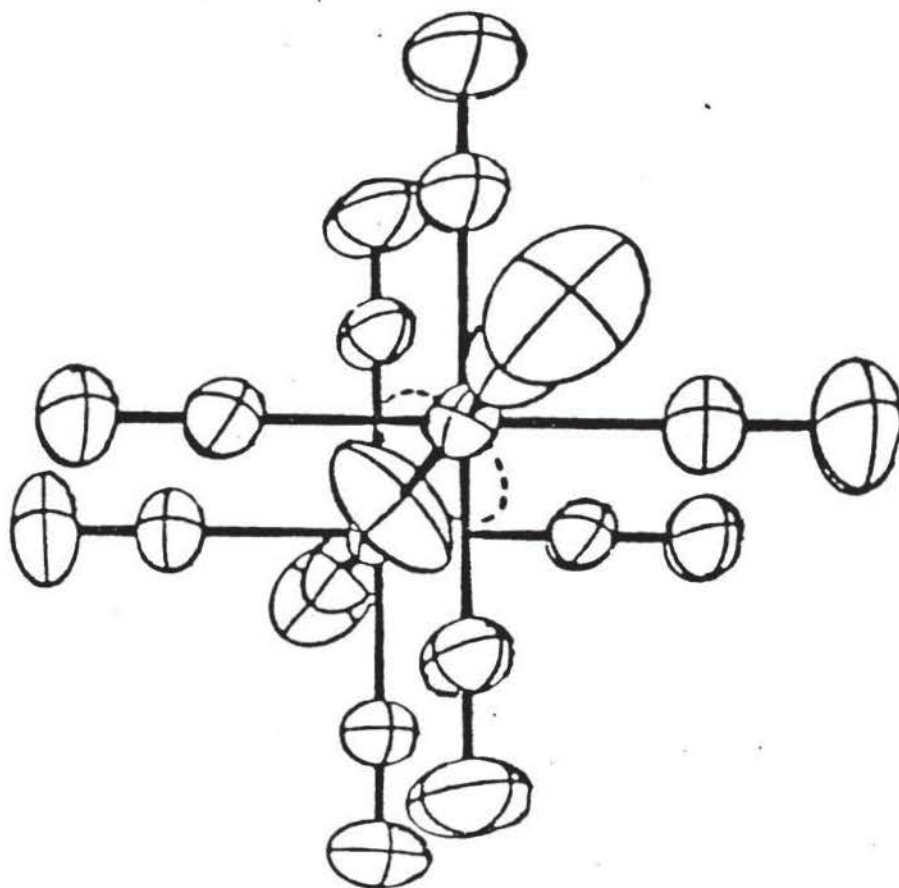
Figure 3. A molecular plot of the $[HW_2(CO)_{10}^-]$ anion in $[Ph_4P^+][HW_2(CO)_{10}^-]$, based on neutron diffraction data collected at 40 K.[26] A crystallographic twofold axis passes through the bridging H atom, bisecting the W-H-W angle. Notice that the axial O-C-W vector is not colinear with the bridging H atom but is directed approximately toward the center of the W-H-W triangle. This is interpreted as evidence that the nature of the overlap in M-H-M bonds is "closed" (see I, page 11).
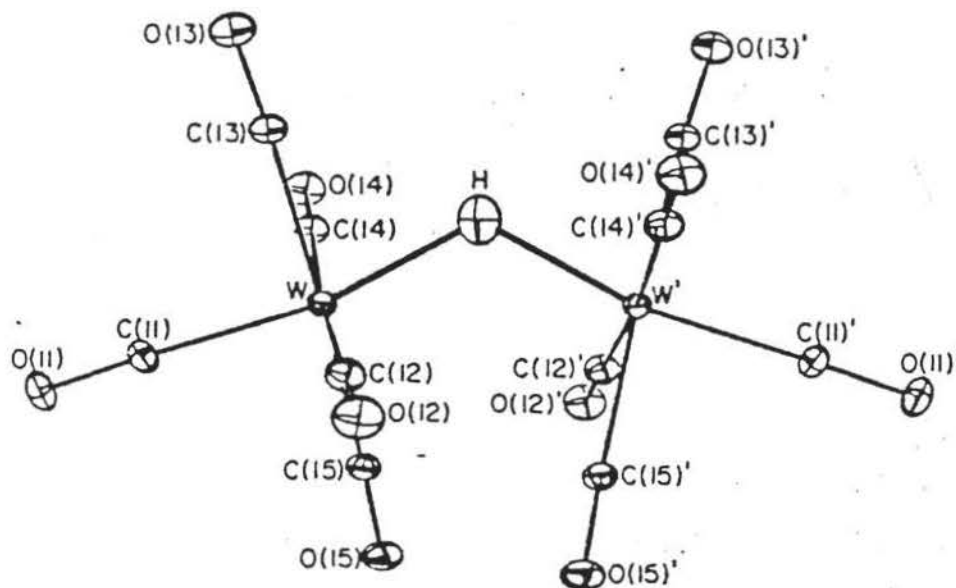
Figure 4. An end-on view of the anion $[HW_2(CO)_{10}^-]$ in $[Ph_4P^+][HW_2(CO)_{10}^-]$, **26** showing the 45° staggering of the equatorial carbonyl groups. Note the planarity of the OC_{ax}-W-H-W-CO_{ax} fragment, which is staggered at 22.5° relative to the equatorial carbonyls.
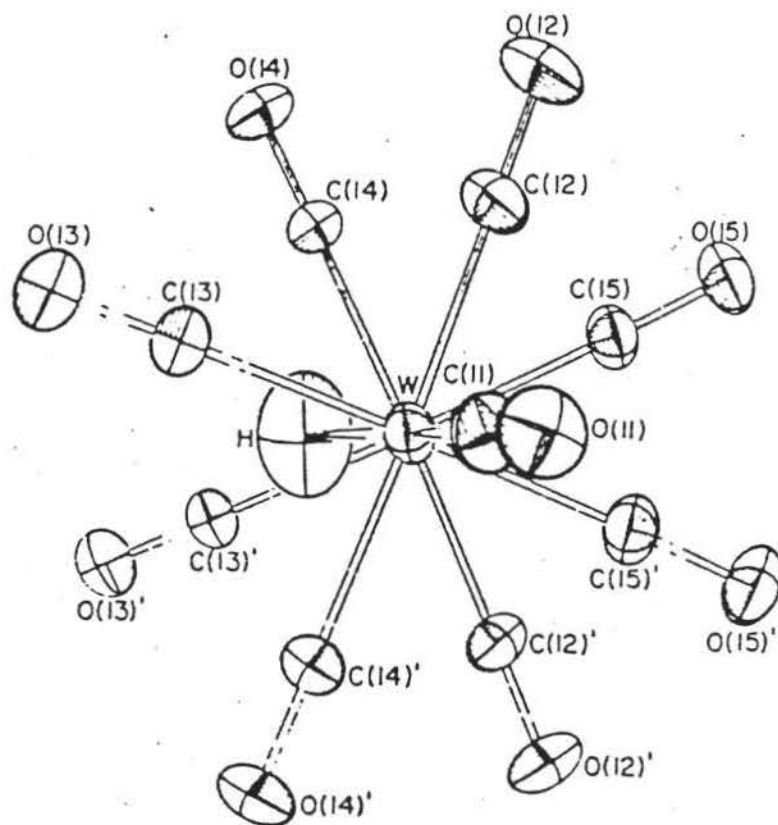
B. M-H-M bonding

Based on the information obtained from the X-ray and neutron diffraction studies, several different symbolisms (**I, II, III**)[33] have been utilized to represent the so-called 3c-2e M-H-M bonds. A molecular orbital (MO) picture has also been proposed and is shown in Figure 5. From Figure 5, it can be seen that three atomic orbitals involved give rise to three molecular orbitals: one bonding (Ψ_1), one slightly antibonding (Ψ_2), and one antibonding (Ψ_3). Since there are only 2e available, only the bonding orbital is filled. The simple MO picture shown is consistent with the observation that the M-H-M bond is bent and supports the contention that this bent configuration is inherent.
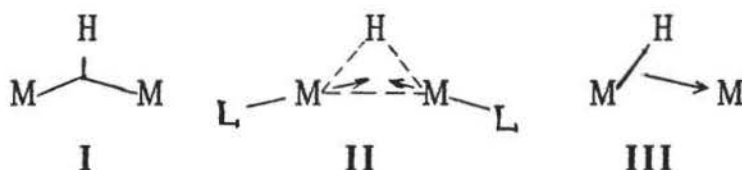
Figure 5. Qualitative molecular orbital scheme for bent 3c-2e M-H-M systems

antibonding

antibonding

bonding

Ψ_3 ——

Ψ_2 ——

Ψ_1

M-H-M
(3c,2e)
bent
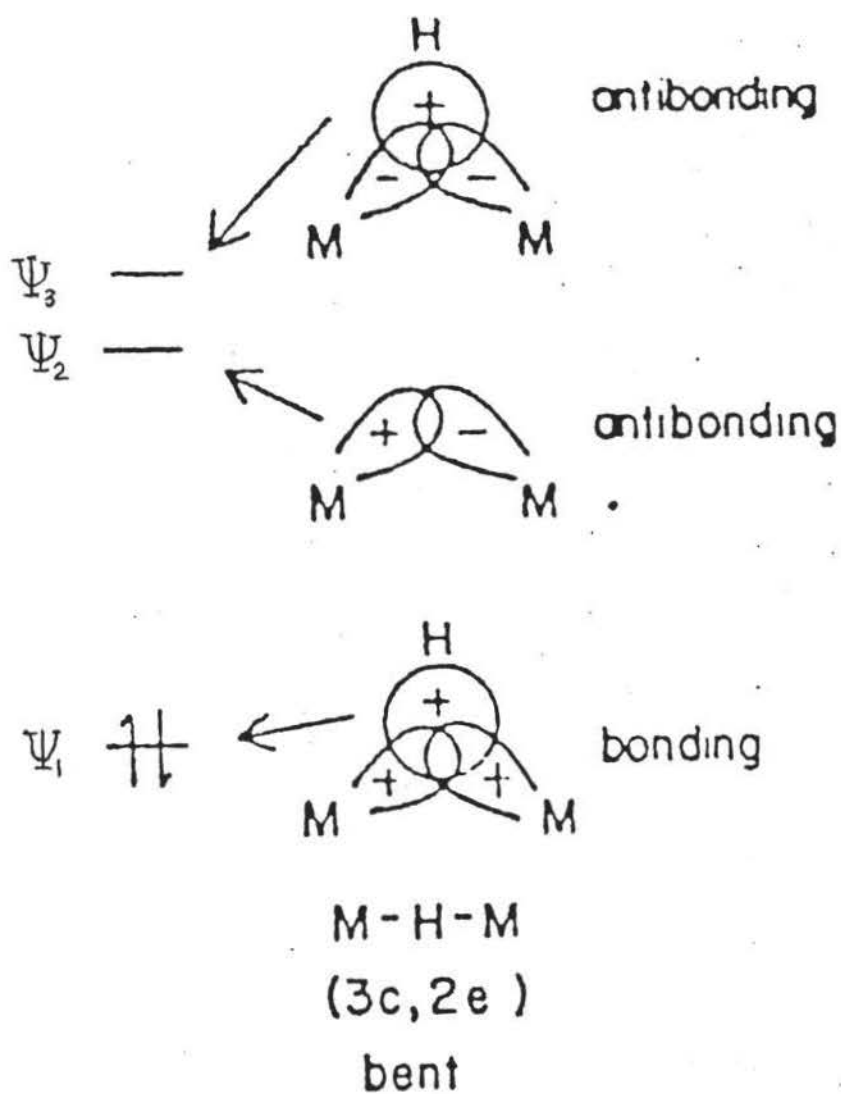
Chapter III
Experimental

A. General considerations

Tungsten and chromium hexacarbonyls, reducing agents $NaBH_4$ and $NaBD_4$, salts tetraethylammonium (Et_4N^+) bromide, bis(triphenylphos-phine)iminium (PPN^+) chloride, and tetraphenylphosphonium (Ph_4P^+) chloride were purchased from various commercial chemical suppliers. They were all reagent grade and were used without further purification.

The infrared (IR) spectra were obtained using a Nicolet 20 DX-B Fourier Transform Infrared Spectrometer. Solid IR spectra were obtained on KBr pellets of the corresponding compounds. Solution IR spectra were obtained from their THF solutions with THF as the background.

NMR spectra were obtained on a Varian T-60 spectrometer from concentrated acetone solution (for PPN^+ and Ph_4P^+ hydrides) and deuterated acetone solution (for Et_4N^+ hydrides) with tetramethylsilane (TMS) as an internal standard. For the TPPO study, THF was used as the solvent.

The anions $[HM_2(CO)_{10}]^-$ (M=Cr, W) are air-sensitive and thus syntheses were carried out under a nitrogen atmosphere. All solvents such as ethanol, THF and hexane were reagent grade. THF was distilled

from sodium and benzophenone while the others were used without further purification. They were all thoroughly degassed and purged with nitrogen gas before use.

B. Preparation of compounds

Twelve bridging hydrides (H and D) were prepared by a published synthesis method[2] or modifications of it. They are $[Et_4N]^+$, $[PPN]^+$, and $[Ph_4P]^+$ salts of $[HCr_2(CO)_{10}]^-$ (μ-hydrido-bis(pentacarbonyl)chromium(0)), $[HW_2(CO)_{10}]^-$ (μ-hydrido-bis(pentacarbonyl)tungsten(0)), and their deuterated forms $[DCr_2(CO)_{10}]^-$ and $[DW_2(CO)_{10}]^-$. The reaction was assumed to occur according to eq 1.

$$2M(CO)_6 + NaBH_4 \longrightarrow Na[HM_2(CO)_{10}] + 2CO + [BH_3] \qquad (1)$$

The borine fragment presumably remains in solution as a THF complex.[2]

The detailed synthesis steps of one of these compounds, $[Et_4N^+][HW_2(CO)_{10}^-]$, are given in the following section.

Preparation of $[Et_4N^+][HW_2(CO)_{10}^-]$: Dry THF solvent (125 mL) and a Teflon coated magnetic stirring bar were added to a two-necked 250-mL round bottomed Pyrex flask. The solution was then degassed and saturated with nitrogen for about 5 minutes. Tungsten hexacarbonyl, $W(CO)_6$ (8.0g, 22.7mmoles) and sodium borohydride, $NaBH_4$ (0.5g, 13.2mmoles) were added in turn while a good nitrogen stream was passing through the solution. With the side narrow neck sealed and the main neck connected to a condenser which had an outlet to a nitrogen bubbling system, the flask was immersed halfway in an oil bath with a

14

temperature about 80°C, and the whole mixture was refluxed for 18 hours. The oil-bath temperature and stirring bar's speed were adjusted so that the dripping from the reflux condenser was about 1 drop/second. The reaction solution was initially colorless, but rapidly became yellow and gradually deepened to brown-yellow. After the reaction was complete (18 hours), the heating was stopped and the solution was allowed to cool down to room temperature without stopping the nitrogen stream. Then the solution was filtered through degassed Celite filteraid and the solvent was removed with a vacuum pump, leaving an oily orange to red residue (less than 3 mL). Dry ethanol (ca. 100 mL) and a concentrated solution of [Et$_4$N]Br (2.4g, 11.4 mmoles) in ethanol were added. Precipitation of a yellow crystalline solid began at once and was completed by cooling overnight in a refrigerator. The yellow product was filtered, washed with ethanol, dried under vacuum for 2 hours, and then saved in a vial in a dessicator. The purity of the product [Et$_4$N$^+$]-

[HW$_2$(CO)$_{10}$$^-$] was checked by IR in THF solution, which showed only three characteristic bands of the [HW$_2$(CO)$_{10}$$^-$] (1878.6, 1938.6 and 2041.6 cm^{-1}; lit.:[2] 1880, 1943 and 2043 cm^{-1}) in the CO stretching region. The characteristic CO stretching absorption of the starting material W(CO)$_6$ at around 1974 cm^{-1} was not observed. Hence recrystallization of this product was not necessary.

For those products for which the IR showed a considerable CO stretching band characteristic of its corresponding starting material M(CO)$_6$ (1978 cm^{-1} for M=Cr, 1974 cm^{-1} for M=W), recrystallization from ethanol or tetrahydrofuran-hexane was performed. This was repeated until the unwanted peak was reasonably small or had disappeared.

15

Summaries of the preparations and some properties of the products are given in Table 2.

C. Spectroscopic measurements

1. Solution IR

The solution IR spectra for all these twelve compounds are given in Appendix I (Fig. A01–Fig. A12). Table 3 (next chapter) includes frequencies for the three characteristic CO stretching modes of each of these $[HM_2(CO)_{10}^-]$ anions in THF solution.

2. NMR

The presence of the H in M-H-M in $[HM_2(CO)_{10}]^-$ was checked by ^1H NMR. The H peak disappeared in the corresponding D compounds. (See Table 3 of the next chapter.) The NMR spectra of these twelve compounds are given in Appendix I (Fig. A13 - Fig. A24). The ^1H NMR also can act as a tool to verify the cation being $[Et_4N]^+$, $[PPN]^+$, or $[Ph_4P]^+$. (See Fig. A13 - Fig. A24 to compare different salts of same cation.)

3. Solid IR

The KBr pellets of all of the twelve compounds were made and the solid IR spectra were obtained at room temperature. These spectra are given in Fig. A25 - Fig. A36.

Table 2 Summary of preparations for M-H-M complexes

Product, color	Starting material 2:1	Salt added after 18 hrs reaction	Recrystallization solvent
$[Et_4N][HW_2(CO)_{10}]$ yellow powder		$[Et_4N]Br$	
$[PPN][HW_2(CO)_{10}]$ yellow powder	$W(CO)_6$: $NaBH_4$	$[PPN]Cl$	
$[Ph_4P][HW_2(CO)_{10}]$ yellow crystal		$[Ph_4P]Cl$	
$[Et_4N][HCr_2(CO)_{10}]$ brownish yellow powder		$[Et_4N]Br$	
$[PPN][HCr_2(CO)_{10}]$ yellow orange powder	$Cr(CO)_6$: $NaBH_4$	$[PPN]Cl$	
$[Ph_4P][HCr_2(CO)_{10}]$ orange crystal		$[Ph_4P]Cl$	
$[Et_4N][DW_2(CO)_{10}]$ yellow powder		$[Et_4N]Br$	Ethanol
$[PPN][DW_2(CO)_{10}]$ yellow crystal	$W(CO)_6$: $NaBD_4$	$[PPN]Cl$	
$[Ph_4P][DW_2(CO)_{10}]$ yellow powder		$[Ph_4P]Cl$	
$[Et_4N][DCr_2(CO)_{10}]$ orange crystal		$[Et_4N]Br$	
$[PPN][DCr_2(CO)_{10}]$ yellow orange crystal	$Cr(CO)_6$: $NaBD_4$	$[PPN]Cl$	
$[Ph_4P][DCr_2(CO)_{10}]$ yellow orange crystal		$[Ph_4P]Cl$	THF/Hexane

D. Attempted preparation

Synthesis of $[HM_2(CO)_{10}]^-$ (M=W) as the K^+ salt using another published method[4] also was tried. This reaction was supposed to proceed according to eq. 2.

$$2M(CO)_6 + 4\,OH^- \longrightarrow [HM_2(CO)_{10}]^- + CO_3^{2-} + H_2O + HCO_2^- \quad (2)$$
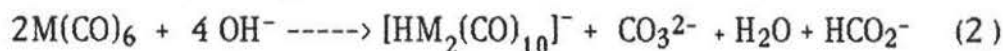
After 19 hours of reaction, yellow solid did separate from the pale yellow solution in agreement with the literature report. But among the solid there were also potassium salts of CO_3^{2-} and HCO_2^-. In the next step water was introduced to separate the unwanted inorganic salts K_2CO_3 and $KHCO_2$ from the product. It appeared that during this step much of the yellow solid turned white. The infrared spectrum showed an intensive peak characteristic of the starting material $W(CO)_6$ as well as three peaks characteristic of $[HW_2(CO)_{10}]^-$. The method obviously offers another approach from $M(CO)_6$ to $[HM_2(CO)_{10}]^-$ (yellow), but it needs a lot of care in order to avoid the decomposition mentioned above.

E. Interaction with triphenylphosphine oxide (TPPO)

1. Solid IR measurements

Mixtures of TPPO and $[Ph_4P^+][HW_2(CO)_{10}^-]$ in molar ratios 1:1 and 1.5:1, a mixture of TPPO and $[Ph_4P^+][HCr_2(CO)_{10}^-]$ in molar ratio 1:1, and a mixture of TPPO and $[PPN^+][HW_2(CO)_{10}^-]$ in molar ratios 1:1 were separately prepared and dissolved in THF solution. The solvent was evaporated gradually in the hood. The vacuum pump was used for the Cr

mixture. When most solvent was gone, the W mixtures were also further dried by vacuum. Solid IR spectra (KBr pellets) were obtained for the remaining dried solids of the above mixtures and for pure TPPO. The solid IR spectra and their corresponding ratios are summarized in Table 4 in the next chapter. These spectra are shown in Figs. A37-A48.

2. Solution NMR measurements

Mixtures of TPPO and $[Ph_4P^+][HW_2(CO)_{10}^-]$ in molar ratios 1:1, 1.5:1, 4:1 and 8:1 were prepared in different flasks. THF was added to each flask to just dissolve these solid samples in order to obtain a saturated solution. THF solutions of pure TPPO and pure $[Ph_4P^+][HW_2(CO)_{10}^-]$ were prepared in the same manner.

Mixtures of TPPO and $[Ph_4P^+][HCr_2(CO)_{10}^-]$ in molar ratios 1:1, 2:1 and 4:1 were prepared in the same way as for the W complexes above.

The solution NMR spectra were obtained for all these samples. A representation spectrum is shown in Fig. A49. The results are summarized in Table 5 in the next chapter.

3. Solution IR measurements

Mixtures of TPPO and $[Ph_4P^+][HW_2(CO)_{10}^-]$ in molar ratios 1:1, 2:1, 3:1, 4:1 and 8:1 were prepared in different flasks. THF was added into each flask to dissolve the sample. The concentrations of these solution mixtures were adjusted so that their CO stretching peaks characteristic of $[HW_2(CO)_{10}^-]$ in the window 1700-2200 cm^{-1} were not over scale in the transmittance IR spectra. Solutions of mixtures of TPPO and $[Ph_4P^+][HCr_2(CO)_{10}^-]$ in molar ratios 1:1 and 2:1, a mixture of TPPO and $[Et_4N^+][HW_2(CO)_{10}^-]$ in molar ratio 1:1, a mixture of TPPO and $[Ph_4P]Cl$ in

19

molar ratio 1:1 and a mixture of TPPO and [Et$_4$N]Br in molar ratio 1:1 as well as pure components TPPO, [Et$_4$N$^+$][HW$_2$(CO)$_{10}$$^-$], [Ph$_4P^+$][HW$_2(CO)_{10}$$^-$] and [Ph$_4P^+$][HCr$_2(CO)_{10}$$^-$] were also prepared in the same way.

Solution IR spectra were obtained for all these samples (with THF as the background). These spectra are shown in Figs. A50-A57. Results of these spectra are summarized in Table 6 in the next chapter.

F. NQDR measurements

The six deuteride samples, [DM$_2$(CO)$_{10}$]$^-$ (M=Cr, W) of [Et$_4$N]$^+$, [PPN]$^+$, and [Ph$_4$P]$^+$, were sent to Louisiana State University for deuterium NQR measurements.

Chapter IV
Results and discussion

The spectroscopic results of the ^{1}H NMR, solution IR and solid IR for the title hydrides are summarized in Table 3. The discussion based on this table will be separated into IR and NMR sections. The interaction with TPPO will be discussed in its own section.

A. IR spectra

There certainly are infrared-active vibrations for the M-H-M backbone of $[HM_2(CO)_{10}^-]$. Unfortunately the M-H modes of hydride-bridged metal compounds frequently give weak and broad bands in IR spectra, and it is often not possible to detect the hydride absorptions of the M-H-M system in a spectrum obtained at room temperature.[34] Though low temperature (10 K to 50 K) IR affords significant improvements in the ease of detecting bridging M-H modes,[34] it was not available for this study.

Fortunately, the bands associated with the carbonyl stretching modes of the anion $[HM_2(CO)_{10}^-]$ are observable. All twelve compounds in THF solution exhibit three characteristic carbonyl stretching vibrations which strongly suggest a structure with a fourfold axis of symmetry (see Appendix III). Their frequencies are listed in Table 3. The IR spectra could not determine whether these anions are D_{4h} or D_{4d} in solution. Isotopic labelling studies with ^{13}CO accompanied by force-field analyses

21

Table 3 Summary of IR and ^1H NMR spectral data for M-H-M and M-D-M complexes

(1)

Compounds	Solid IR bands (cm^{-1})	Solution IR bands (cm^{-1})[a]	δ (M-H-M), ppm[b] (TMS = 0)
[Et$_4$N][HW$_2$(CO)$_{10}$]	2046.2 1872.1 1918.3 1924.2 1935.7 1964.5	2041.6 1878.6 1938.5	-12.51
[Et$_4$N][DW$_2$(CO)$_{10}$]	2046.2 1863.6 1917.1 1934.9 1962.6	2041.5 1875.3 1938.4	
[Ph$_4$P][HW$_2$(CO)$_{10}$]	2040.6 1863.4 1883.9 1909.8 1944.2 1959.0	2041.5 1878.4 1938.4	-12.49
[Ph$_4$P][DW$_2$(CO)$_{10}$]	2041.0 1822.9 1861.6 1909.1 1944.2 1959.1	2041.4 1875.2 1938.4	

22

Table 3 continued

(2)

Compounds	Solid IR bands (cm^{-1})	Solution IR bands (cm^{-1})[a]	δ(M-H-M) ,ppm[b] (TMS = 0)
[PPN][HW$_2$(CO)$_{10}$]	2040.4 1870.2 1898.6 1928.1 1964.1	2041.5 1878.4 1938.5	-12.54
[PPN][DW$_2$(CO)$_{10}$]	2040.3 1865.8 1898.1 1924.6 1931.3 1964.3	2041.4 1875.2 1938.2	
[Et$_4$N][HCr$_2$(CO)$_{10}$]	2037.8 1868.6 1927.1 1933.8 1968.0	2030.8 1879.0 1940.5	-19.49
[Et$_4$N][DCr$_2$(CO)$_{10}$]	2036.5 1865.1 1934.1 1965.6	2031.0 1877.0 1940.4	

Table 3 continued

(3)

Compounds	Solid IR bands (cm^{-1})	Solution IR bands (cm^{-1})[a]	(M-H-M) ,ppm[b] (TMS - 0)
[Ph$_4$P][HCr$_2$(CO)$_{10}$]	2028.0	2030.7	-19.54
	1872.7	1878.6	
	1897.5	1940.4	
	1921.5		
	1938.3		
	1965.9		
[Ph$_4$P][DCr$_2$(CO)$_{10}$]	2028.2	2030.9	
	1871.4	1876.5	
	1895.2	1940.4	
	1898.6		
	1910.4		
	1921.6		
	1936.1		
	1965.1		
[PPN][HCr$_2$(CO)$_{10}$]	2034.1	2030.6	-19.51
	1879.4	1878.6	
	1925.9	1940.4	
	1935.5		
	1970.7		
[PPN][DCr$_2$(CO)$_{10}$]	2033.7	2030.8	
	1877.2	1876.5	
	1925.5	1940.5	
	1934.1		
	1971.6		

---

[a] THF solution

[b] Acetone solution

have shown that a model that includes some interaction between the carbonyl groups in the two halves of the complex across the M-H-M bridge is consistent with observations.[35,36] The observed bands are assigned, in order of decreasing frequency, as A_{2u}, E_{2u}, and A_{2u}.

The solution IR spectra contrast with the solid IR spectra in that there are more than three bands in the solid IR spectrum for each anion. This means the symmetry of the anion $[HM_2(CO)_{10}^-]$ is not D_{4h} or D_{4d} in the solid state and is likely to be lower than either of these. For C_{2v} symmetry, for example, nine infrared-active CO stretching bands would be expected[2] and some overlaps would be probable. As is evident from Table 3, this is consistent with observations for the solid state spectra.

Another point of contrast between the solution and solid state spectra is that in the solution samples, once the M is chosen, the three characteristic stretching frequencies of $[HM_2(CO)_{10}^-]$ are found to be essentially independent of the cation. However, for $[HCr_2(CO)_{10}^-]$ the bands for the Et_4N^+ salt occur at slightly higher frequencies than those for the PPN^+ and Ph_4P^+ salts in the solution spectra. This is in keeping with slightly greater cation-anion interaction for $[Et_4N][HCr_2(CO)_{10}]$ than for $[PPN][HCr_2(CO)_{10}]$, as shown by conductance measurements.[37] On the other hand, the solid IR spectrum of a certain anion $[HM_2(CO)_{10}^-]$ in the CO stretching region changes more dramatically (e.g., from 2046.2 cm^{-1} of $[Et_4N][HW_2(CO)_{10}]$ to 2040.6 cm^{-1} of $[Ph_4P][HW_2(CO)_{10}]$) as the cation it is bound to changes. This is not surprising in view of the solid state structural differences that are known to accompany changes in the identities of cations for these compounds (Table 1).

25

Upon substitution of D for H in each of the anions, a small change in one of the CO stretching frequencies (the lower-energy A_{2u} band) was observed in the solution IR spectrum (see Table 3). For example, it shifted from 1879 cm^{-1} in $[Et_4N^+][HCr_2(CO)_{10}{}^-]$ to 1877 cm^{-1} in $[Et_4N^+][DCr_2(CO)_{10}{}^-]$. This is consistent with an assignment which attributes this mode primarily to symmetric stretching of the axial CO ligands.[35,36]

B. NMR spectra

NMR is a valuable tool for the characterization of these compounds. The most reliable spectroscopic evidence for the presence of hydride ligands in transition metal complexes is said to be provided by the resonances observed to high field of TMS in the proton NMR spectrum. The chemical shifts of the bridging H in these complexes in acetone solution are given in Table 3. The values are -12.5 ppm for $[HW_2(CO)_{10}{}^-]$ (lit.:[2] -12.60 ppm in THF) and -19.5 ppm for $[HCr_2(CO)_{10}{}^-]$ (lit.:[2] -19.47 ppm in THF). For the tungsten compounds the coupling between the hydride ligand and ^{183}W (14.28% abundant, I-1/2)was observed (see Fig. A17) and was calculated to be 43 Hz (lit.:[2] 42.3 Hz). In contrast to the H compounds, such high field resonances were not observed in the D compounds. This provides indirect evidence for the existence of the M-D-M bond. In addition, the IR spectra of the D compounds in solution closely resemble the H forms, strongly suggesting that the only difference between them is substitution of D for H. The chemical shifts of the hydrides are found to be independent of the cations in the solution (see Table 3 and Figs. A13-A24).

In this study, ^{1}H NMR has also been used to confirm the identities of the cations of the synthesized complexes. The [Et_4N^+] salts of either [$HW_2(CO)_{10}^-$] or [$HCr_2(CO)_{10}^-$] or their D forms (Figs. A13-A16) display very similar spectra contributed from the same cation [Et_4N^+]: There is a quartet at around 3.6 ppm which is due to the resonance of CH_2 groups under the influence of three neighboring protons from the CH_3 groups. Each CH_2 group seems to have the same environment. There is a triplet at around 1.5 ppm which is due to the resonances of the CH_3 groups coupled to two neighboring hydrogens from the CH_2 group. Interestingly, each peak of the triplet is further split into three smaller lines. This splitting can be attributed to coupling of the methyl protons to the [14]N ($I=1$) nucleus. Coupling of this type frequently is not observable because the nonzero quadrupole moment of a ^{14}N nucleus imparts to it a mode of rapid spin relaxation.[38] Consequently, coupling to neighboring spin-1/2 nuclei typically is manifest as signal broadening rather than as discrete splitting. However, under some conditions the relaxation rate of the quadrupolar nucleus is slow enough relative to the magnitude of J_{N-H} that the splitting is observable. At the other extreme, the rate of relaxation may be fast enough relative to J_{N-H} that the proton signal is a single sharp peak, i.e., that the two nuclei are effectively decoupled. The rate of quadrupolar relaxation depends greatly on the extent of interaction between the nuclear quadrupole moment and the surrounding electric field gradient, q, with a larger value of q leading to a stronger interaction and more efficient relaxation. The magnitude of the field gradient, in turn, depends on the symmetry of the charge distribution in the immediate environment of the quadrupolar nucleus, becoming larger with greater departure from axial symmetry. For the highly symmetric

27

tetraethylammonium ion, the magnitude of q should be quite small and thus the rate of relaxation for the nitrogen nucleus via the quadrupolar mechanism should be relatively slow. This is undoubtedly what accounts for the resolvable N-H coupling observed for the methyl protons in Et_4N^+.

The proton resonances contributed from $[PPN]^+$ of the M-H-M salts occur at about 7.6 ppm and the shapes of the resonance peaks in this region are independent of the counteranions. The resonance from $[Ph_4P]^+$ occurs at around 8.0 ppm and shape of its resonance peaks are also independent of the counteranion.

C. Interaction with triphenylphosphine oxide (TPPO)

As described in the Introduction, this portion of the overall study was initiated as a means of experimentally deriving information about the charge distribution and reactivity of the complexes of interest. By studying the interaction of the complexes with the electron donor triphenylphosphine oxide (TPPO), it was hoped that regions of relative electron deficiency could be identified. TPPO and other trialkyl- and triarylphosphine oxides have been shown to associate with proton donors of various strengths from oxyacids to phenols to C-H groups.[31,32,39] In addition, TPPO has been found to function as a catalyst for migratory insertion reactions of alkyl metal carbonyls[40] and for certain substitution reactions of metal carbonyls.[41] In neither case is the mode of catalytic action well understood, but an association of some type between the phosphoryl oxygen and a carbonyl carbon has been postulated.[42] Thus TPPO appeared to be particularly well suited to this investigation.

28

In considering the potential sites with which the electron-rich oxygen of TPPO might interact to form a donor-acceptor complex, several possibilities were recognized: 1) the carbon atom of a bound CO group; 2) the bridging H site; 3) one of the metal atoms; and 4) a site on the cation. The possibility that a reaction might occur, such as disruption of the bridge or substitution of TPPO for a CO ligand, was also acknowledged but was regarded as quite improbable under the experimental conditions chosen.

Of the possible interactions cited above, the second is particularly intriguing for several reasons. The distribution of charge density in the M-H bond in transition metal hydrides, in general, poses an interesting question because of the range of reactivity patterns these species exhibit. Some, such as $HCo(CO)_4$, are strongly acidic while others, such as cis-$[HW(CO)_4PMe_3^-]$ almost exclusively behave as hydride (H^-) donors. Homolytic M-H cleavage is a third mode of reaction shown by several species. The complex $HMn(CO)_5$ shows all three tendencies, depending on the reaction conditions.[30(b)] Clearly, elucidation of reaction mechanisms for these processes would be aided by information about the character of the M-H bond in the starting complexes.

For the bridging hydride complexes, the question is even more open because, as a group, they are less well studied. A recent theorectical study has assigned a net charge of -0.25 electron to this site in $[HCr_2(CO)_{10}^-]$.[43] However, there is no conclusive experimental verification of this assignment. For example, in solution ion pairing studies involving a number of monometallic anionic metal carbonyl hydrides and a variety of cations, including PPN^+ and Na^+ as well as other alkali metal ions, it has been established that Na^+ has the strongest

tendency to specifically associate with the H or M-H site of the hydrido complexes. However, for [Na][HW$_2$(CO)$_{10}$] there is no evidence for this interaction, suggesting that the hydride site in this complex is not sufficiently negative to specifically attract even the most accommodating positive ion.[30] Moreover, the failure of the M-H stretching vibration to yield an observable IR band for these species has been attributed to the small M-H dipole, a further indication that prediction of the charge distribution in these M-H bonds is not a simple matter.[30(b)]

Evidence for donor-acceptor interaction between TPPO and the bridging hydride complexes was sought primarily in solution with IR and ^{1}H NMR spectroscopy as the probing methods. Some attempt was also made to induce formation of a discrete solid state adduct based on TPPO's reported capacity for cocrystallization with proton donors.[44] Solid state IR spectroscopy was utilized to test formation of new solid state materials. The results are described in the following sections.

1. Solid state IR results

The solid samples were prepared by mixing the desired ratios of TPPO and the M-H-M complexes in THF solution and then THF was evaporated. The mixtures were examined as KBr pellets. A solid IR spectrum of TPPO was also obtained for comparison. The following mixtures were prepared: TPPO: [Ph$_4$P][HW$_2$(CO)$_{10}$] = 1:1, 1.5:1; TPPO: [Ph$_4$P][HCr$_2$(CO)$_{10}$] = 1:1; TPPO: [PPN$^+$][HW$_2$(CO)$_{10}$$^-$] = 1:1. The solid IR spectra (4600-400 cm^{-1}) of these mixtures were carefully compared with those of pure TPPO and pure corresponding M-H-M complex. Spectra were expanded in three regions: 2200-1700 cm^{-1}, 1700-1000 cm^{-1} and 1000-400 cm^{-1}.

30

Because of the complexity of the solid state spectra, the carbonyl stretching region (2200-1700 cm^{-1}, Figs. A37 - A40) was judged to be the most amenable to interpretation. Table 4 summarizes the data for this region. As is evident from the table and the related figures, the spectra of the mixtures in this frequency range are very similar to those of the corresponding M-H-M complexes. Although there are small differences in some of the peak minima detected by the spectrometer, they are not regarded as significant in view of the strong intensities, large bandwidths, and overlapping nature of the absorptions. It is clear that the gross spectral pattern in this region for each bridging hydrido complex has not been altered by the addition of TPPO, indicating that the overall symmetry of the carbonyl groups has not been perturbed. At the very least this rules out the possibility that TPPO has reacted with the metal center and strongly suggests that there is also no strong interaction between TPPO and any of the carbonyl groups.

For the other two expanded regions, the spectra of the mixtures (Figs. A43, A44, A47 and A48) appear to be mere superimpositions of the spectra of the corresponding compounds (Figs. A41 and A42, Figs. A45 and A46), with intensities changing as expected upon alteration of the ratios. Although the position and lineshape of the P=O stretching band (at 1190.0 cm^{-1} for pure TPPO) should in principle be a good indication as to whether the phosphoryl group is interacting with any other species, it was not useful for these solid state mixtures because of interfering bands from the hydride complexes.

31

Table 4 Selected solid state IR data (2200-1700 cm⁻¹) for mixtures of TPPO and M-H-M complexes

Mixture	Ratio	Observed bands (cm⁻¹)
TPPO:[Ph$_4$P][HW$_2$(CO)$_{10}$]	1:1	2041.0 1824.8 1864.7 1884.0 1909.3 1944.5 1959.0
	1.5:1	2041.1 1825.4 1864.1 1884.3 1908.2 1943.9 1959.0
TPPO:[PPN][HW$_2$(CO)$_{10}$]	1:1	2040.4 1869.6 1898.3 1928.2 1964.2
TPPO:[Ph$_4$P][HCr$_2$(CO)$_{10}$]	1:1	2027.9 1872.6 1897.3 1910.6 1922.0 1964.2

32

There is thus no conclusive evidence for the formation of an adduct between TPPO and any of the hydride compounds by the methods utilized for preparing the samples. It is possible that by making greater efforts to induce formation of crystals that new compounds could be isolated.

2. Solution NMR results

Saturated solution mixtures of TPPO and $[Ph_4P][HW_2(CO)_{10}]$ in THF in ratios of 1:1, 1.5:1, 4:1 and 8:1 were prepared and a ^1H NMR spectrum was obtained for each of them. Similarly, saturated solution mixtures of TPPO and $[Ph_4P][HCr_2(CO)_{10}]$ in THF in ratios of 1:1, 2:1 and 4:1 were prepared and a ^1H NMR spectrum was obtained for each. The spectrum of one representative mixture (TPPO:$[Ph_4P][HW_2(CO)_{10}]$ = 2:1) is shown in Fig. A49 and the measured chemical shifts for the bridging hydrogen atoms are given in Table 5. As is apparent from the table, the chemical shifts associated with the bridging hydride sites in the mixtures are altered slightly (by up to 0.07 ppm) from the values (-12.77 and -19.64 ppm, respectively) for pure $[Ph_4P][HW_2(CO)_{10}]$ and pure $[Ph_4P][HCr_2(CO)_{10}]$. It is questionable whether these variations have any real significance, given their small magnitude and the precision of the measurements (estimated to be 0.03 ppm, at best).

The absence of a marked effect on the hydride chemical shift values certainly cannot be taken as conclusive evidence that there is no association between TPPO and the complexes in solution. In ion pairing studies of monometallic hydrido carbonylates with various cations, it has

33

Table 5 ^{1}H NMR chemical shifts for M-H-M complexes and mixtures with TPPO in THF

Component(s)	Ratio	δ (TMS = 0) (ppm)
[Ph$_4$P][HW$_2$(CO)$_{10}$]	pure	-12.77
TPPO:[Ph$_4$P][HW$_2$(CO)$_{10}$]	1:1	-12.73
	1.5:1	-12.70
	4:1	-12.70
	8:1	-12.70
[Ph$_4$P][HCr$_2$(CO)$_{10}$]	pure	-19.64
TPPO:[Ph$_4$P][HCr$_2$(CO)$_{10}$]	1:1	-19.57
	2:1	-19.60
	4:1	-19.60

been observed that association of a cation with a carbonyl group does not alter the position of the hydridic proton NMR signal.[45] Thus it is possible that TPPO is interacting with a nonhydridic portion of a given complex. Moreover, for any association to be observable by NMR, its lifetime would have to be on the order of 10^{-2} s or longer, a condition that may not be met for the systems under investigation. It is also difficult to estimate how strong an interaction between TPPO and a hydridic site would have to be in order to perturb the ^1H chemical shift because M-H chemical shifts in general present problems in interpretation.[30(a),46] For example, anionic metal hydrides have no higher field shifts than do their neutral analogs, a fact that cannot be easily rationalized in terms of the nature of the electronic environment at the hydridic site. Furthermore, based on ion pairing studies with transition metal hydridic carbonylates, it is expected that interactions that are significantly mediated by solvent would not be detectable by NMR.[30(a),45] Hence, even if there was an association between TPPO and a hydridic site, it may be too short-lived or too weak to cause an observable change in its ^1H NMR spectrum.

Both the chemical shift and the line shape associated with the cations in these mixtures do not vary markedly from those of corresponding pure complexes. This can be seen, e.g., by comparing the ^1H NMR signal for $[Ph_4P]^+$ in the mixture TPPO:$[Ph_4P][HW_2(CO)_{10}]$ = 2:1 (Fig. A49) with that of pure $[Ph_4P][HW_2(CO)_{10}]$ (Fig. A17). Thus, the ^1H NMR results do not provide information regarding interaction between TPPO and the cations.

3. Solution IR results

Solution IR samples were prepared by dissolving various ratios of TPPO and M-H-M complexes in THF. The specific mixtures examined were TPPO and $[Ph_4P][HW_2(CO)_{10}]$ in ratios of 1:1, 2:1, 3:1, 4:1, and 8:1; TPPO and $[Ph_4P][HCr_2(CO)_{10}]$ in ratios of 1:1 and 2:1 and TPPO and $[Et_4N][HW_2(CO)_{10}]$ in a 1:1 ratio. In addition, mixtures consisting of TPPO and $[Ph_4P]Cl$ (1:1) and TPPO and $[Et_4N]Br$ (1:1) were examined to investigate possible interactions between TPPO and countercations. Spectra were expanded in the same three regions (2200-1700, 1700-1000, and 1000-400 cm^{-1}) as for the solid IR samples. Careful comparisons were made between the solution spectra of the mixtures and those of the pure components in THF in an attempt to determine whether there was significant interaction between the solution components. In addition, comparisons were made among the spectra of the mixtures to ascertain whether there were any effects associated with variations in ratio, complex anion, and countercation.

Within each of the three expanded spectral regions, there was at least one key absorption that could be regarded as a potential indicator of interaction between solution components. In order of decreasing frequency, these were the lines associated with CO stretching, PO stretching, and M-C-O bending motions. Table 6 summarizes the data for these three regions, each of which will be discussed in turn.

Within the 2200-1700 cm^{-1} spectral range, each of the M-H-M complexes exhibits three characteristic bands assigned to C-O stretching

36

Table 6 Selected IR data for M–H–M complexes, TPPO, Ph_4PCl, Et_4NBr, and TPPO mixtures, all in THF

(a) 2200–1700 cm^{-1}

Component(s)	Ratio	Observed bands (cm^{-1})
TPPO	pure	
$[Ph_4P][HW_2(CO)_{10}]$	pure	2041.5, 1878.4, 1938.4
	1:1	2041.6, 1878.5, 1938.4
	2:1	2041.5, 1878.5, 1938.4
TPPO:$[Ph_4P][HW_2(CO)_{10}]$	3:1	2041.6, 1878.4, 1938.4
	4:1	2041.6, 1878.5, 1938.4
	8:1	2041.6, 1878.5, 1938.4
$[Ph_4P][HCr_2(CO)_{10}]$	pure	2030.7, 1878.6, 1940.4
TPPO:$[Ph_4P][HCr_2(CO)_{10}]$	1:1	2030.4, 1878.6, 1940.4
	2:1	2030.4, 1878.6, 1940.3
$[Et_4N][HW_2(CO)_{10}]$	pure	2041.6, 1878.6, 1938.5
TPPO:$[Et_4N][HW_2(CO)_{10}]$	1:1	2041.7, 1878.6, 1938.5
Ph_4PCl	pure	
TPPO:Ph_4PCl	1:1	
Et_4NBr	pure	
TPPO:Et_4NBr	1:1	

Table 6   Continued

(b)   1700-1000 cm^{-1}

Component(s)	Ratio	Observed bands (cm^{-1})
TPPO	pure	1118.9, 1203.7, 1438.9, 1485.3
[Ph$_4$P][HW$_2$(CO)$_{10}$]	pure	1109.4, 1196.9, 1438.9, 1486.7
TPPO:[Ph$_4$P][HW$_2$(CO)$_{10}$]	1:1	1109.4, 1118.9, 1185.9, 1191.4, 1202.3, 1438.9, 1459.4, 1485.3
	2:1	1109.4, 1118.9, 1190.0, 1203.7, 1438.9, 1459.4, 1485.3
	3:1	1109.4, 1118.9, 1185.9, 1192.8, 1203.7, 1438.9, 1460.7, 1485.3
	4:1	1109.4, 1118.9, 1190.0, 1203.7, 1438.9, 1460.7, 1485.3
	8:1	1109.4, 1118.9, 1203.7, 1438.9, 1460.7, 1485.3
[Ph$_4$P][HCr$_2$(CO)$_{10}$]	pure	1099.8, 1181.8, 1464.8
TPPO:[Ph$_4$P][HCr$_2$(CO)$_{10}$]	1:1	1109.4, 1118.9, 1188.7, 1203.7, 1438.9
	2:1	1118.9, 1192.8, 1202.3, 1438.9, 1485.3
[Et$_4$N][HW$_2$(CO)$_{10}$]	pure	1463.5
TPPO:[Et$_4$N][HW$_2$(CO)$_{10}$]	1:1	1118.9, 1181.8, 1203.7, 1396.5, 1438.9, 1485.5
Ph$_4$PCl	pure	1181.8, 1194.1, 1464.8
TPPO:Ph$_4$PCl	1:1	1118.9, 1180.5, 1203.7, 1438.9, 1485.3
Et$_4$NBr	pure	
TPPO:Et$_4$NBr	1:1	1180.5, 1188.7, 1203.7

Table 6   Continued

(c)   1000-400 cm^{-1}

Component(s)	Ratio	Observed bands (cm^{-1})
TPPO	pure	543.0, 697.7, 721.1, 749.2
[Ph$_4$P][HW$_2$(CO)$_{10}$]	pure	528.9, 584.0, 594.5, 691.8, 725.8
TPPO:[Ph$_4$P][HW$_2$(CO)$_{10}$]	1:1	528.9, 543.0, 593.4, 696.5, 722.3, 755.1
	2:1	528.9, 543.0, 593.4, 696.5, 722.3, 753.9
	3:1	528.9, 543.0, 593.4, 696.5, 722.3, 753.9
	4:1	528.9, 543.0, 593.4, 696.5, 722.3, 755.1
	8:1	528.9, 543.0, 593.4, 696.5, 722.3, 753.9
[Ph$_4$P][HCr$_2$(CO)$_{10}$]	pure	497.3, 530.1, 666.0, 693.0, 724.6
TPPO:[Ph$_4$P][HCr$_2$(CO)$_{10}$]	1:1	528.9, 543.0, 664.8, 693.0, 723.4
	2:1	530.1, 543.0, 664.8, 696.5, 722.3
[Et$_4$N][HW$_2$(CO)$_{10}$]	pure	594.5
TPPO:[Et$_4$N][HW$_2$(CO)$_{10}$]	1:1	543.0, 594.5, 697.7, 721.1, 749.2
Ph$_4$PCl	pure	
TPPO:Ph$_4$PCl	1:1	543.0, 697.7, 722.3, 749.2
Et$_4$NBr	pure	
TPPO:Et$_4$NBr	1:1	543.0, 697.7, 722.3, 749.2

39

modes, as described in section A of this chapter. The spectrum of pure TPPO in THF exhibits no peaks in this range. The CO stretching bands have been shown to be very sensitive to interactions of carbonylate species with countercations in solution.[30] For the current study, probably the most remarkable change in this region would occur if TPPO were to bind to one or more of the metal atoms. Because this would disrupt the symmetry of the molecule, it should affect not only the frequencies but also the pattern of the CO stretching modes. As can be ascertained from a glance at Table 6, the number of CO stretching bands for a given complex is not altered when TPPO is present in the same solution; thus it is reasonable to conclude that TPPO is not strongly interacting with the metal sites.

It is expected that if an association developed between TPPO and a carbonyl ligand, it would involve the oxygen of TPPO and the carbon of CO in an O---C interaction. This would result in a reduction in the CO bond order which should lead to a decrease in the CO stretching frequency for the affected ligand. The stretching modes for the other CO groups in the complex may also be shifted. Examination of Table 6 reveals that for the Ph_4P^+ and Et_4N^+ salts of $[HW_2(CO)_{10}]$, the CO stretching frequencies are unaffected when TPPO is added, even up to an 8:1 ratio of TPPO to complex. This can be taken as an indication that there is not a strong association between TPPO and a specific carbonyl ligand in these complexes. For the $[Ph_4P][HCr_2(CO)_{10}]$, however, the absorption that occurs at 2030.7 cm^{-1} in the pure salt is shifted slightly to 2030.4 cm^{-1} in the presence of TPPO. The shift, although small, is identical for both of the ratios (1:1 and 2:1) examined, suggesting that it is probably not simply a result of experimental error. The other two CO stretching bands

40

for the complex appear to be unaffected. This spectral change could result from a loose association between TPPO and an equatorial carbonyl ligand. The assignment specifically to an equatorial CO is based on infrared analyses of similar complexes which conclude that the higher-frequency A_{2u} band is due mainly to symmetric stretching of the equatorial carbonyl groups.[35,36,47] Although it would be reasonable to expect that the other two bands would also be affected by a TPPO---CO_{eq} association, the effects on them should be less dramatic. In view of the small shift in CO stretching frequency (0.3 cm^{-1}) observed for the ligand most affected, it would not be surprising if these more minor effects were unobservable. Thus the solution IR data for the carbonyl stretching region suggest that there is a specific interaction between TPPO and an equatorial CO ligand in $[HCr_2(CO)_{10}^-]$.

In the $1700-1000$ cm^{-1} window, the vibrational mode of interest is that associated with the symmetric PO stretch, which appears as a strong sharp peak at 1203.7 cm^{-1} for pure TPPO in THF solution. In a number of studies, this band has been shown to be quite sensitive to interactions between the phosphoryl oxygen of TPPO and various centers, including proton donors[48] and metal ions.[49] The effect of these interactions is to broaden, shift, or split the PO stretching band or to cause some combination of these changes. In general, the perturbations are toward lower frequency, which can be rationalized in terms of a decrease in the P-O bond order upon association with an electron acceptor.

The observations for the PO stretching region for the mixtures of this study are summarized in Table 6(b); the spectra are shown in Figs. A58-A60. The greatest perturbations in this domain are exhibited by the spectra for mixtures of TPPO and the Ph_4P^+ salt of the bridging tungsten

41

hydrido complex. For the 1:1 mixture, the PO stretching band is shifted by 1.4 cm^{-1} to 1202.3 cm^{-1} and two new lines appear at 1191 and 1186 cm^{-1}; all three of these absorptions have similar intensities. As the ratios of TPPO to complex are increased, the absorption for unperturbed TPPO at 1203.7 cm^{-1} grows in intensity with the lower-frequency bands finally appearing as a broad shoulder on this peak. These results are clearly consistent with an interaction of TPPO through its phosphoryl oxygen with at least one other component of the mixture, i.e., with the hydrido anion, the countercation, or both.

The spectra for mixtures of TPPO and the Ph$_4$P$^+$ salt of the Cr-H-Cr complex show features similar to those for the tungsten analogs. For the 1:1 mixture of TPPO and Cr-H-Cr complex, the PO peak is strongly broadened and a new broad line is evident at 1189 cm^{-1}. For the 2:1 mixture of TPPO with this complex, the PO stretching band is shifted to 1202.3 cm^{-1} and there is a band at 1193 cm^{-1}. It appears that the interactions of this complex with TPPO are more dependent on the ratio of components than they are for the W-H-W analog, but are similar in other respects. In contrast, the spectrum for the mixture of TPPO with the Et$_4$N$^+$ salt of the W-H-W complex, shows no shift in the PO stretching frequency and only slight broadening of this peak to the lower frequency side, suggesting that TPPO is experiencing a much reduced interaction in this mixture compared to those containing Ph$_4$P$^+$.

To further test the possibility of TPPO-cation interactions, the spectra of TPPO:Ph$_4$PCl and TPPO:Et$_4$NBr mixtures were examined in the PO stretching region . For the Ph$_4$PCl mixture, the 1203.7 cm^{-1} band was unshifted but broadened slightly compared to that for pure TPPO and it had shoulders on the lower-frequency side. This certainly suggests that

an association exists between TPPO and the cation. When the spectral features for this mixture are compared with those for the mixtures of TPPO with Ph_4P^+ salts of the M-H-M complexes, however, there are distinct contrasts in line shapes, shifts, and numbers of peaks. A plausible explanation is that, when mixed with $[Ph_4P][HM_2(CO)_{10}]$, TPPO associates with both cation and anion.

The spectrum for the TPPO:Et_4NBr mixture shows sharp peaks, at 1203.7 and 1188.7 cm^{-1}, suggesting that there is a stronger association of TPPO with Et_4N^+ in this mixture than in the one with $[Et_4N][HW_2(CO)_{10}]$. This somewhat puzzling result can be rationalized on the basis of competing interactions. In section A of this chapter, evidence was presented that Et_4N^+ forms more strongly bound ion pairs with M-H-M carbonylates than does Ph_4P^+. Thus it is possible that TPPO is not able to very successfully disrupt the ion pairing interaction in the $[Et_4N]$-$[HW_2(CO)_{10}]$ case but can do so in the $[Ph_4P][HM_2(CO)_{10}]$ cases.

On the basis of the spectral analysis presented thus far, there is significant evidence that TPPO associates with the bridging hydride complexes in THF solution when the countercation is Ph_4P^+. Further support for this view, as well as additional insight into the specific participating sites on the anion, was provided by examination of the 1000-400 cm^{-1} region of the solution IR spectra. The important vibrational modes within this range for this study were those associated with M-C-O bending motions. In the spectra for the Cr-H-Cr and W-H-W complexes (with all cations studied), these bands appear at 666.0 and 594.5 cm^{-1}, respectively. Their assignment to the M-C-O bending mode is based on analyses for the corresponding $M(CO)_6$ species.[50] Table 6 lists these frequencies as well as those for the mixtures with TPPO. As the

43

data show, the (M-C-O) lines are shifted by about 1.2 cm^{-1} to lower frequency in the mixtures of TPPO with [Ph$_4$P][HCr$_2$(CO)$_{10}$] and with [Ph$_4$P][HW$_2$(CO)$_{10}$]. In contrast, there is no shift upon adding TPPO to [Et$_4$N][HW$_2$(CO)$_{10}$]. These results are consistent with the earlier conclusion that there is some association between TPPO and the M-H-M anions in the [Ph$_4$P$^+$] salts but little or none in the [Et$_4$N$^+$] salt.

As for the site or sites within the hydrido carbonylates that interact with TPPO, it seems most likely that the CO carbon is a point of contact and, for the Cr-H-Cr case, there is evidence that the CO ligand involved is specifically in an equatorial position. This provides concrete support for mechanisms that postulate nucleophilic attack at the CO carbon in reactions of these complexes.

The data for the PO stretching region suggest that TPPO is engaging in more than one type of association, especially in the [Ph$_4$P$^+$] salts. For these salts, it seems quite evident that both cation and anion are interacting with TPPO. It is possible that ^{31}P NMR could allow determination of the number of sites with which TPPO is interacting in a given mixture. Whether more than one type of site on the anion might be involved is less clear. In particular, the possibility of interaction between TPPO and the bridging hydride atom is not ruled out by the available data. Thus the question of the charge distribution in the M-H-M bond is still open. It is expected that ^{2}H NQDR data for the bridging hydride complexes will help to answer this question.

References

1. (a) Behrens, H.; Klek, W. Z. Anorg. Allgem. Chem. **1957**, 292, 151

   (b) Behrens, H.; Haag, W. Chem. Ber. **1961**, 94, 312

   (c) Behrens, H.; Vogl, J. Chem. Ber. **1963**, 96, 2220

2. Hayter, R. G. J. Am. Chem. Soc. **1966**, 88, 4376

3. Anders, U.; and Graham, W.A.G. Chem. Commun. **1965**, 499

4. Grillone, M.D. In Inorganic Synthesis; Kirschner, S., Ed.; Wiley: New York, 1985; Vol.23, p25

5. Darensbourg, D. J.; Ovalles, C. J. Am. Chem. Soc. **1984**, 106, 3750

6. Darensbourg, D. J.; Ovalles, C. J. Am. Chem. Soc. **1987**, 109, 333

7. Bau, R.; Teller, R. G.; Kirtley, S. W.; Koetzle, T. F. Acc. Chem. Res. **1979**, 12, 176

8. Teller, R. G. and Bau, R. Structure and Bonding **1981**, 44, 1

9. Moore, D. S.; Robinson, S. D. Chem. Soc. Rev. **1983**, 12, 415

10. Pearson, R. G. Chem. Rev. **1985**, 65, 1

11. Dahl, L. F. Ann. N.Y. Acad. Sci. **1983**, 415, 1

12. Handy, L. B.; Treichel, P. M.; Dahl, L. F.; Hayter, R. G. J. Am. Chem. Soc. **1966**, 88, 366

13. Handy, L. B.; Ruff, J. K.; Dahl, L. F. J. Am. Chem. Soc. **1970**, 92, 7312

14. Roziere, J.; Williams, J.M.; Stewart, R.P.; Peterson, J.L.; Dahl, L.F. J. Am. Chem. Soc. **1977**, 99, 4497

15. Andrews, M.A.; Tipton, D.L.; Kirtley, S.W. and Bau, R. J. Chem. Soc. Chem. Commun. **1973**, 181

16. Olsen, J.P.; Koetzle, T.F.; Kirtley, S.W.; Andrews, M.; Tipton, D.L.; Bau, R. J. Am. Chem. Soc. **1974, 96**, 6621

17. Wilson, R.D.; Graham, S.A.; Bau, R. J. Organomet. Chem. **1975, 91**, C49

18. Love, R.A.; Chin, H.B.; Koetzle, T.F.; Kirtley, S.W.; Wittlesey, B.R. and Bau, R. J. Am. Chem. Soc. **1976, 98**, 4491

19. Peterson, J.L.; Dahl, L.F.; Williams, J.M. In Transition Metal Hydrides; Bau, R., Ed.; Advances in Chemistry 167; American Chemical Society: Washington, DC., 1978; p11

20. Peterson, J.L.; Johnson, P.L.; O'Connor, J.; Dahl, L.F.; Williams, J.M. Inorg. Chem. **1978, 17**, 3460

21. Darensbourg, M.Y.; Atwood, J.L.; Burch, R.R.; Hunter, W.E.; Walker, N. J. Am. Chem. Soc. **1979, 101**, 2633

22. Peterson, J.L.; Brown, R.K.; Williams, J.M.; McMullan, R.K. Inorg. Chem. **1979, 18**, 3493

23. Peterson, J.L.; Brown, R.K.; Williams, J.M. Inorg. Chem. **1981, 20**,158

24. Peterson, J.L.; Masino, A.; Stewart, R.P. J. Organomet. Chem. **1981, 208**, 55

25. Roziere, J.; Teulon, P.; Grillone, M.D. Inorg. Chem. **1983, 22**, 557

26. Hart, D.W.; Bau, R.; Koetzle, T.F. Organometallics **1985, 4**, 1590

27. (a) Hiyama, Y.; Keiter, E. A.; Brown, T. L. J. Magn. Reson. **1986, 67**, 202

    (b) Keiter, E. A.; Hiyama, Y; Brown, T. L. J. Mol. Struct. **1983, 111**, 1

28. Jarrett, W.L.; Farlee, R.D.; Butler, L.G. Inorg. Chem. **1987, 26**, 1381

29. Guo, K.; Jarrett, W.L.; Butler, L.G. Inorg. Chem. **1987, 26**, 3001

30. (a) Darensbourg, M.Y. Prog. in Inorg. Chem. **1985**, 33, 221

    (b) Darensbourg, M.Y.; Ash, C.E. Advances Organomet. Chem. **1985**, 33,1

31. (a) Etter, M.C.; Baures, P.W. J. Am. Chem. Soc. **1988**, 110, 639

    (b) Etter, M.C.; Panunto, T.W. J. Am. Chem. Soc. **1988**, 110, 5896

32. (a) Etter, M.C.; Gillard, R.D.; Johnson, R.B. J. Org. Chem. **1986**, 51, 5405

    (b) Hadzi, D. J. Chem. Soc. **1962**, 5128

    (c) Aksnes, G.; Gramstad, T. Acta Chem. Scand. **1960**, 14,1485

    (d) Gramstad, T. Acta Chem. Scand. **1961**,15,1337

33. Crabtree, R.H. The Organometallic Chemistry of the Transition Metals; John Wiley & Sons: New York ,1988, p57

34. Cooper III, C.B.; Shriver, D.F.; Onaka, S. In Transition Metal Hydrides; Bau, R., Ed.; Advances in Chemistry 167; American Chemical Society: Washington, DC., 1978; p232

35. Darensbourg, D.J.; Burch, Jr., R.R.; Darensbourg, M.Y. Inorg. Chem. **1978**, 17, 2677

36. Darensbourg, D.J.; Incorvia, M.J. Inorg. Chem. **1979**, 18, 18

37. Darensbourg, M.; Barros, H.; Borman, C. J. Am. Chem. Soc. **1977**, 99, 1647

38. (a) Carrington, A.; McLachlan, A. D. Introduction to Magnetic Resonance; Harper & Row: New York, 1967; p210

    (b) Harris, R.K. Nuclear Magnetic Resonance Spectroscopy; Pitman: London, 1983; p138

39. Halpern, E.; Bouck, J.; Finegold, H.; Goldenson, J. J. Am. Chem. Soc. **1955**, 77, 4472

40. Webb, S.L.; Giandomenico, C.M.; Halpern, J. J. Am. Chem. Soc. **1986,** 108, 345

41. (a) Darensbourg, D.J.; Walker, N.; Darensbourg, M.Y. J. Am. Chem. Soc. **1980,** 102, 1213

    (b) Darensbourg, D.J.; Darensbourg, M.Y.; Walker, N.; Inorg. Chem. **1981,** 20, 1918

42. Collman, J.P.; Hegedus, L.S.; Norton, J.R.; Finke, R.G. Principles and Applications of Organotransition Metal Chemistry; University Science Books: Mill Valley, California, 1987; p366

43. Eyermann, C.J.; Chung-Phillips, A. Inorg. Chem. **1984,** 23, 2025

44. References 31,32a, and 32e

45. (a) Ash, C.E.; Delord, T.; Simmons, D.; Darensbourg, M.Y. Organometallics, **1986,** 5, 17

    (b) Kao, S.C.; Darensbourg, M.Y.; Schenk, W.; Organometallics, **1984,** 3, 871

46. Collman, J.P.; Finke, R.G.; Matlock, P.L.; Wahren, R.; Komoto, R.G.; Brauman, J.I. J. Am. Chem. Soc. **1987,** 100, 1121

47. Cotton, F.A.; Wing, R.M. Inorg. Chem. **1965,** 4, 1328

48. Ref. 32 (b), (c), (d)

49. Goodgame, M.L.; Cotton, F.A. J. Chem. Soc. **1961,** 3735

50. Braterman, P.S. Metal Carbonyl Spectra; Academic: New York, 1975; pp 163-167, 182

APPENDIX I

IR and 1H NMR spectra of M-H-M and M-D-M complexes

(Fig. A01- Fig. A36)

Minima List:
X= 1878.8 Y= 38.418
X= 1938.8 Y= 2.3455
X= 2041.8 Y= 86.828
3 Minima Detected
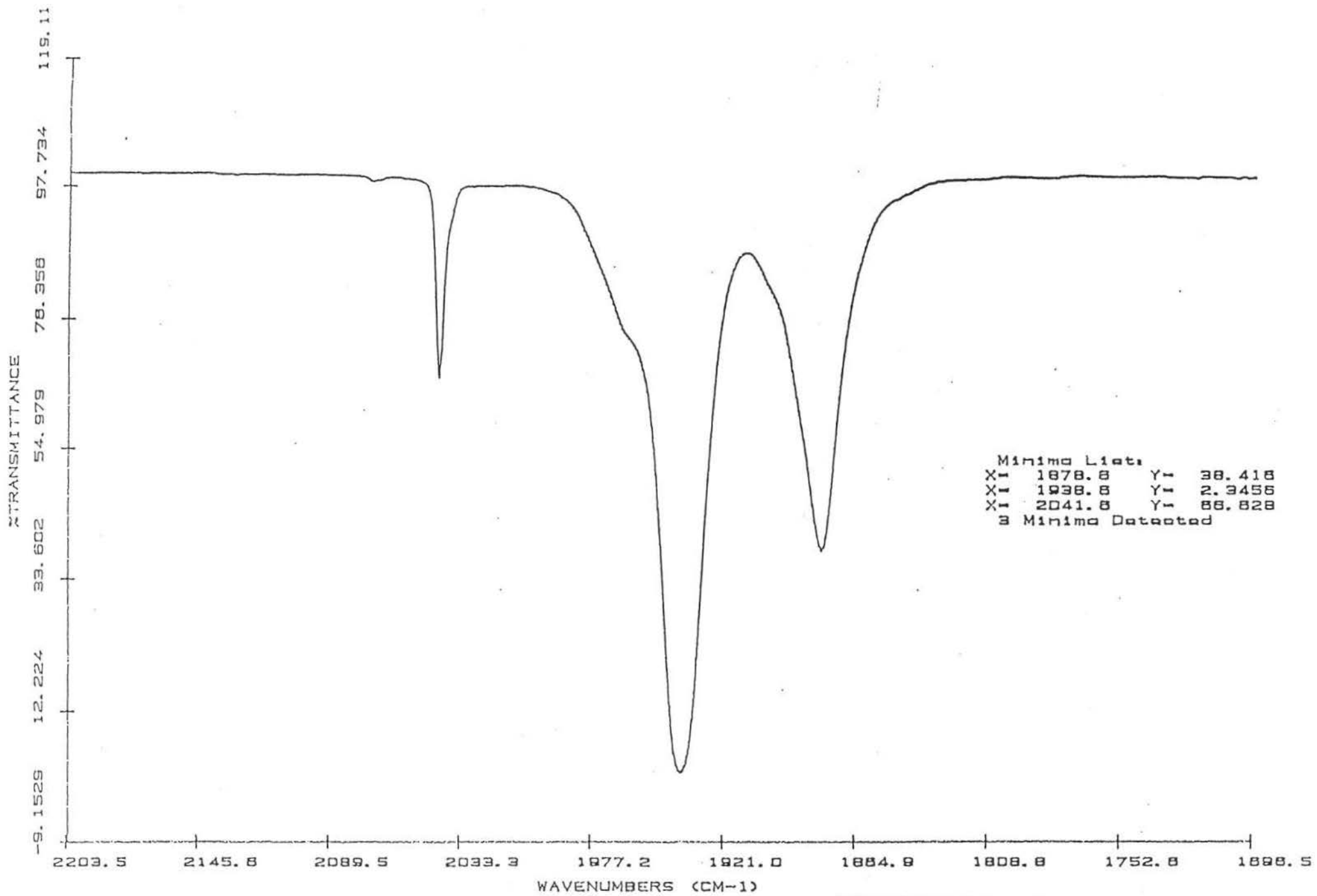
Fig. A01 IR Spectrum of (Et4N)(HW2(CO)10)   (in THF)
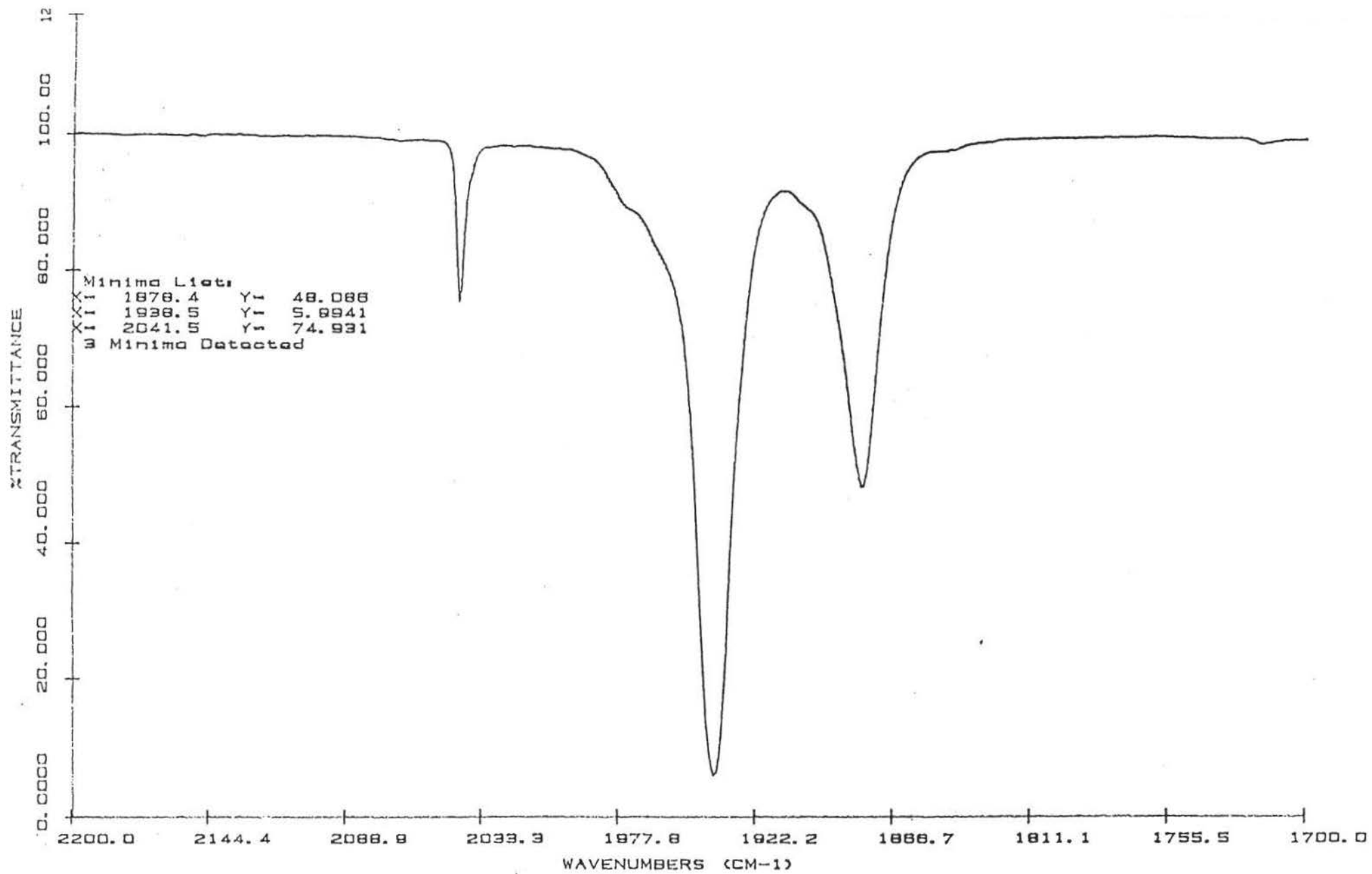
Fig. A02 IR Spectrum of (PPN)(HW2(CO)10)   (in THF)
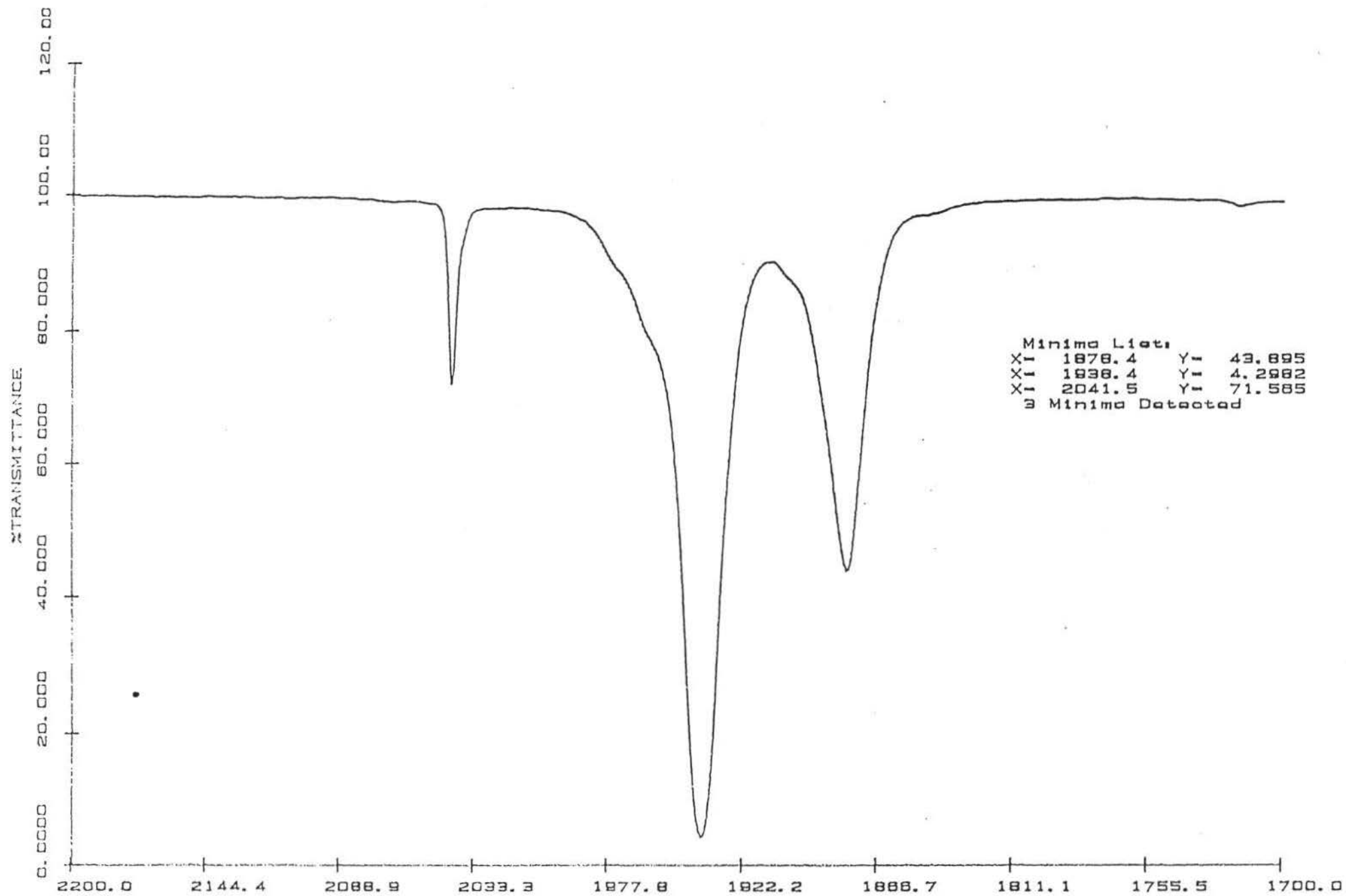
Fig. A03 IR Spectrum of (Ph4P)(HW2(CO)10)   (in THF)

Minima List:
X= 1875.3   Y= 52.525
X= 1938.4   Y= 11.185
X= 1974.8   Y= 77.889
X= 2041.5   Y= 73.797
4 Minima Detected
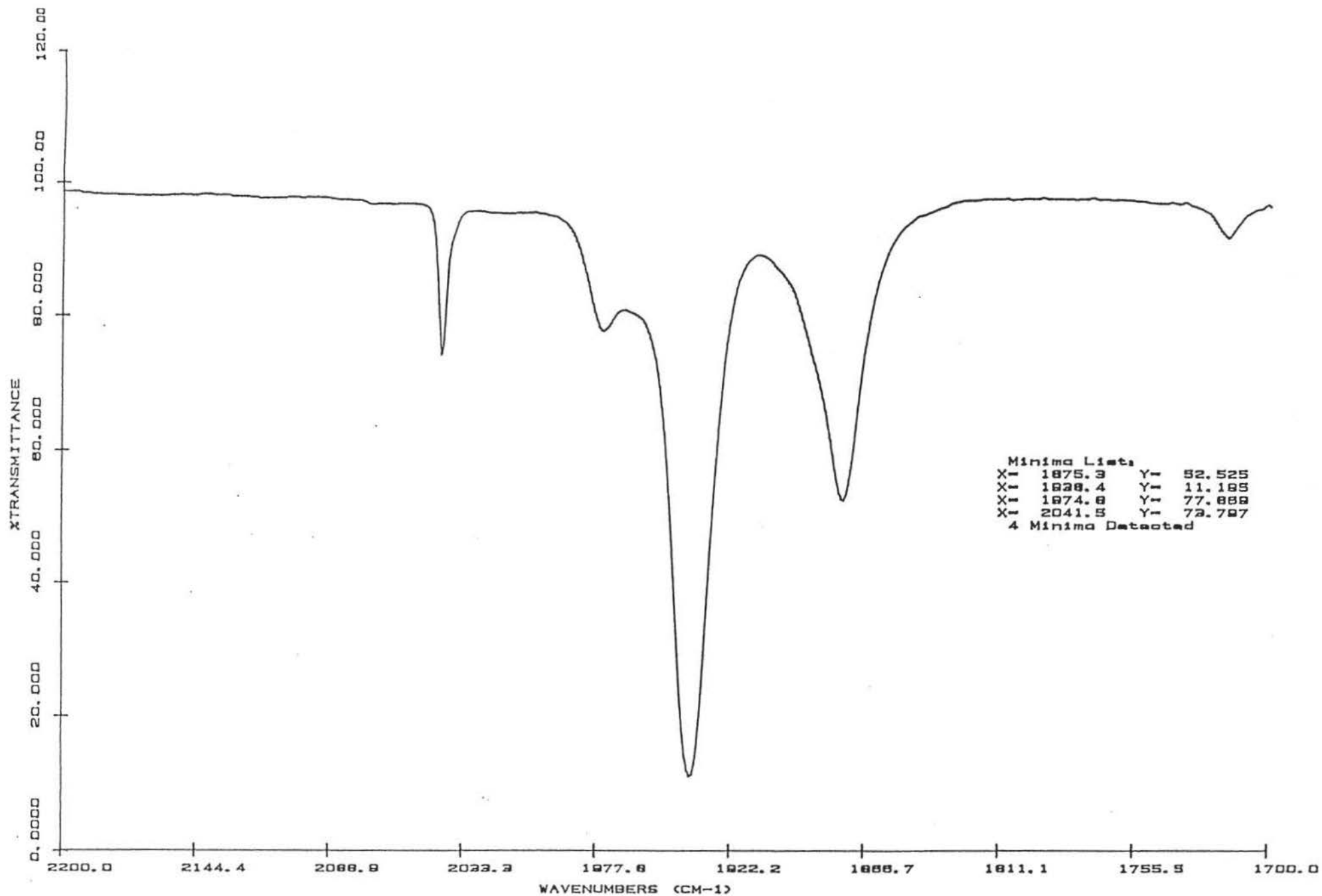
Fig. A04   IR Spectrum of (Et4N)(DW2(CO)10)   (in THF)
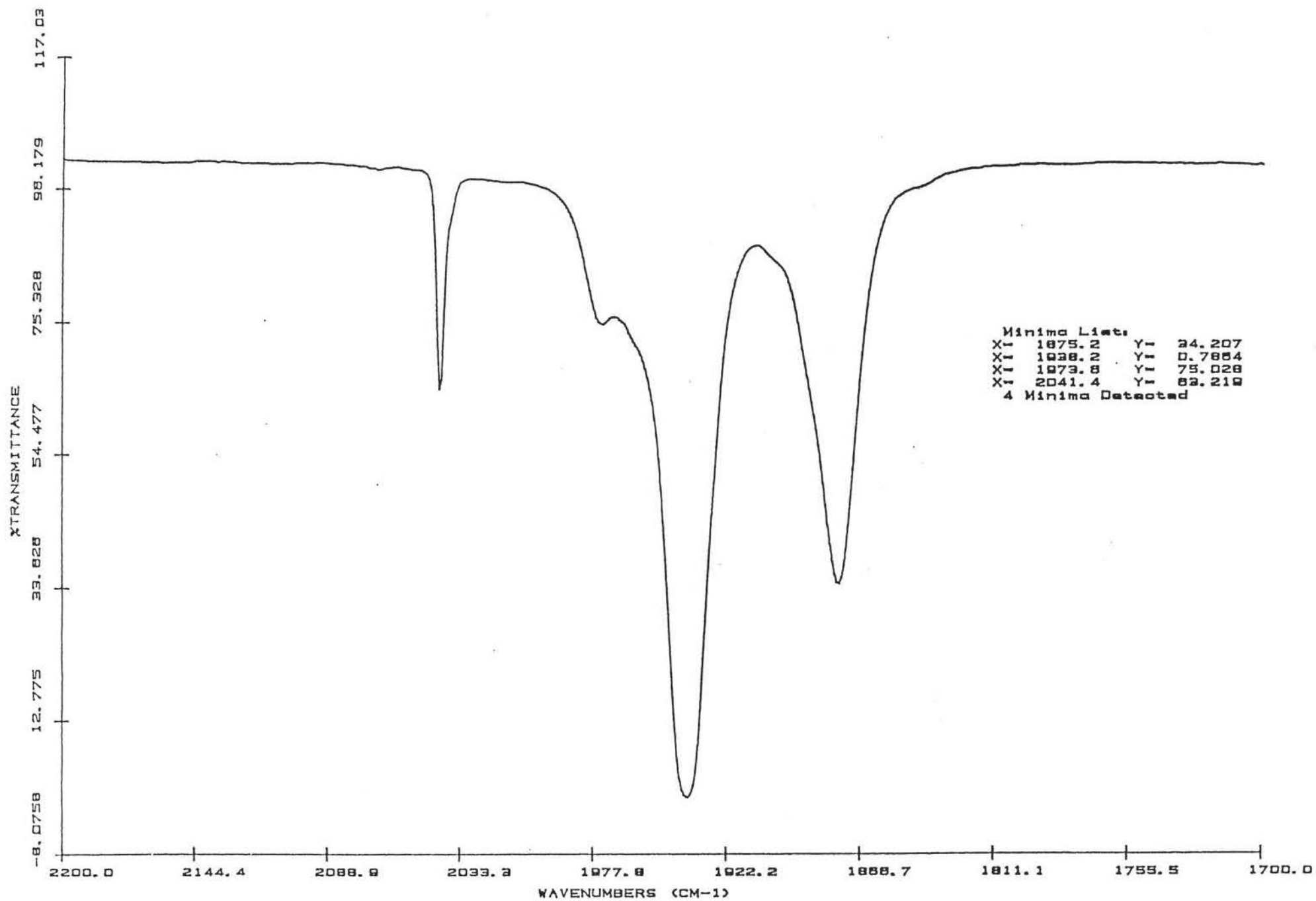
Fig. A05 IR Spectrum of (PPN)(DW$_2$(CO)$_{10}$)   (in THF)
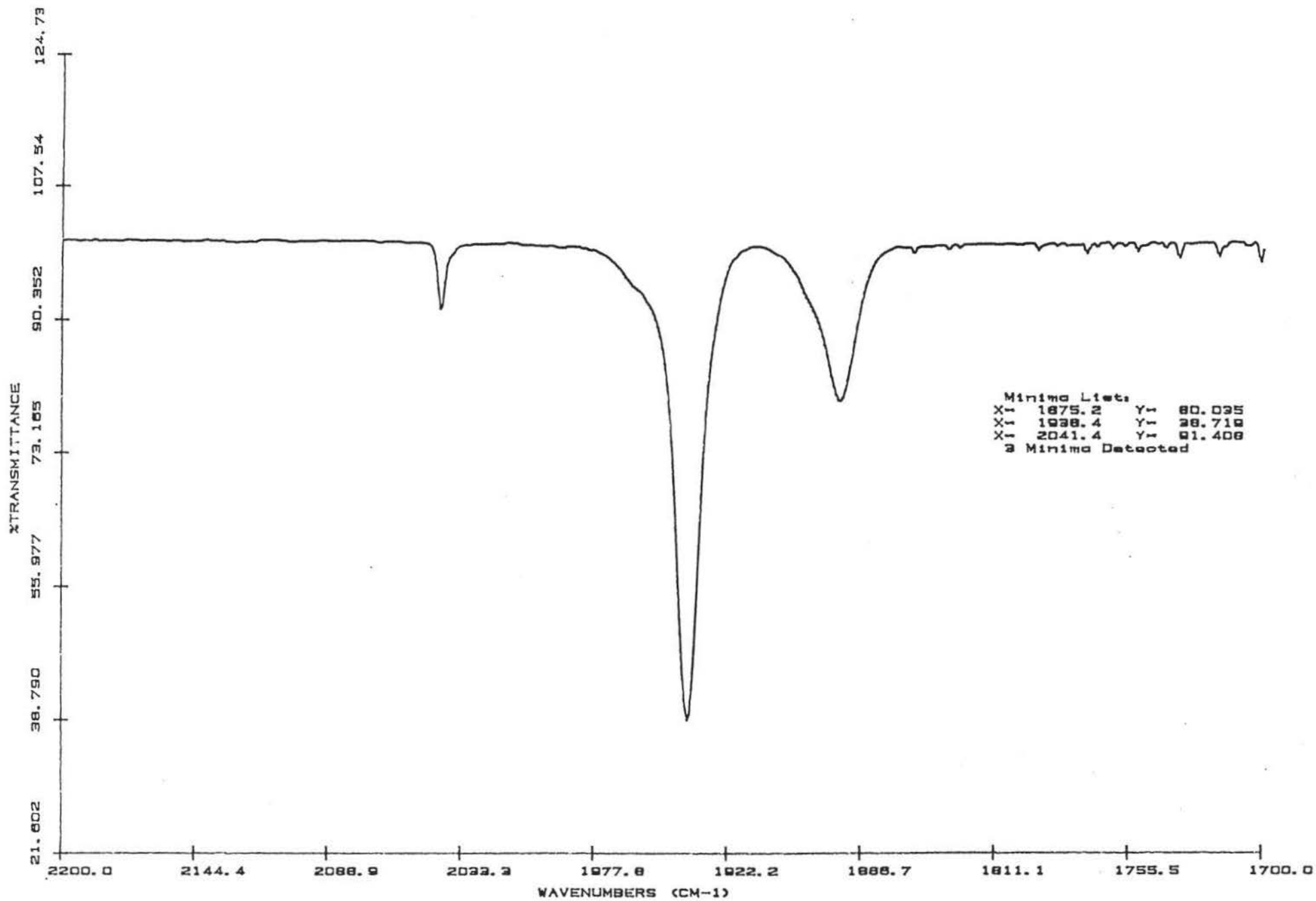
Fig. A06   IR Spectrum of (Ph4P)(DW2(CO)10)   (in THF)
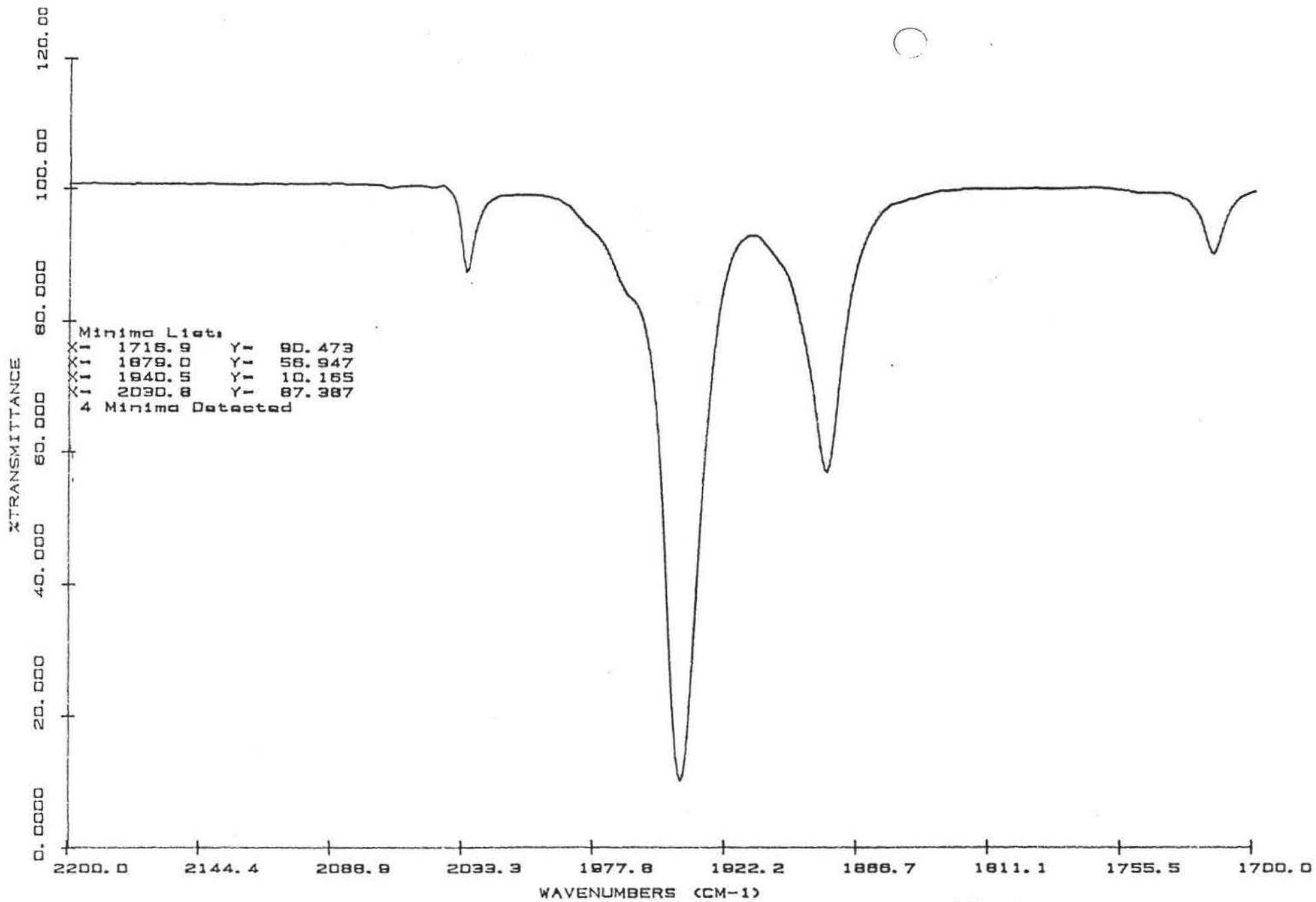
Fig. A07   IR Spectrum of (Et4N)(HCr2(CO)10)   (in THF)
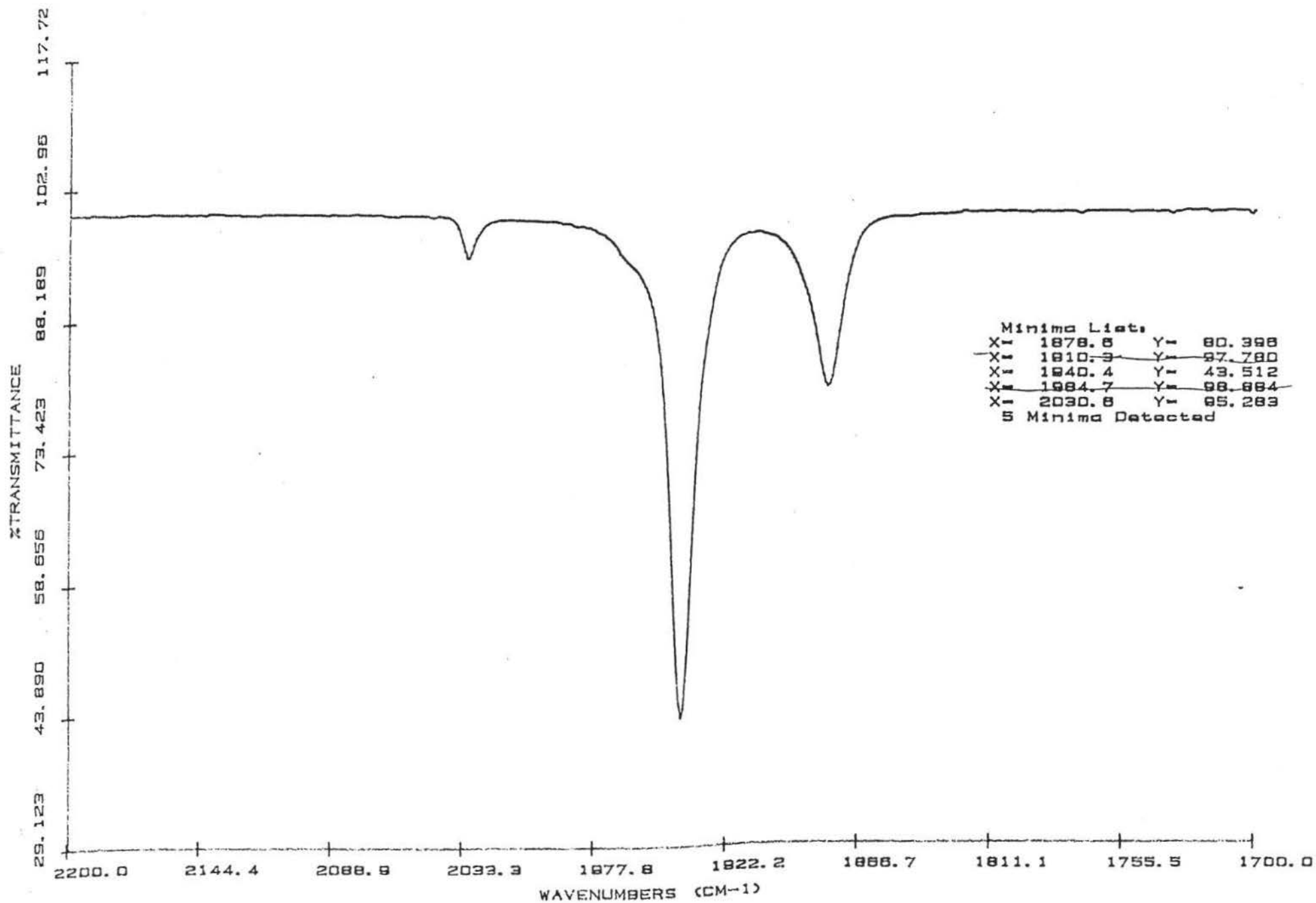
Fig. A08   IR Spectrum of (PPN)(HCr2(CO)10)   (in THF)

Minima List:
X = 1878.8   Y = 68.472
X = 1940.4   Y = 22.982
X = 2030.7   Y = 92.352
3 Minima Detected
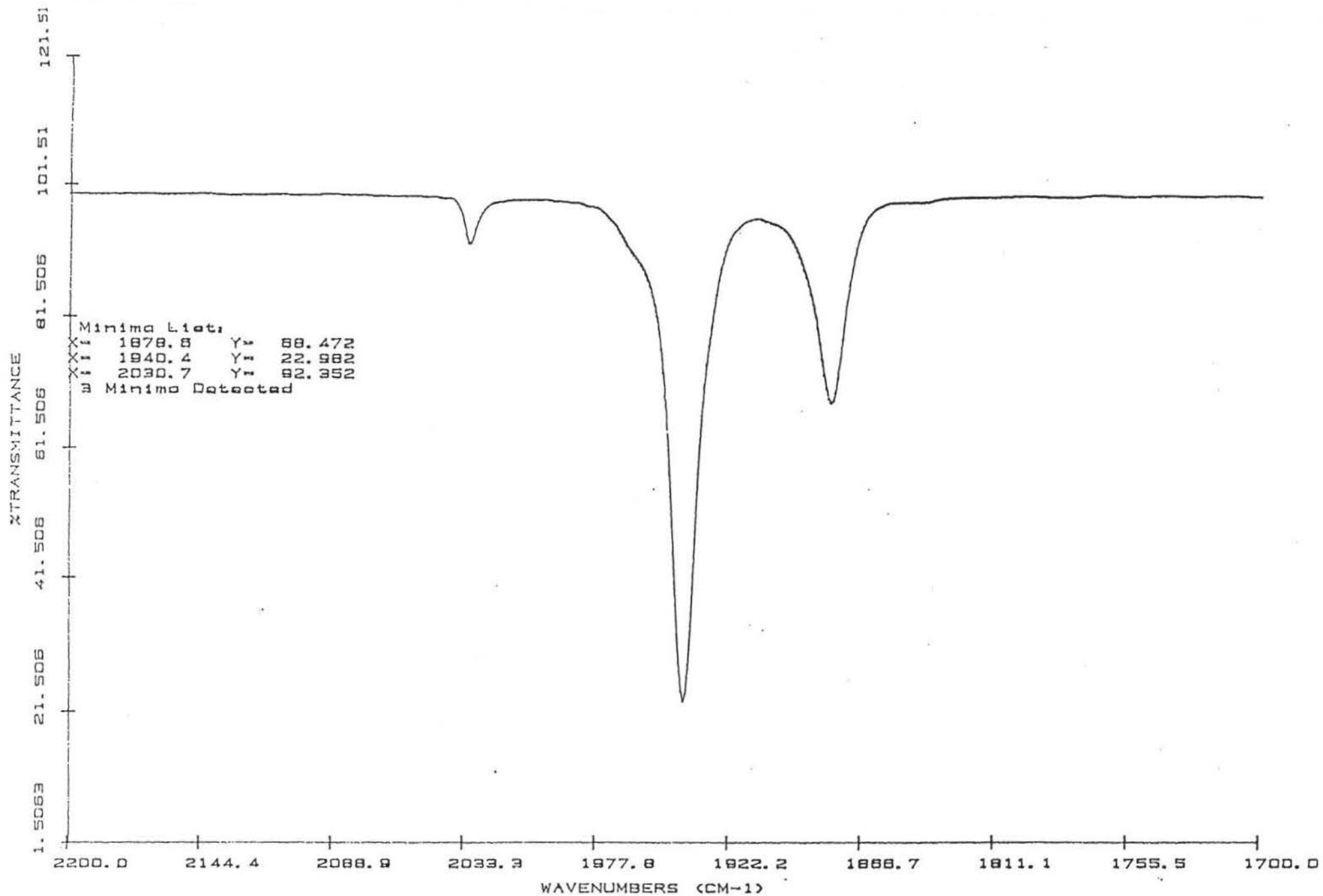
Fig. A09   IR Spectrum of (Ph4P)(HCr2(CO)10)   (in THF)
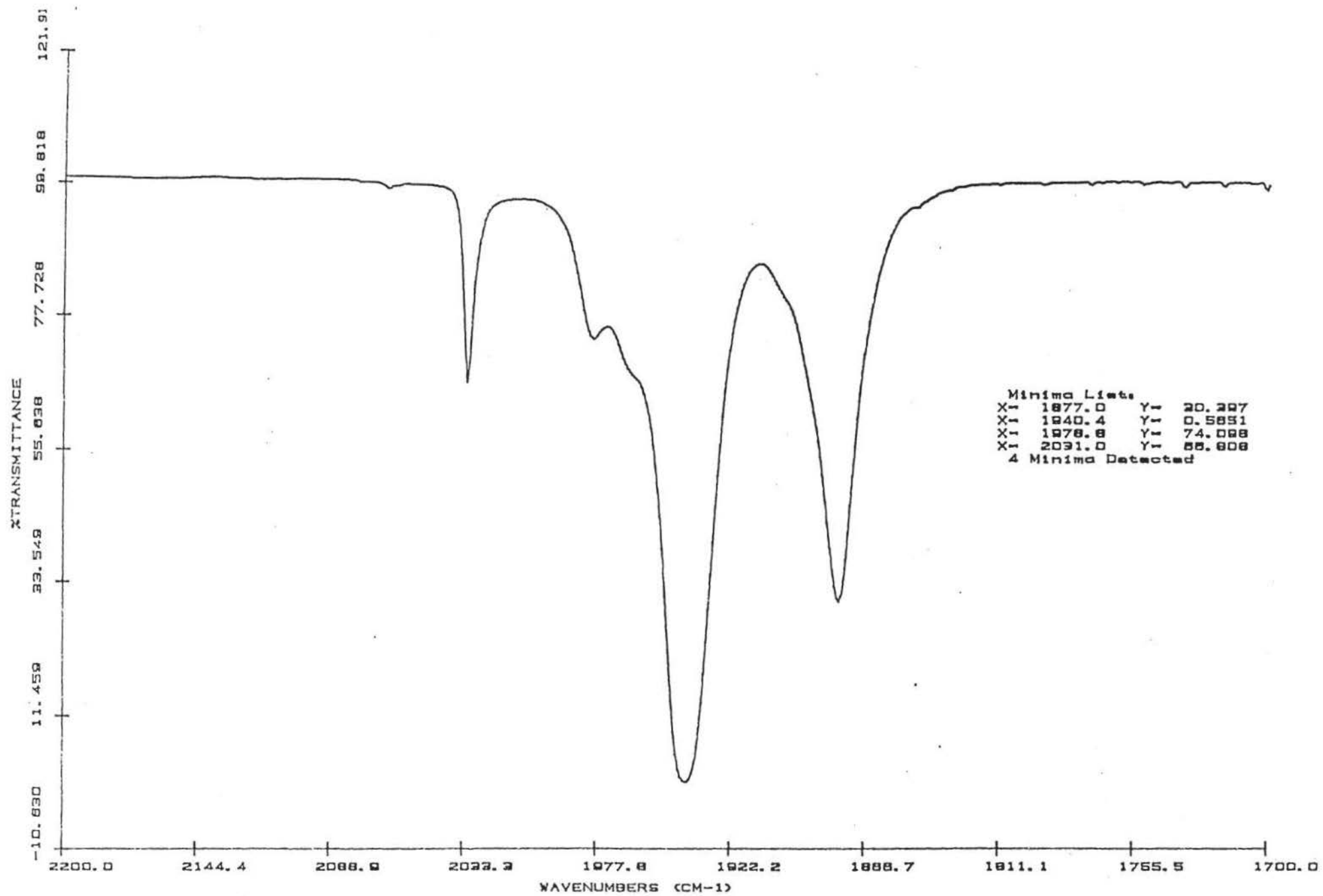
Fig. A10   IR Spectrum of (Et4N)(DCr2(CO)10)   (in THF)
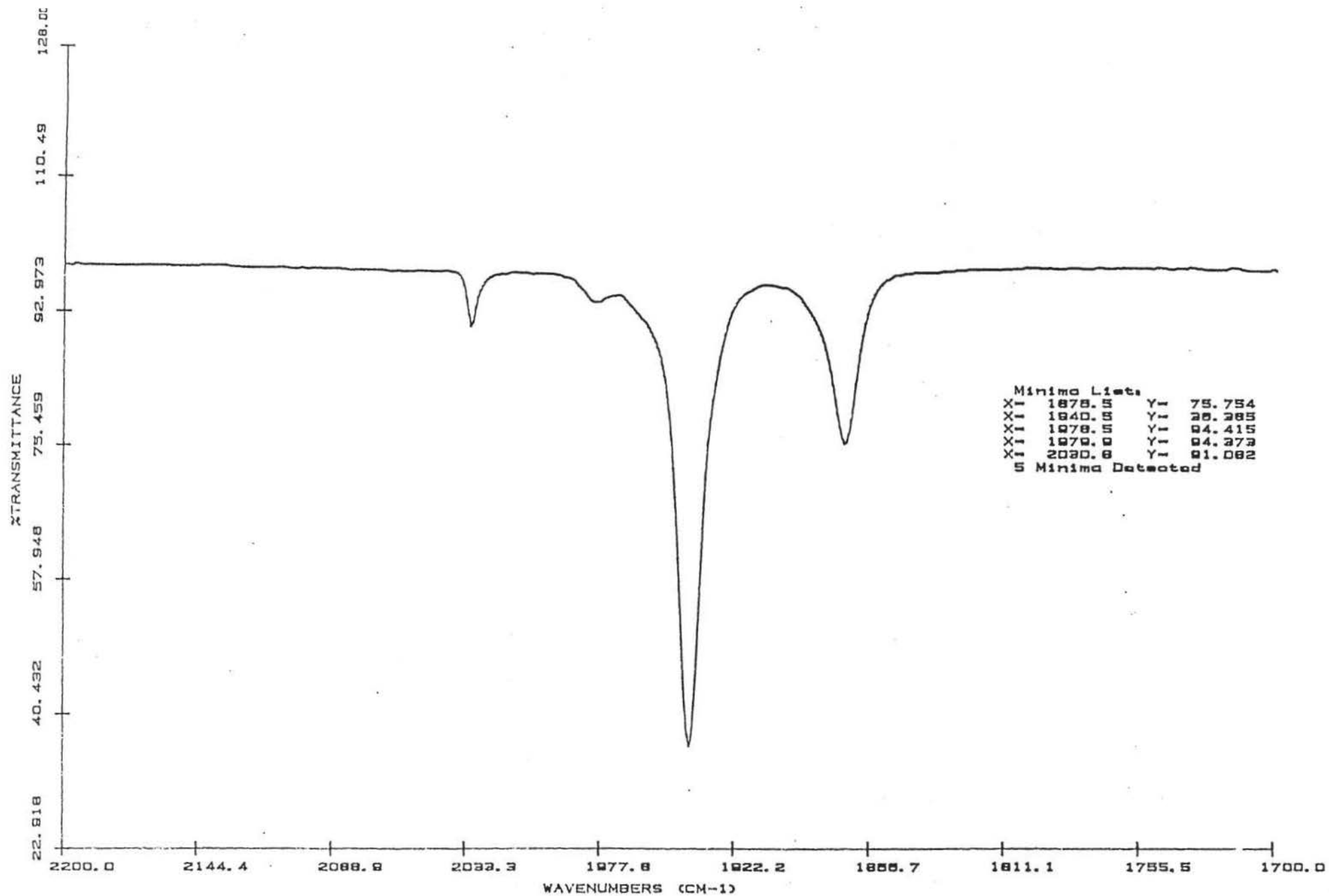
Fig. A11   IR Spectrum of (PPN)(DCr2(CO)10)   (in THF)

Minima List:
X= 1875.4   Y= 70.854
X= 1940.4   Y= 28.493
X= 2030.9   Y= 89.248
3 Minima Detected
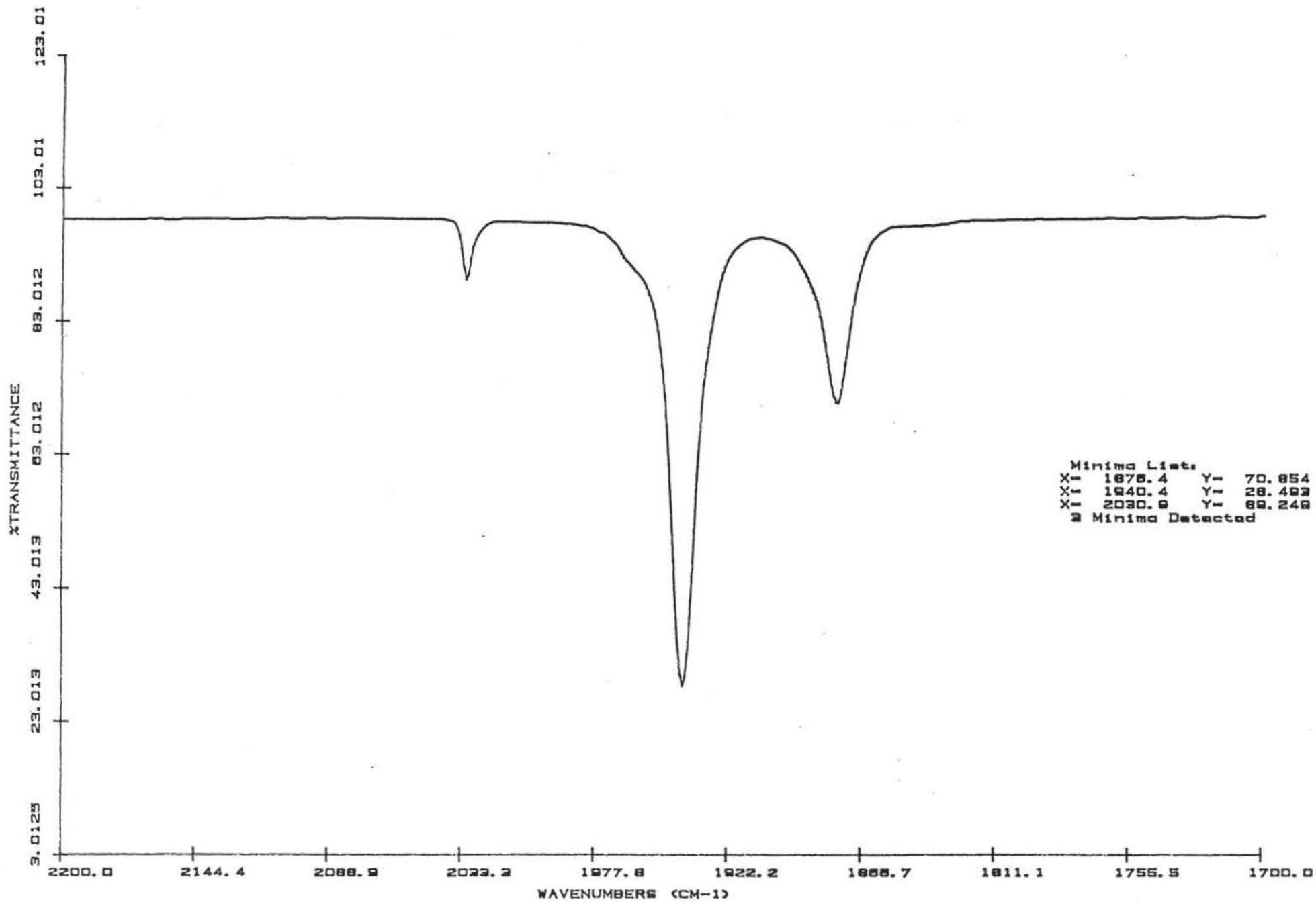
Fig. A12   IR Spectrum of (Ph4P)(DCr2(CO)10)   (in THF)
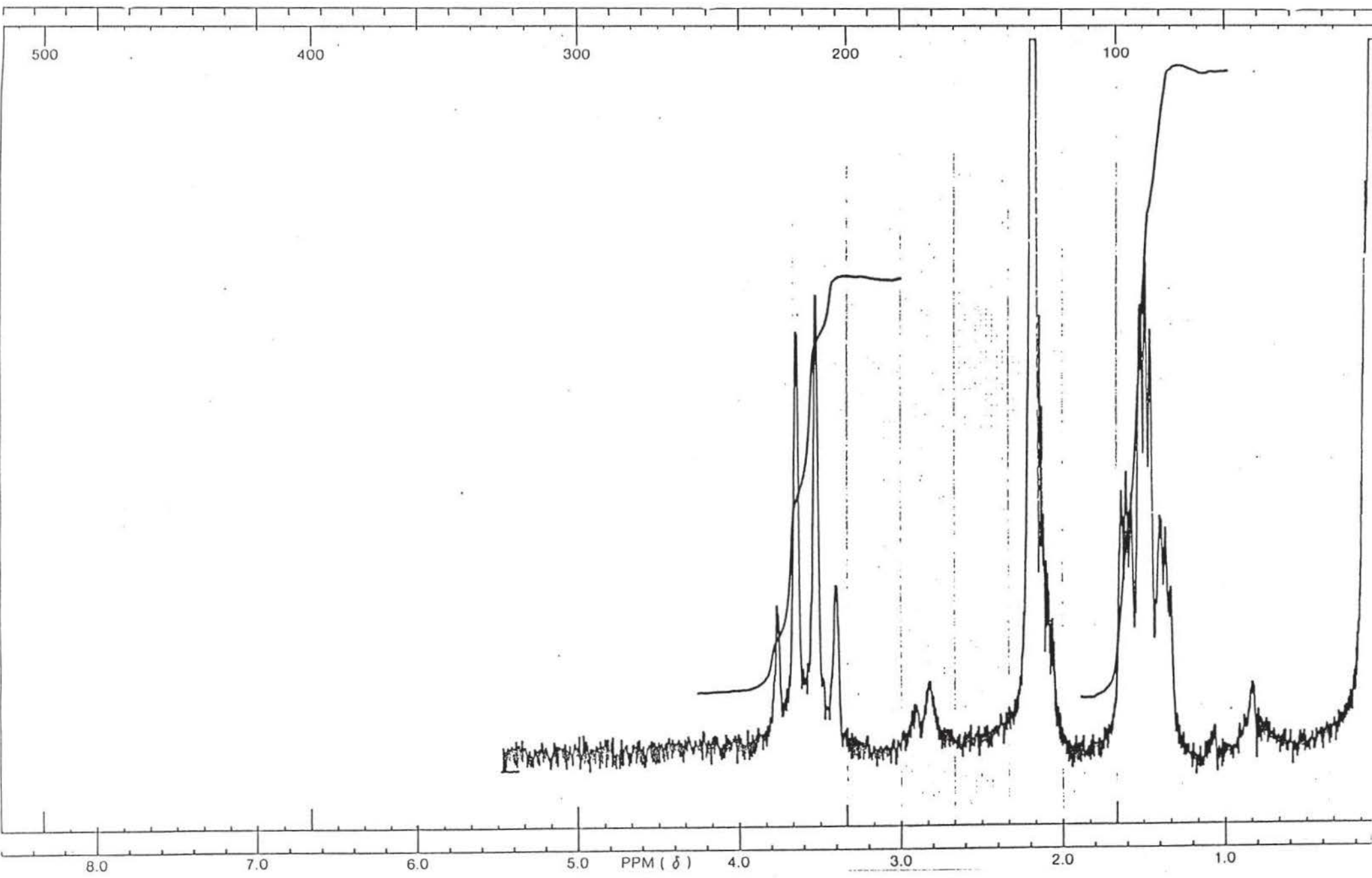
Fig. A13 NMR of (Et4N)(HW2(CO)10) (in deuterated acetone)

500   400   300   200   100   0

(Offset = -1000 Hz)

(Offset = -500 Hz)

8.0   7.0   6.0   5.0   PPM (δ)   4.0   3.0   2.0   1.0   0
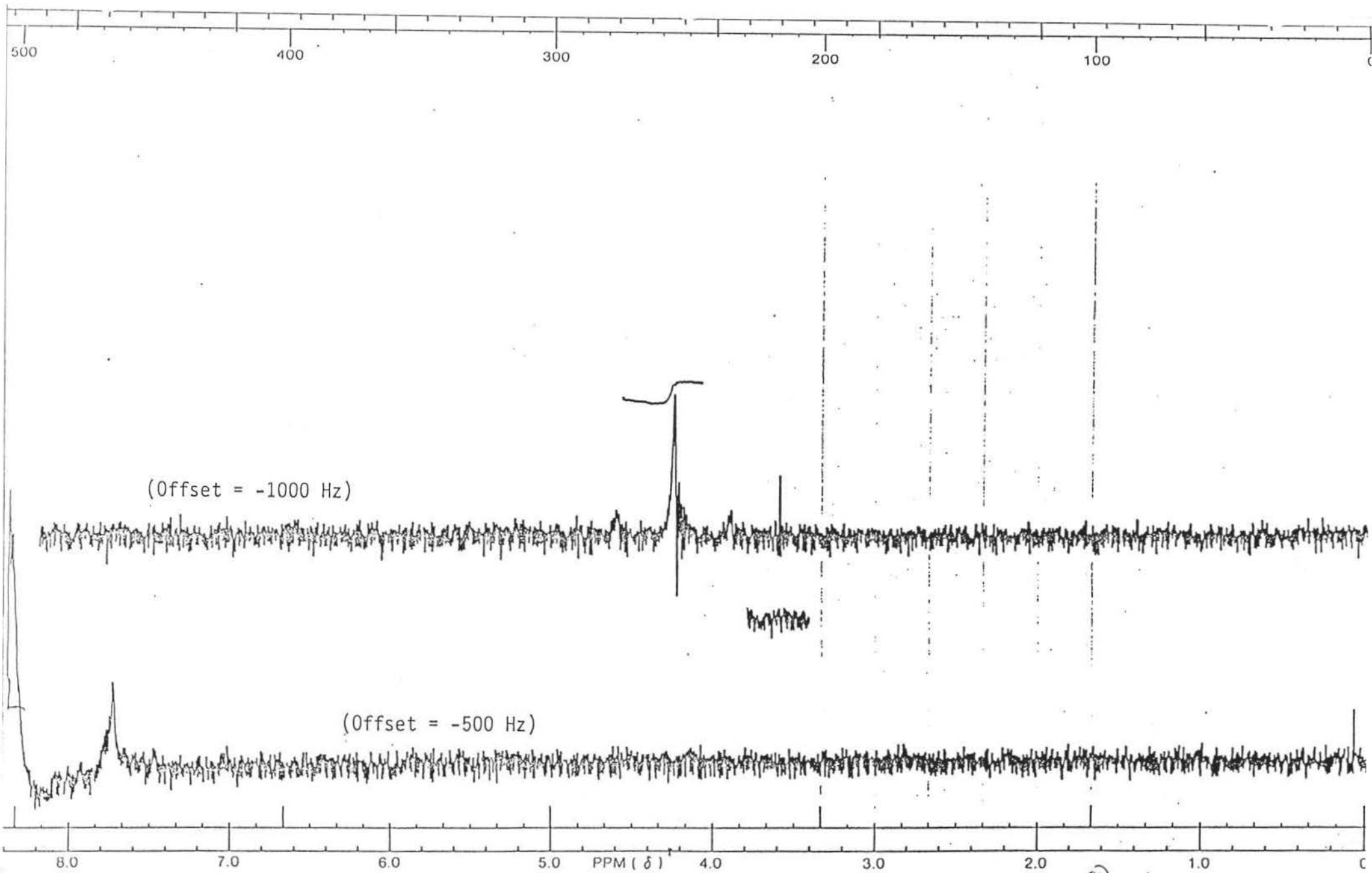
Fig. A13 NMR of (Et4N)(HW2(CO)10) (in deuterated acetone)
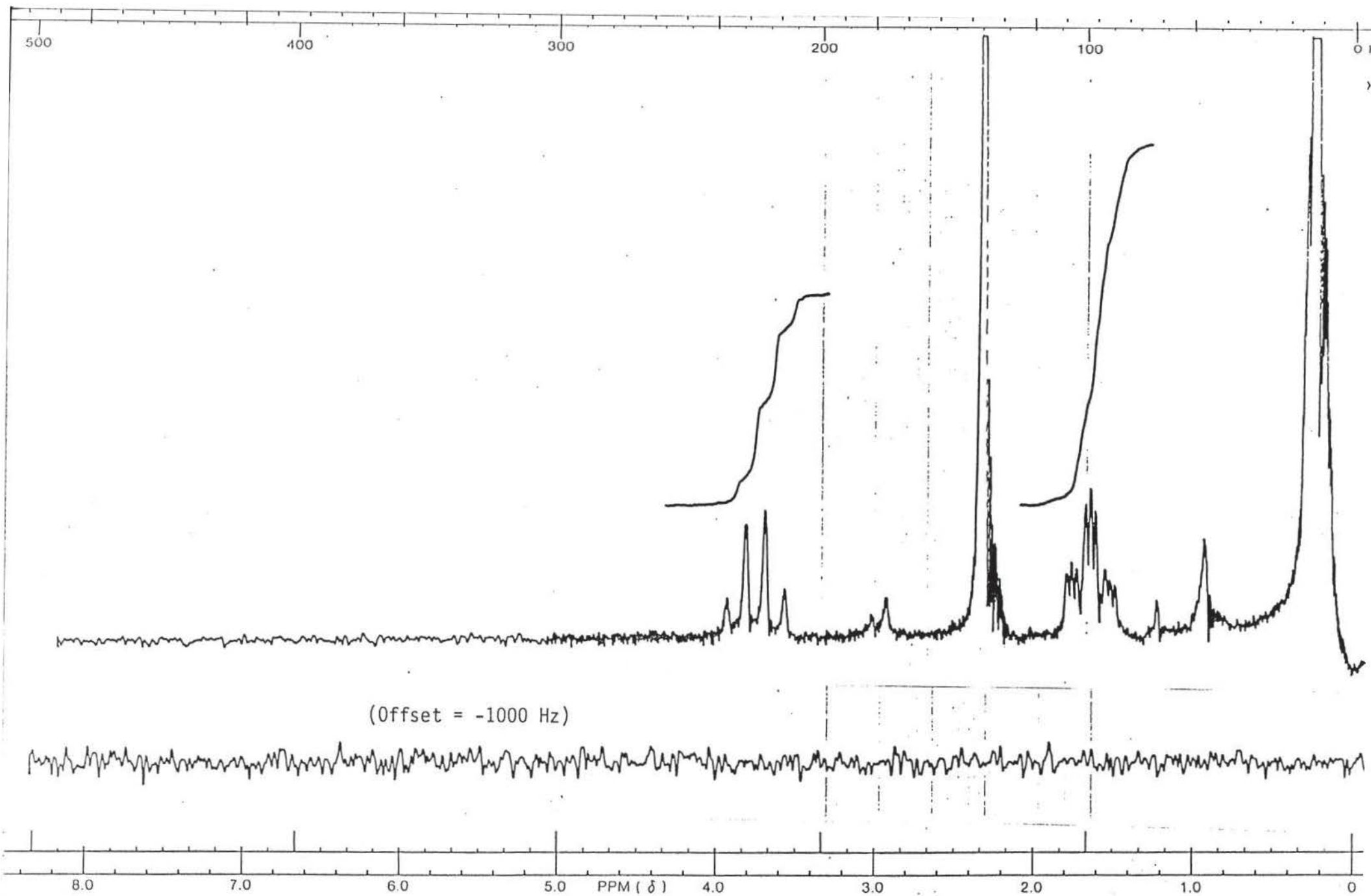
Fig. A14   NMR of (Et4N)(DW2(CO)10)   (in deuterated acetone)
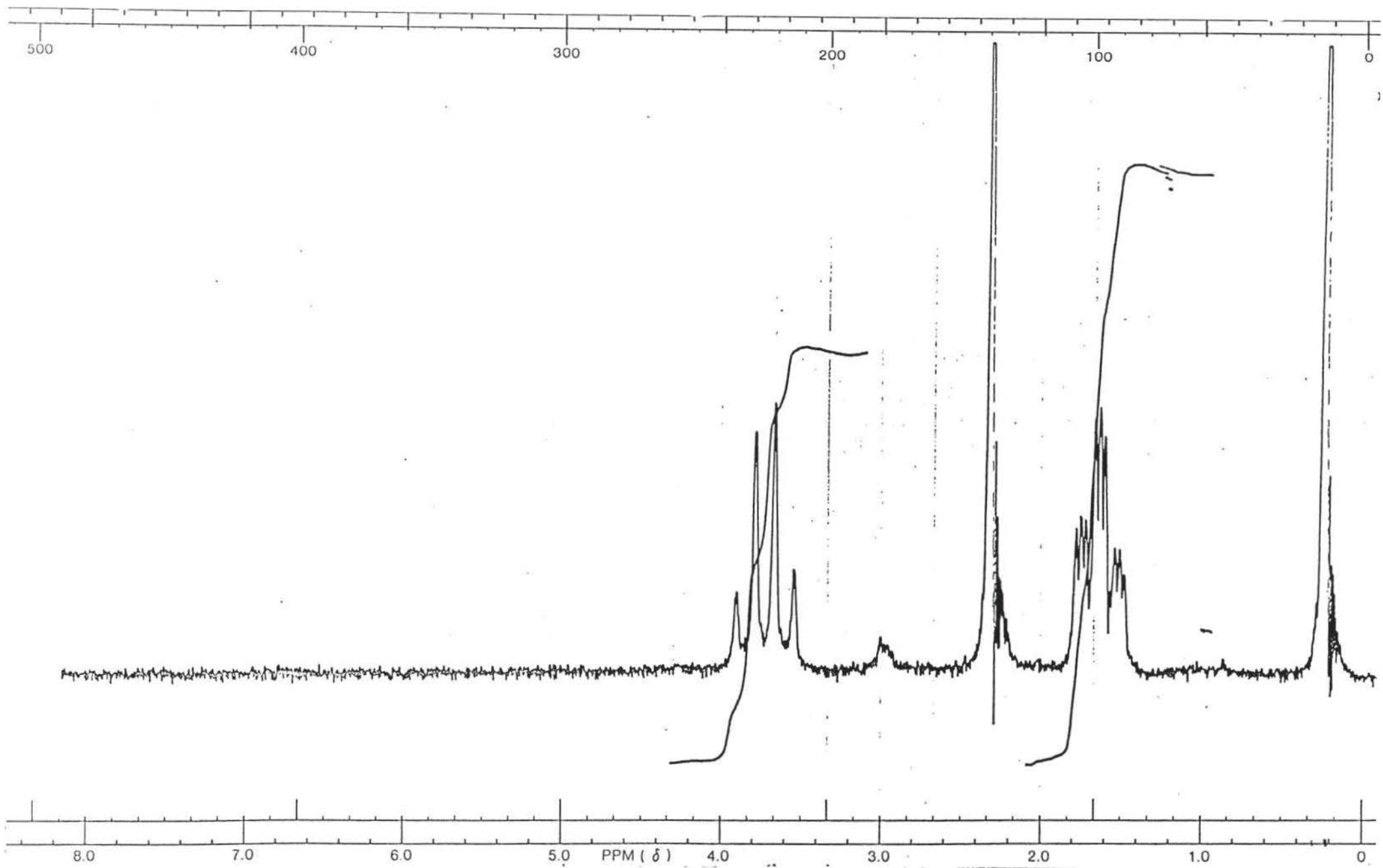
Fig. A15 NMR of (Et4N)(HCr2(CO)10) (in deuterated acetone)

500   400   300   200   100   0

(Offset = -1500 Hz)

(Offset = -1000 Hz)

(Offset = -500 Hz)

8.0   7.0   6.0   5.0   PPM (δ)   4.0   3.0   2.0   1.0   0
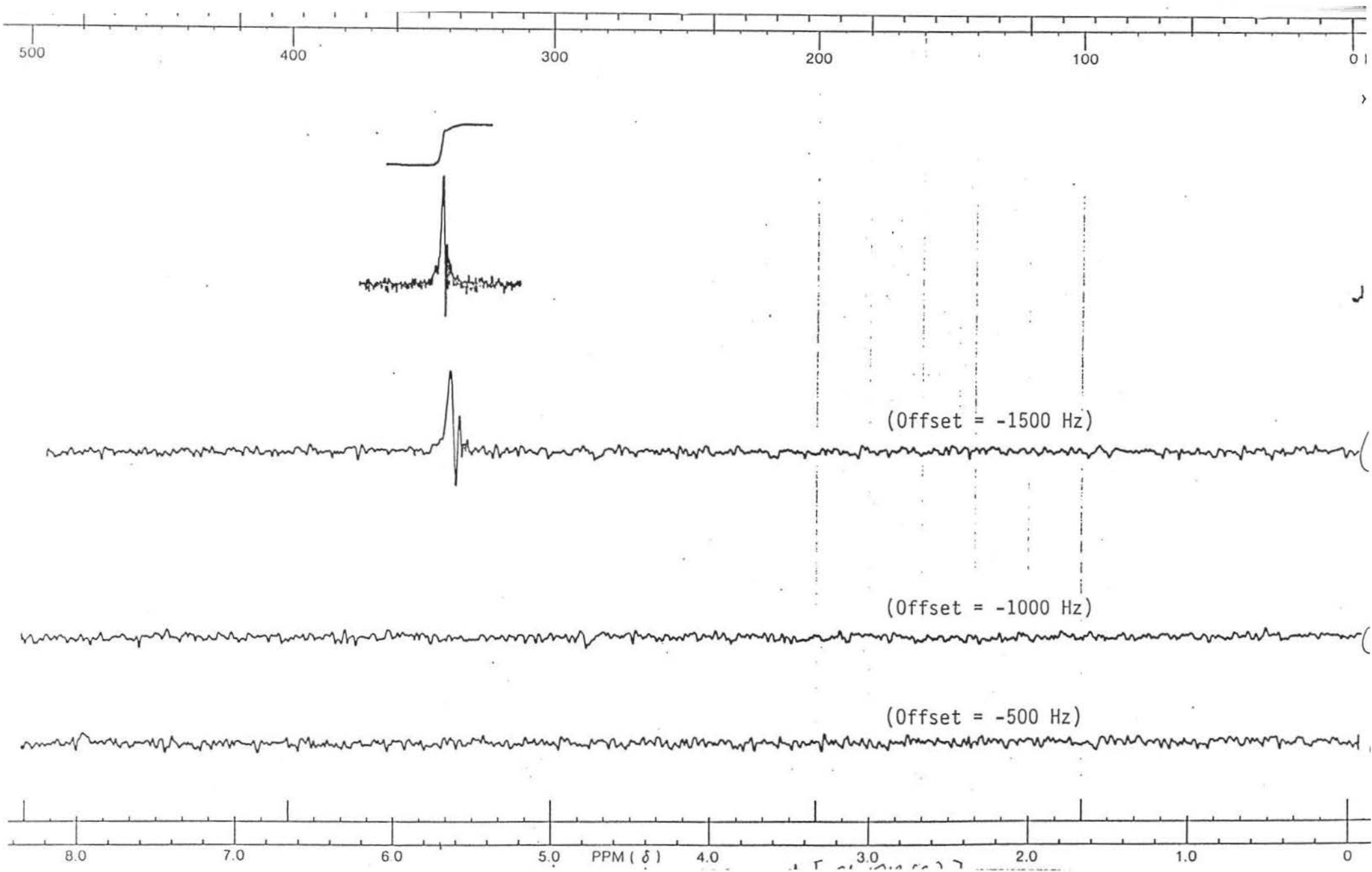
Fig. A15   NMR of (Et4N)(HCr2(CO)10)   (in deuterated acetone)
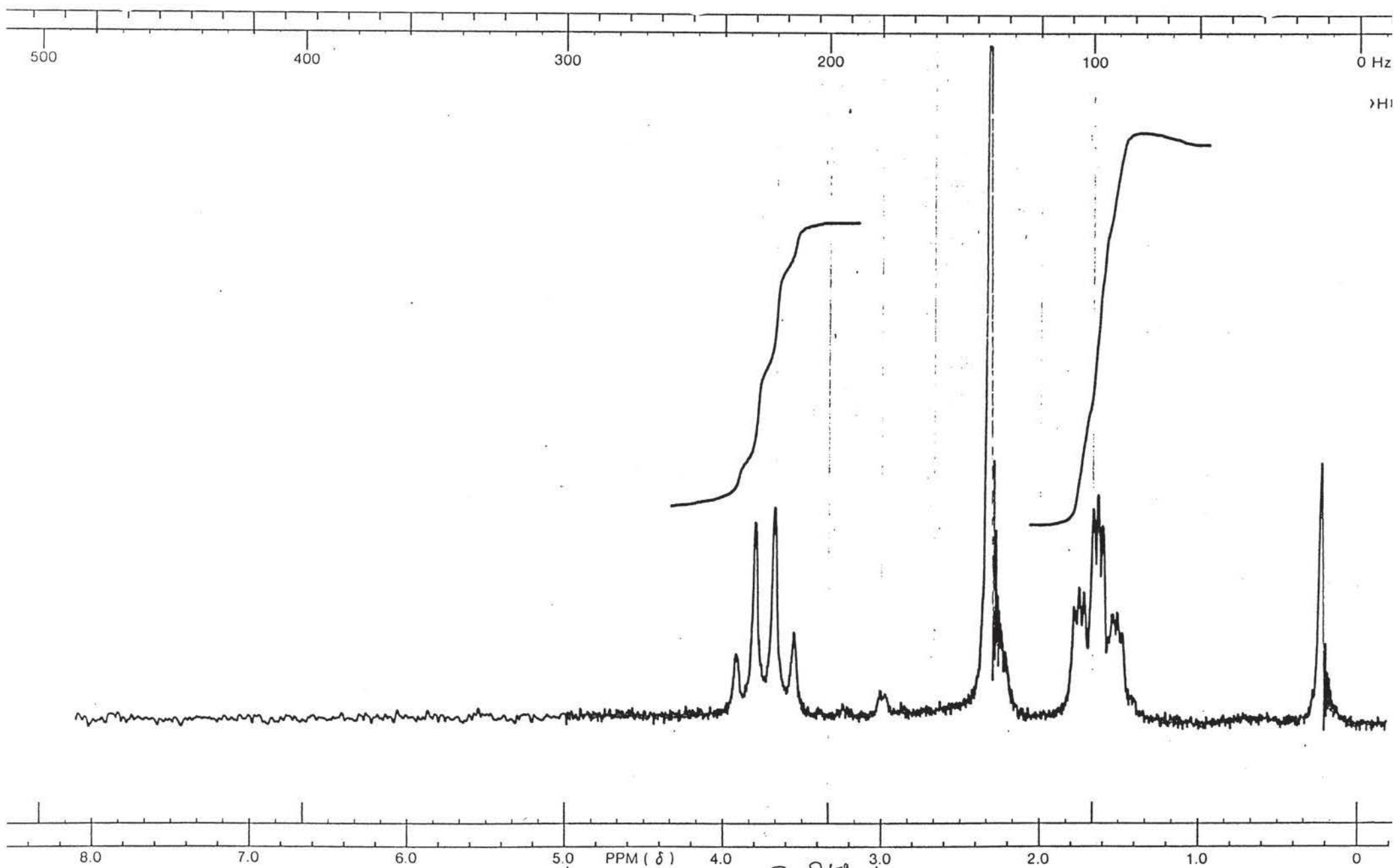
Fig. A16   NMR of (Et4N)(DCr2(CO)10)   (in deuterated acetone)
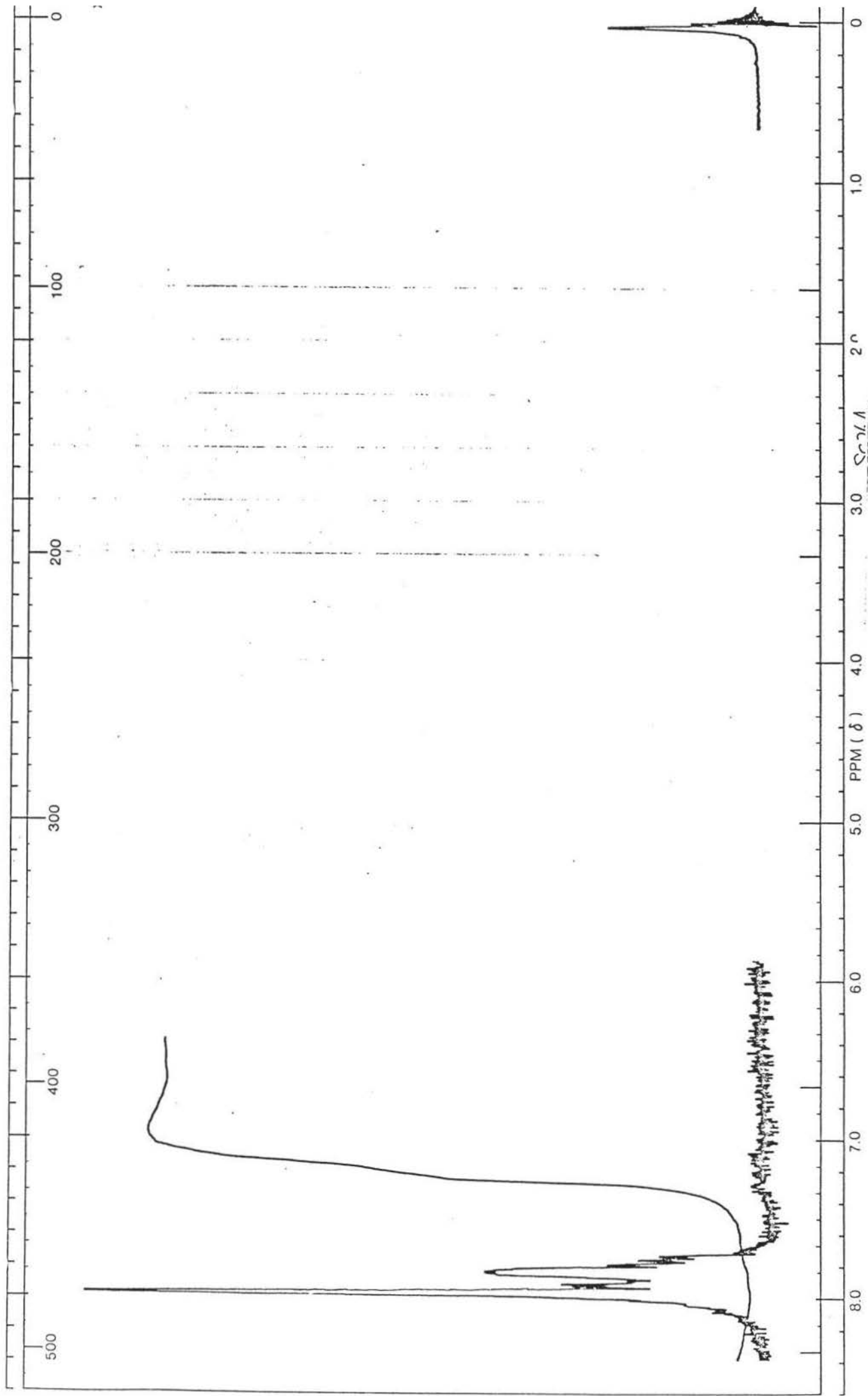
Fig. A17 NMR of (Ph4P)(HW2(CO)10) (in acetone)
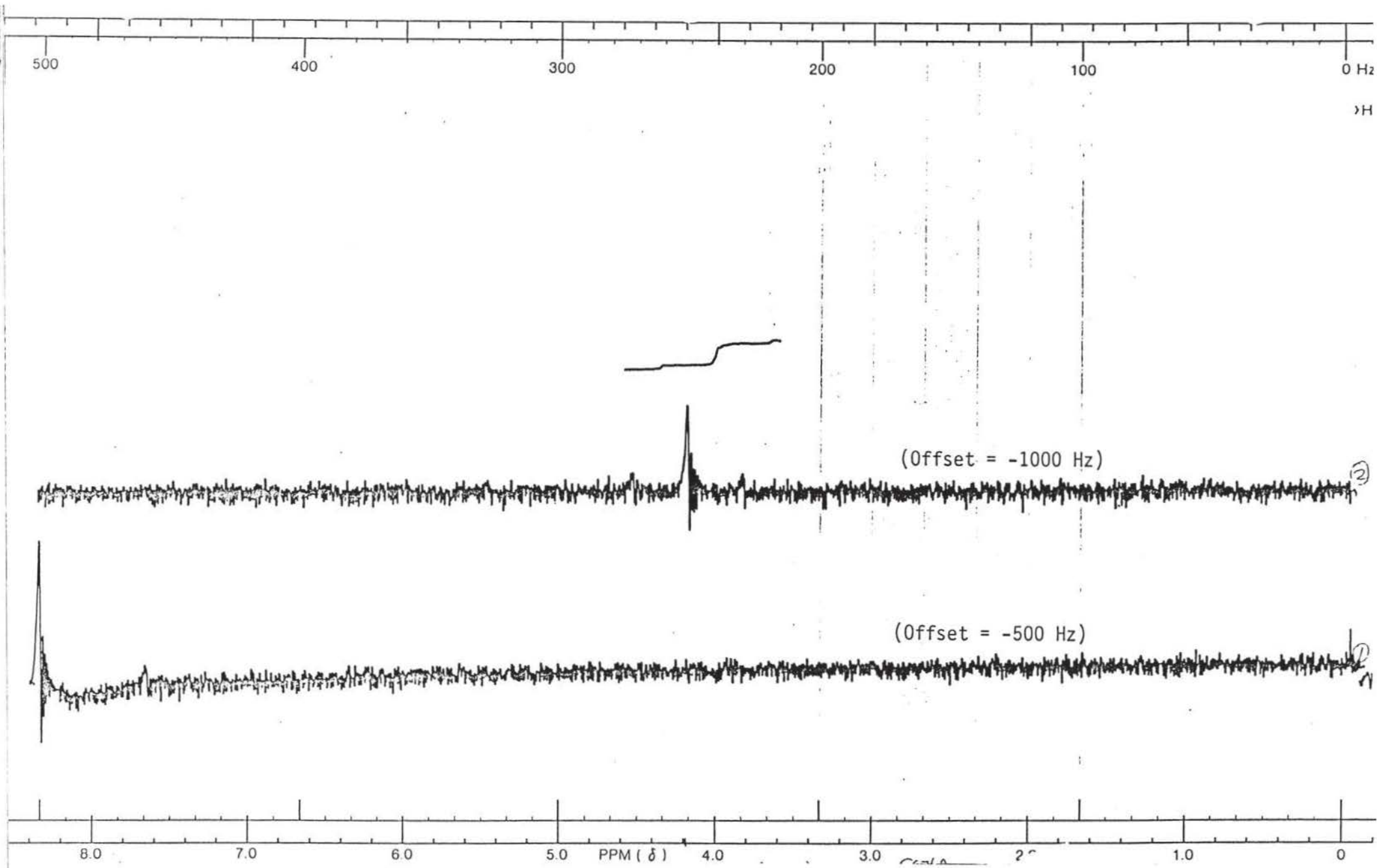
Fig. A17 NMR of (Ph4P)(HW2(CO)10) (in acetone)
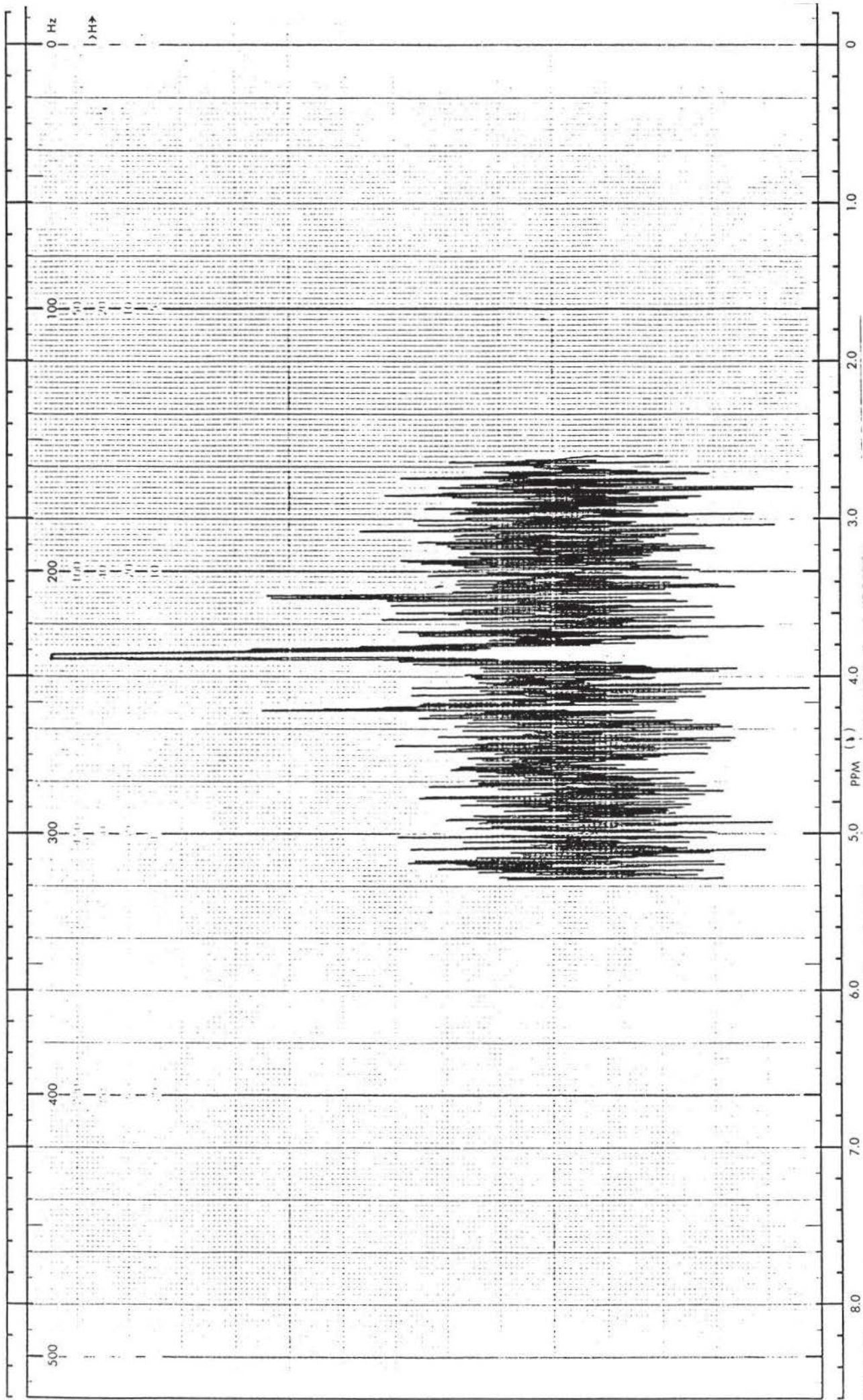
Fig. A17 ^{1}H NMR of $(Ph_4P)(HW_2(CO)_{10})$ (in acetone) $(J_{W-H} = 43\ Hz)$
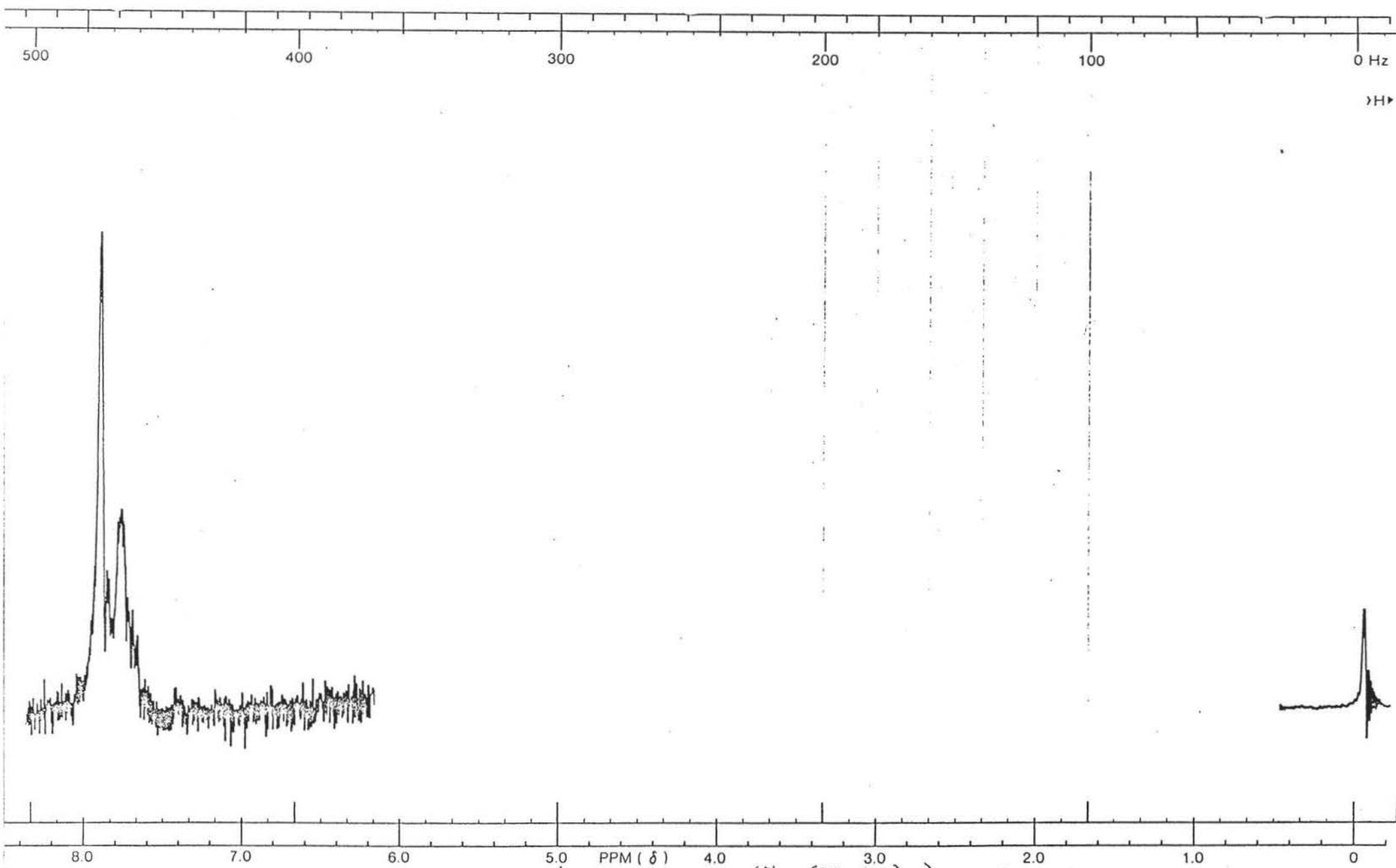
Fig. A18 NMR of (Ph4P)(DW2(CO)10) (in acetone)
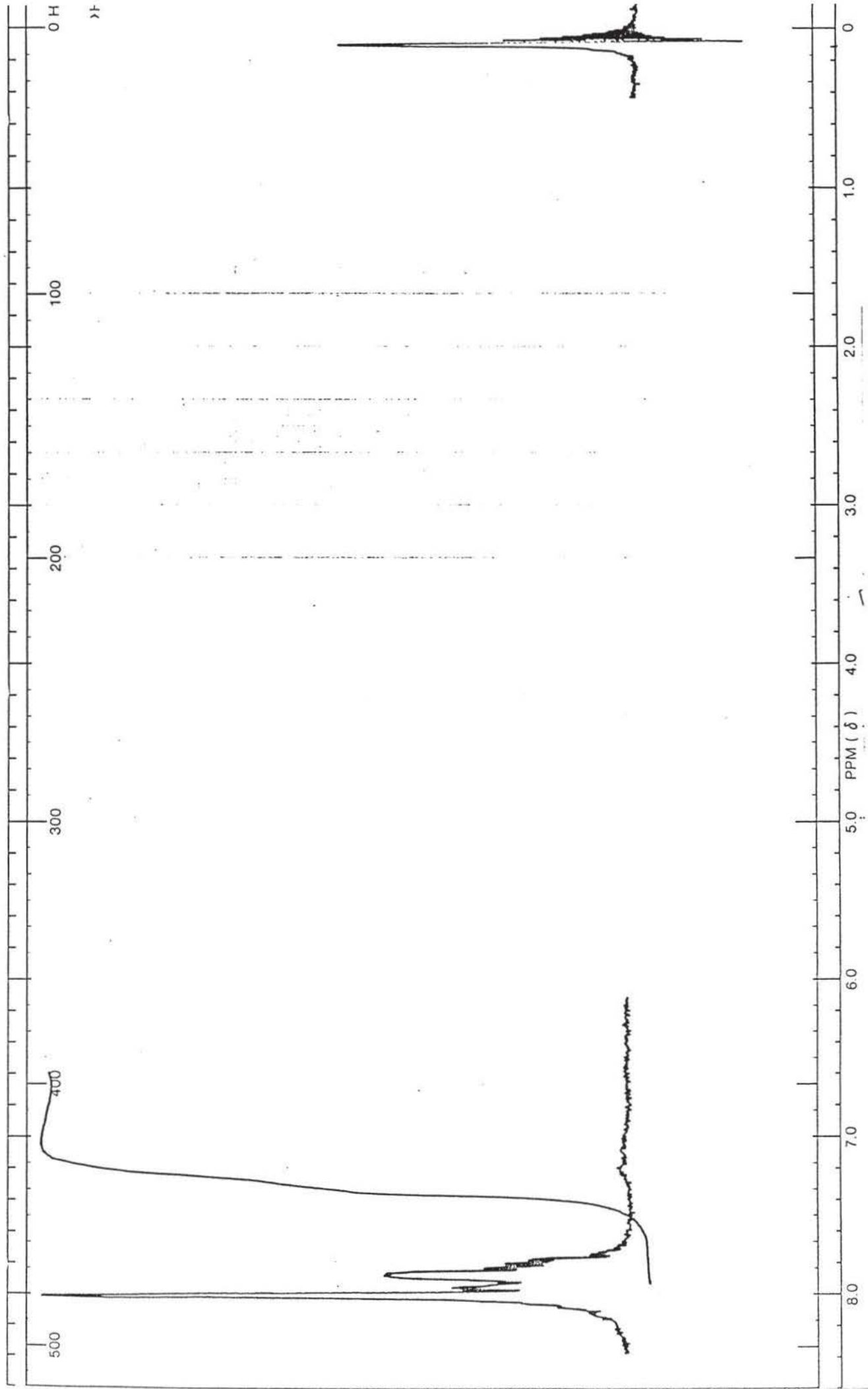
Fig. A19 NMR of (Ph4P)(HCr2(CO)10) (in acetone)
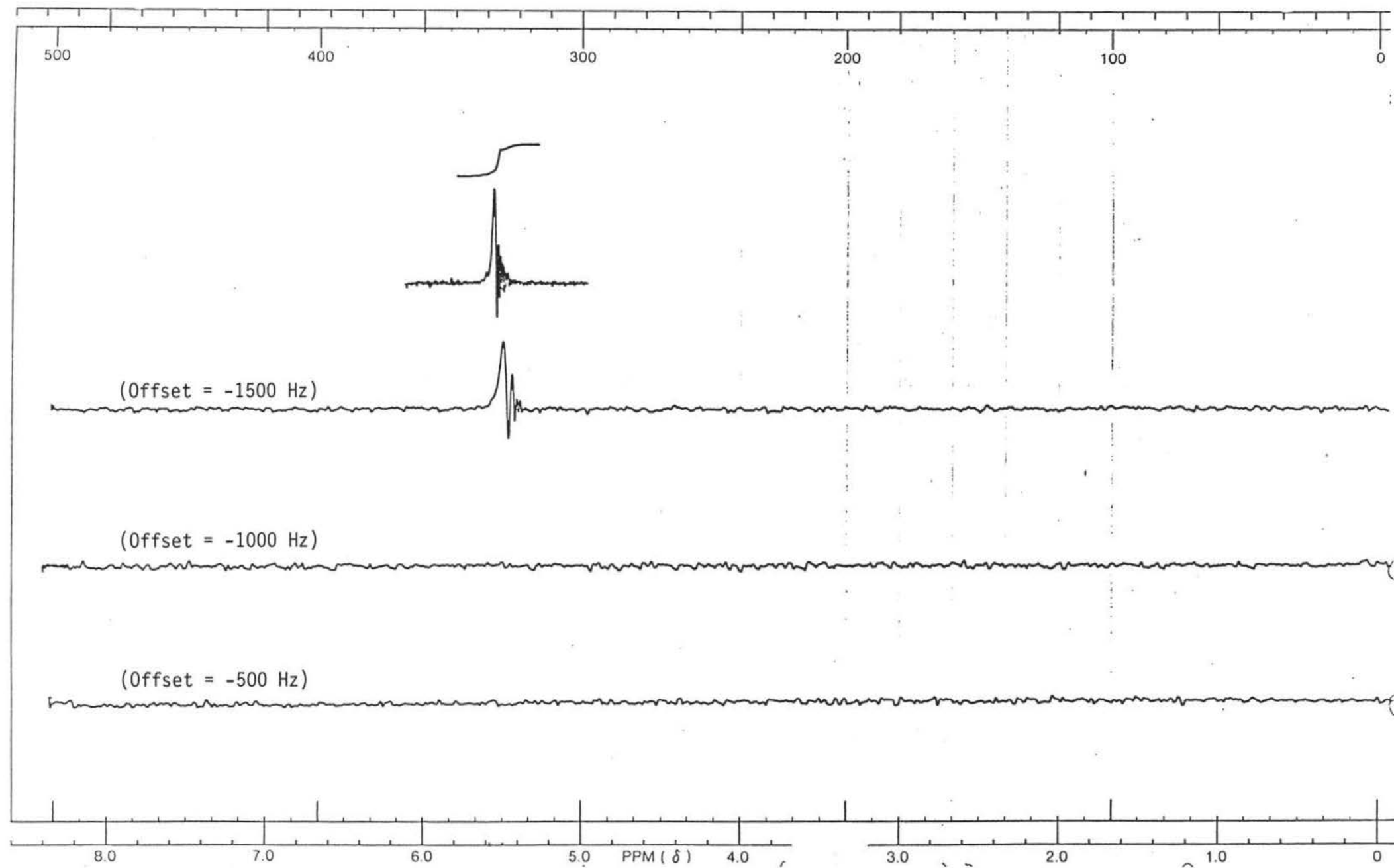
Fig. A19 NMR of (Ph4P)(HCr2(CO)10) (in acetone)
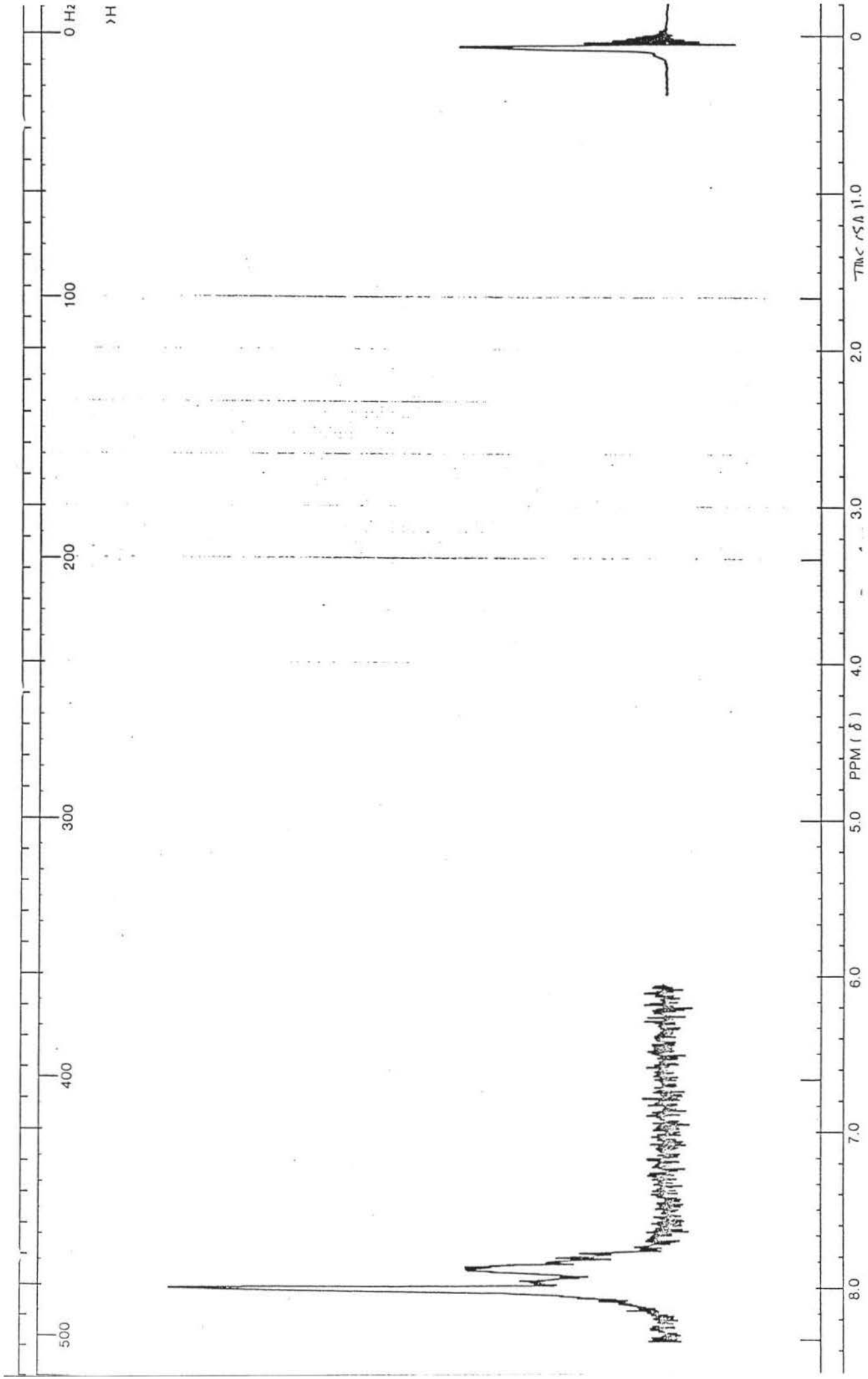
Fig. A20 NMR of (Ph4P)(DCr2(CO)10) (in acetone)
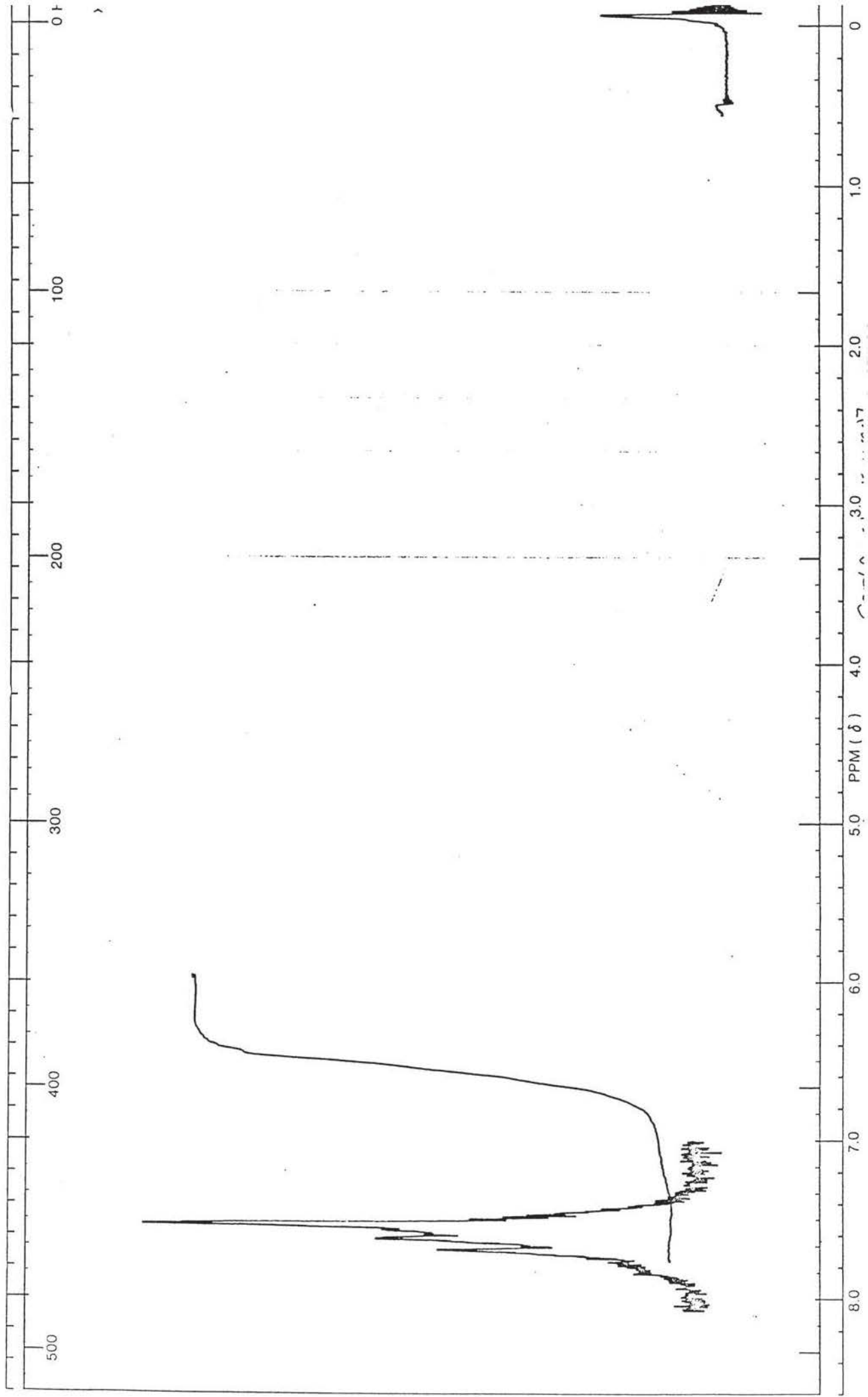
Fig. A21 NMR of (PPN)(HW2(CO)10) (in acetone)

500   400   300   200   100   0 H

(Offset = -1000 Hz)

(Offset = -500 Hz)

8.0   7.0   6.0   5.0   PPM (δ)   4.0   3.0   2.0   1.0   0
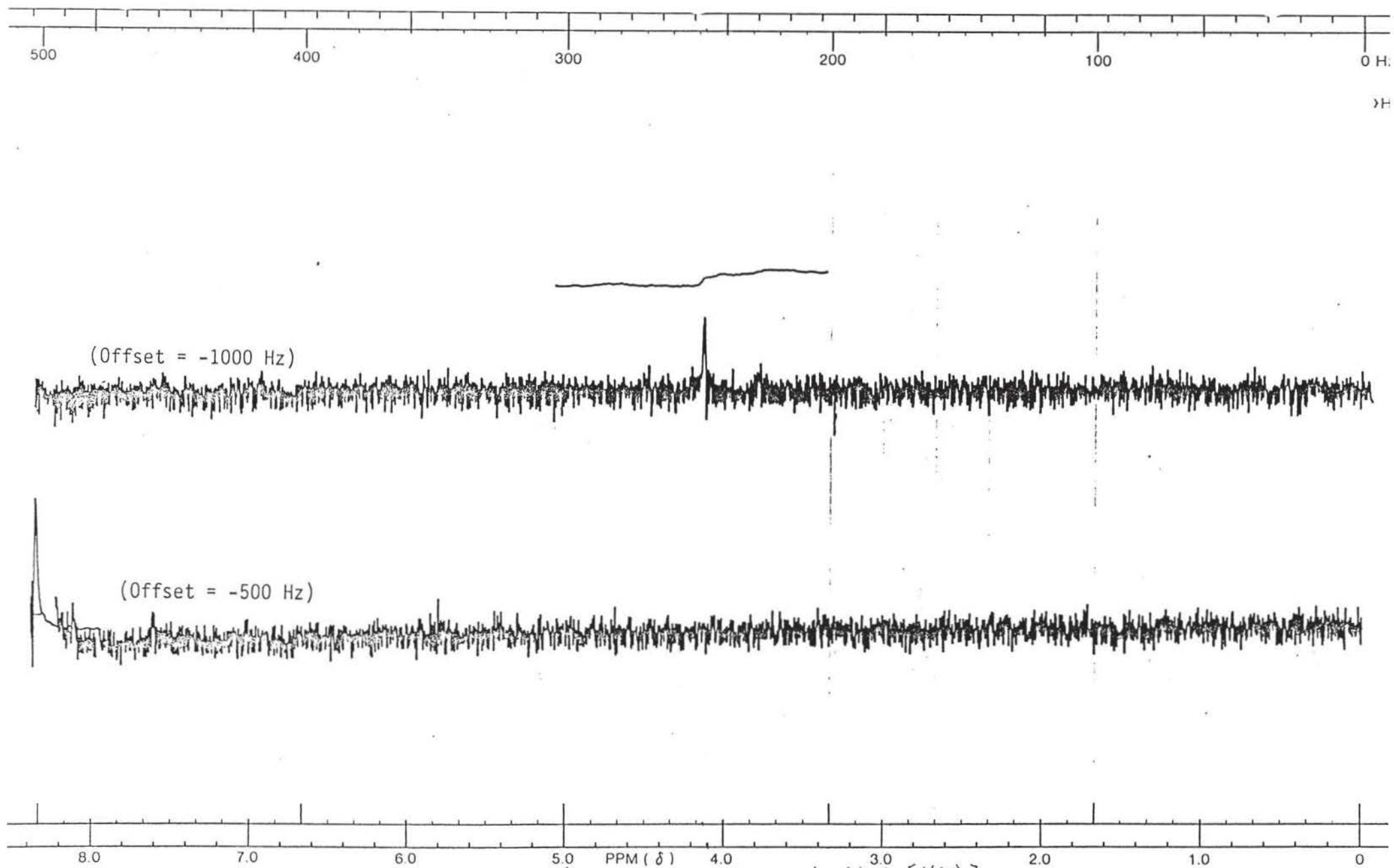
Fig. A21   NMR of (PPN)(HW2(CO)10)   (in acetone)
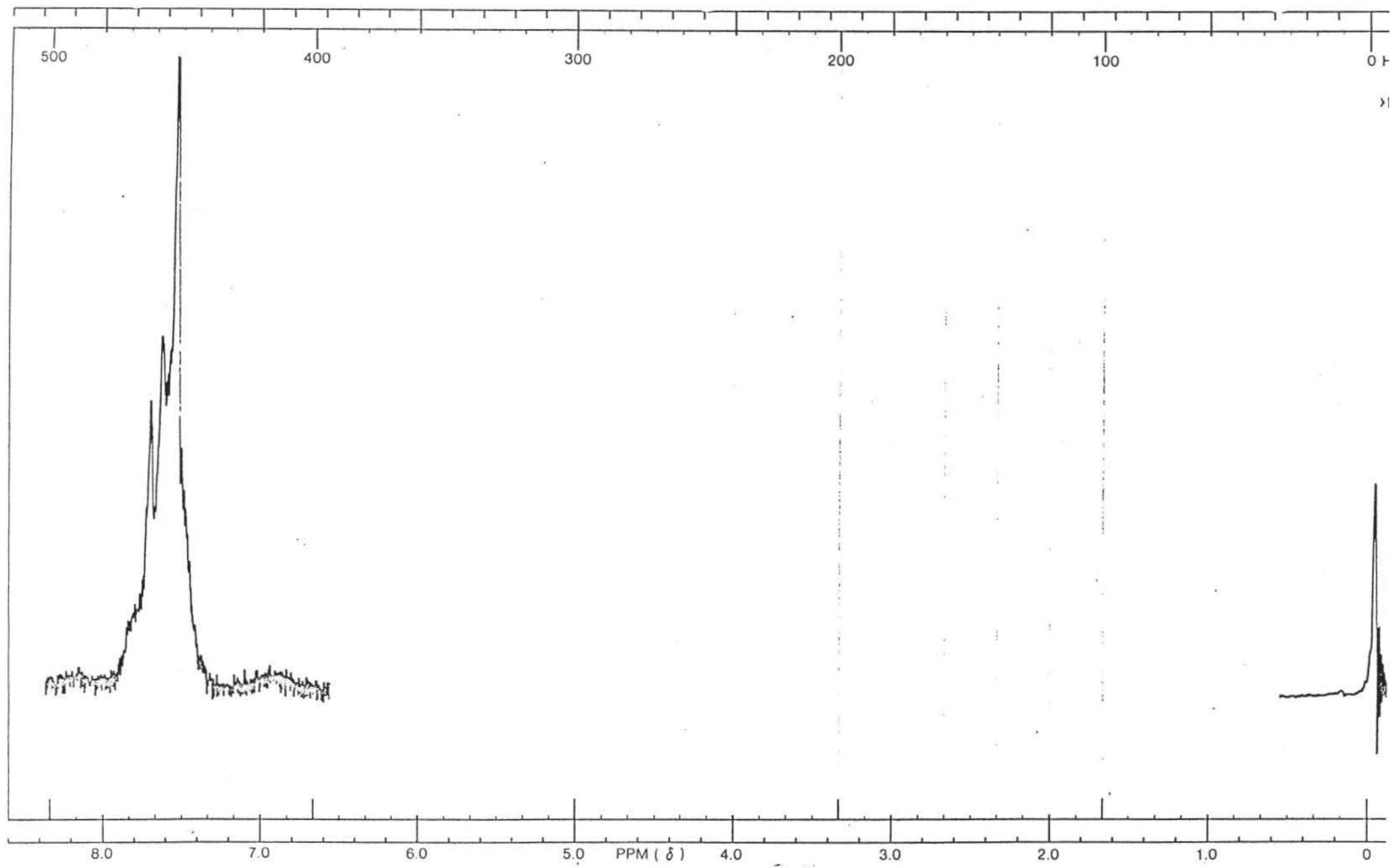
Fig. A22 NMR of (PPN)(DW2(CO)10) (in acetone)
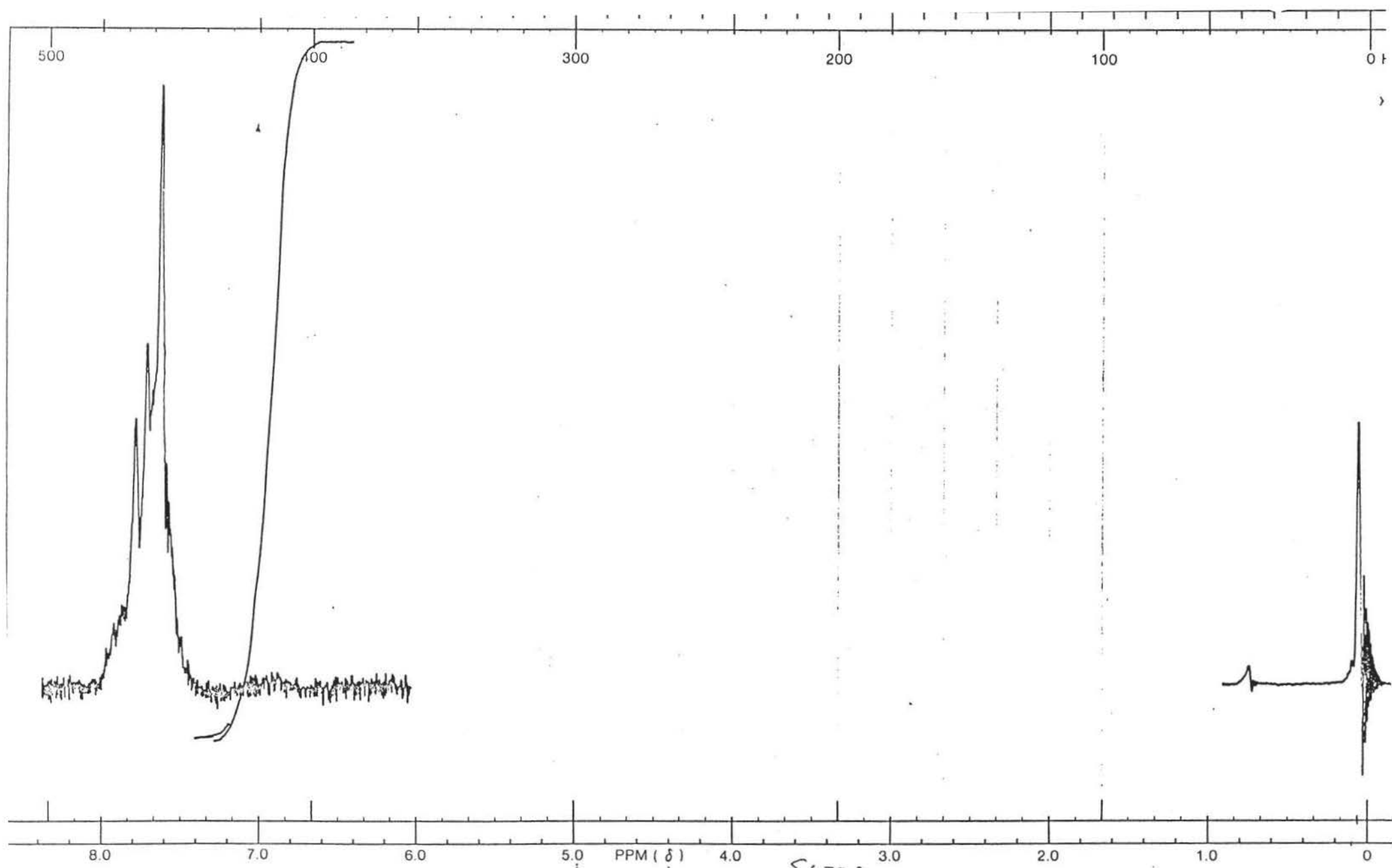
Fig. A23   NMR of (PPN)(HCr2(CO)10)   (in acetone)

500   400   300   200   100   0 Hz

›H

(Offset = - 1500 Hz)

(Offset = -1000 Hz)

(Offset = -500 Hz)

8.0   7.0   6.0   5.0   PPM (δ)   4.0   3.0   2.0   1.0   0
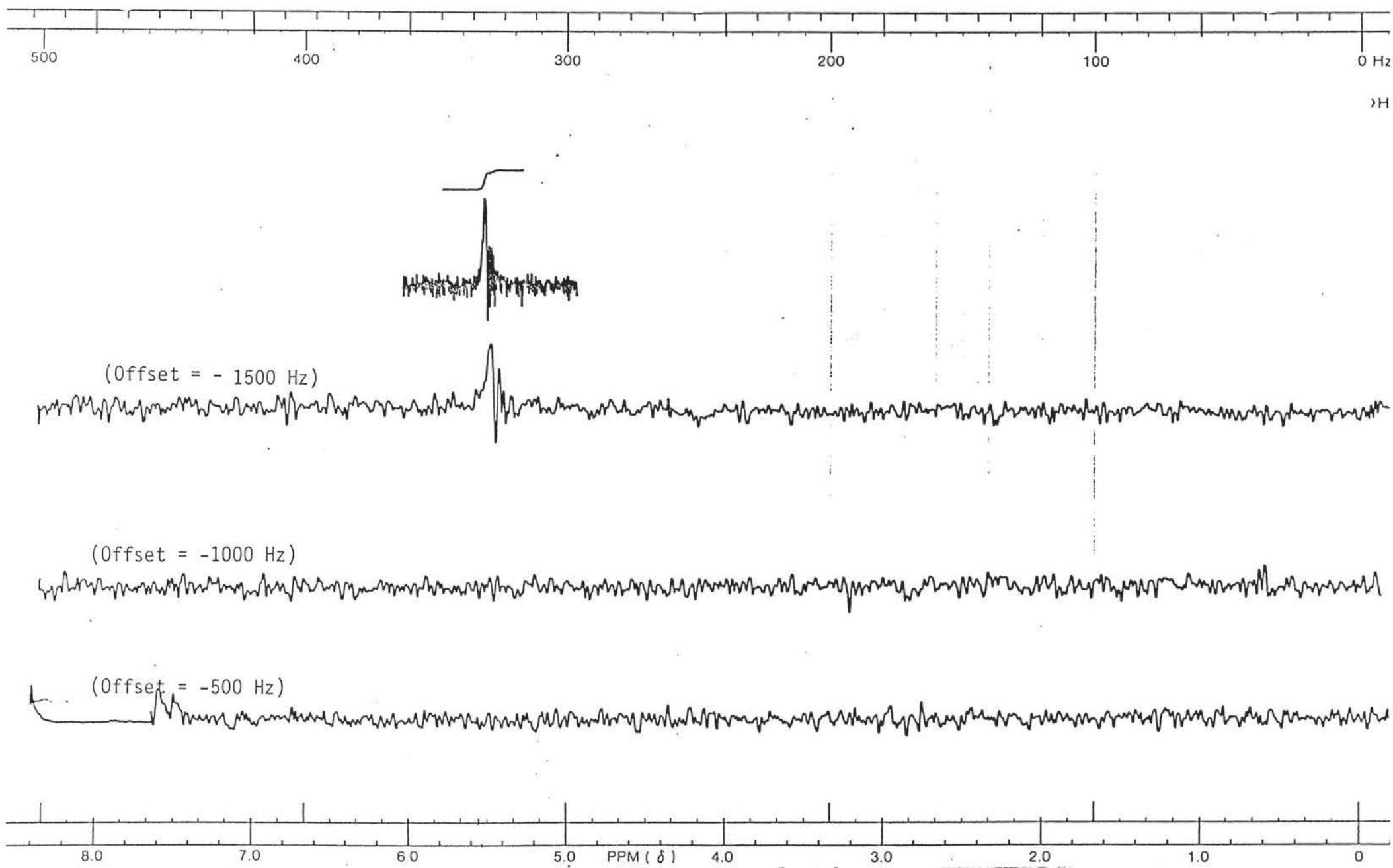
Fig. A23 NMR of (PPN)(HCr2(CO)10) (in acetone)
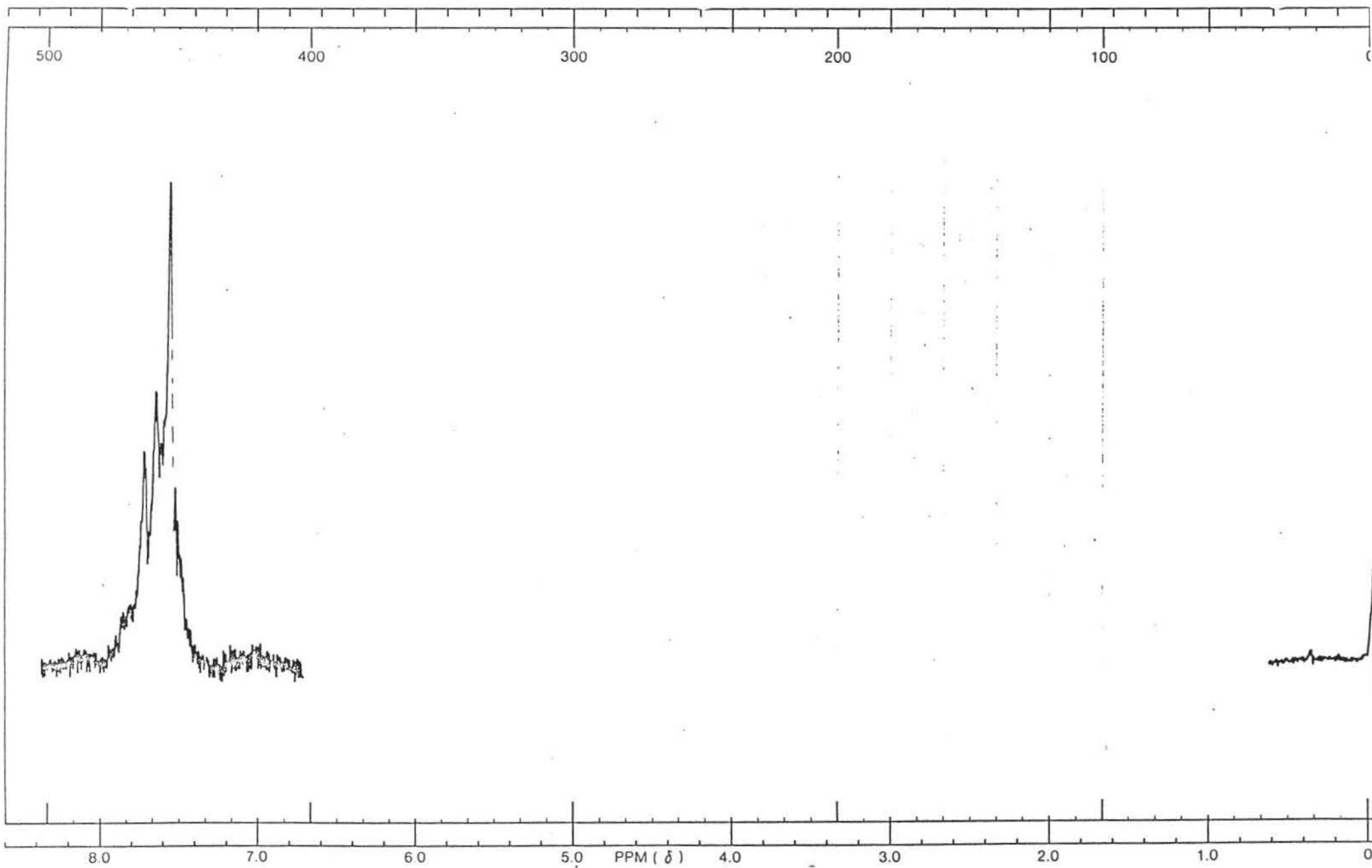
Fig. A24   NMR of (PPN)(DCr2(CO)10)   (in acetone)
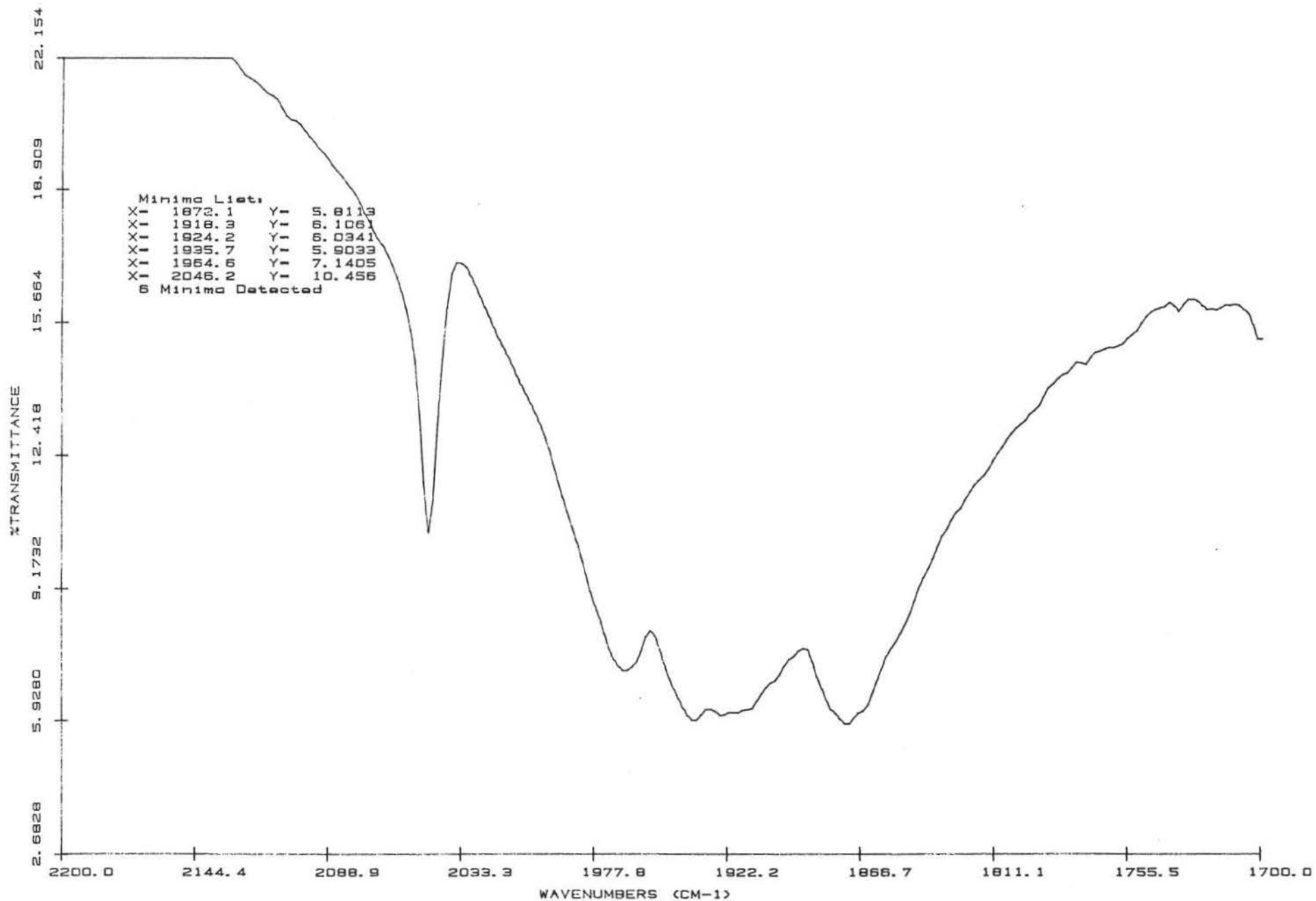
Fig. A25   Solid IR of (Et4N)(HW2(CO)10)
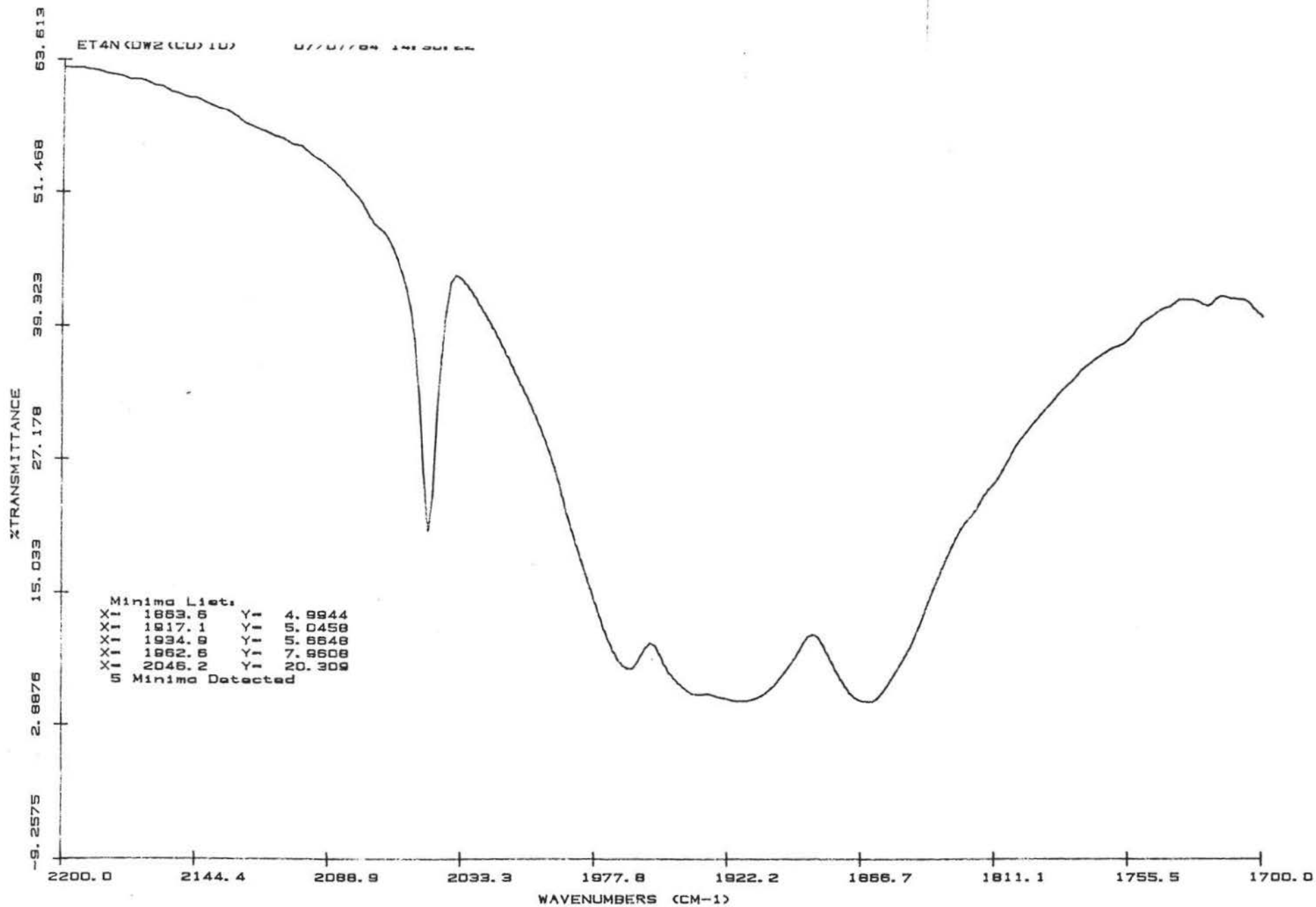
Fig. A26   Solid IR of $(Et_4N)(DW_2(CO)_{10})$
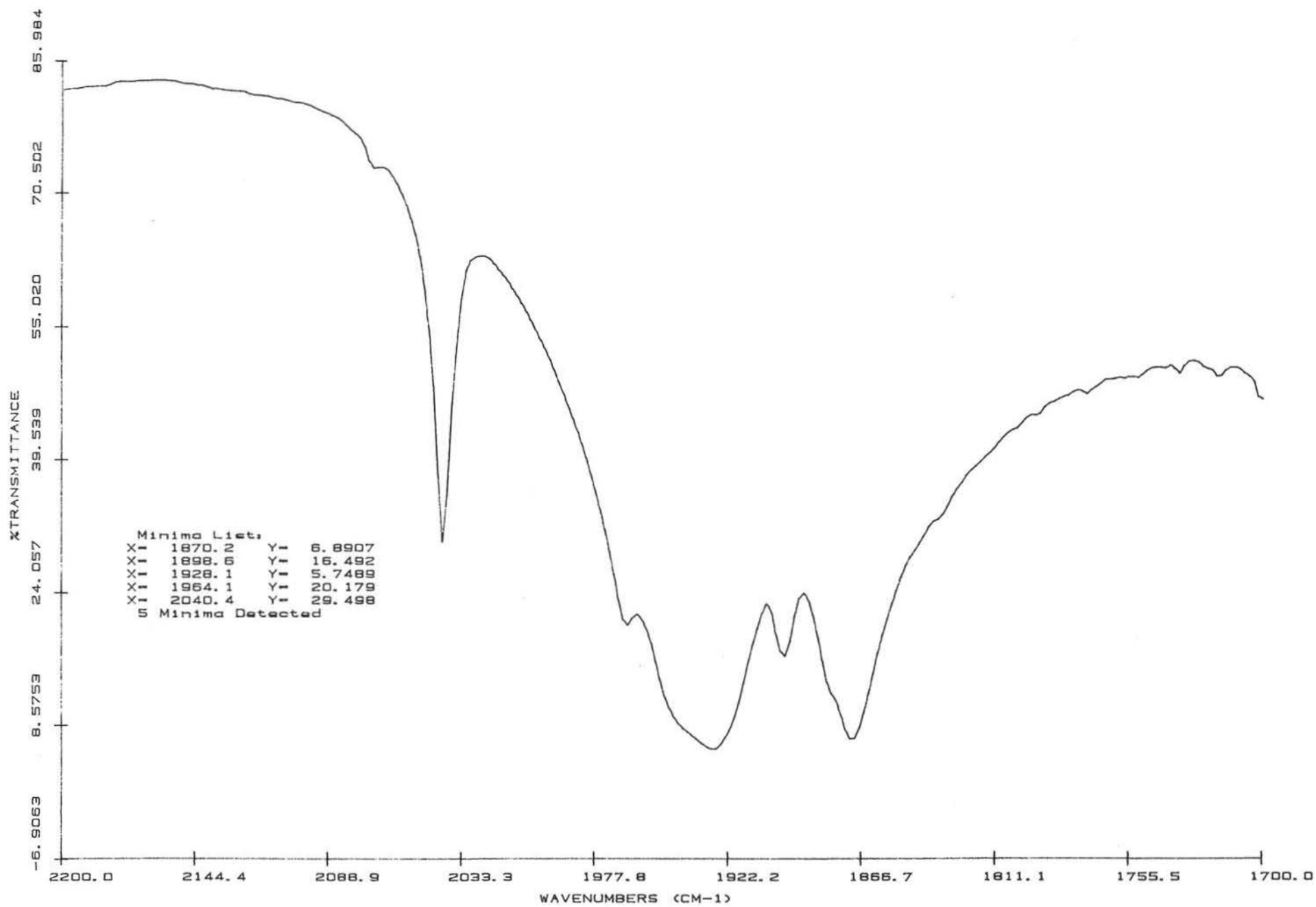
Fig. A27   Solid IR of (PPN)(HW2(CO)10)
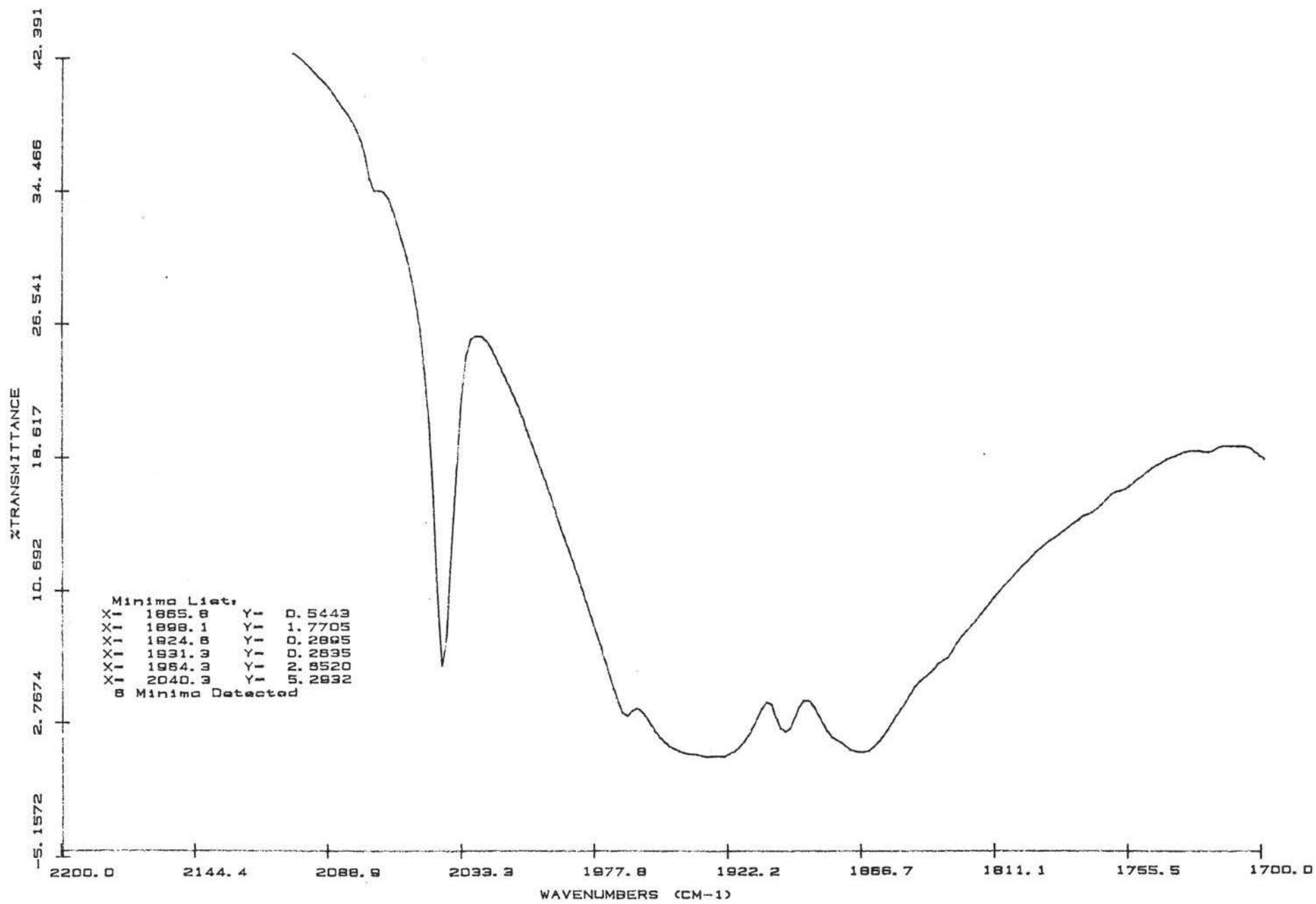
Fig. A28   Solid IR of (PPN)(DW2(CO)10)
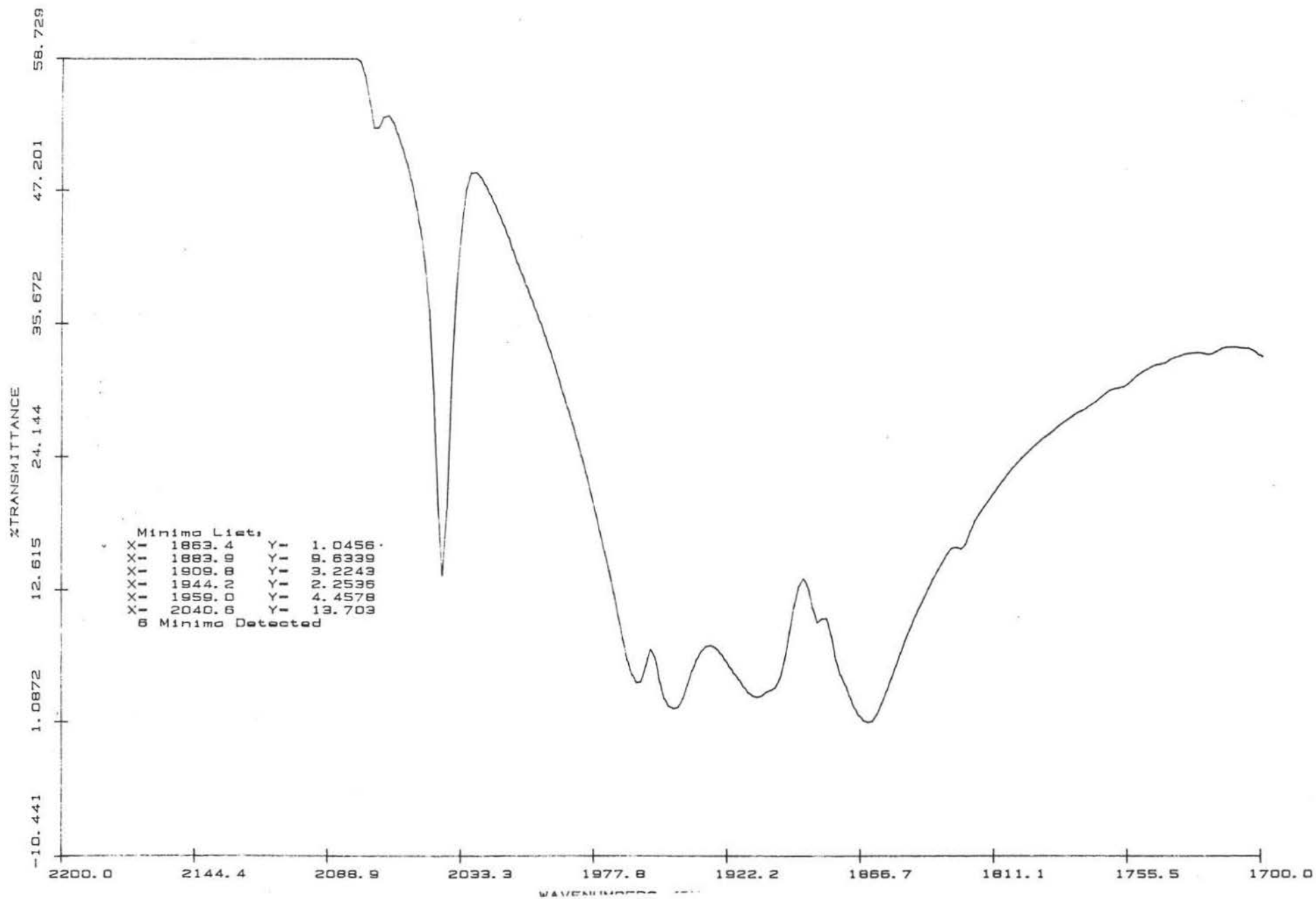
Fig. A29   Solid IR of (Ph4P)(HW2(CO)10)
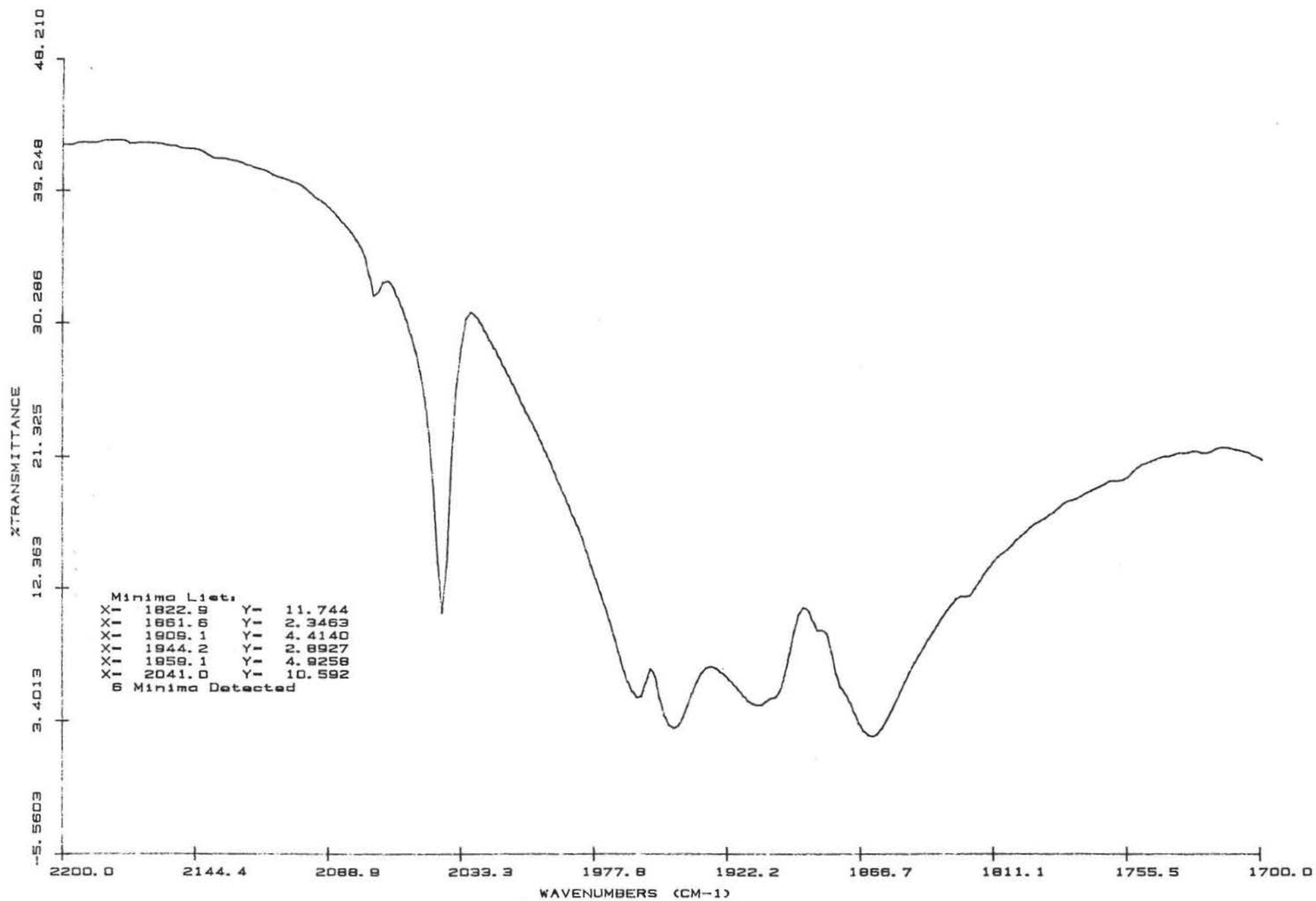
Fig. A30   Solid IR of (Ph4P)(DW2(CO)10)

Minima List:
X= 1822.9   Y= 11.744
X= 1861.6   Y= 2.3463
X= 1909.1   Y= 4.4140
X= 1944.2   Y= 2.8927
X= 1959.1   Y= 4.9258
X= 2041.0   Y= 10.592
6 Minima Detected

Minima List:
X=   1868.6   Y=   3.4925
X=   1927.1   Y=   3.1723
X=   1933.8   Y=   3.0412
X=   1968.0   Y=   3.7351
X=   2037.8   Y=   6.1214
 5 Minima Detected

%TRANSMITTANCE

WAVENUMBERS (CM-1)
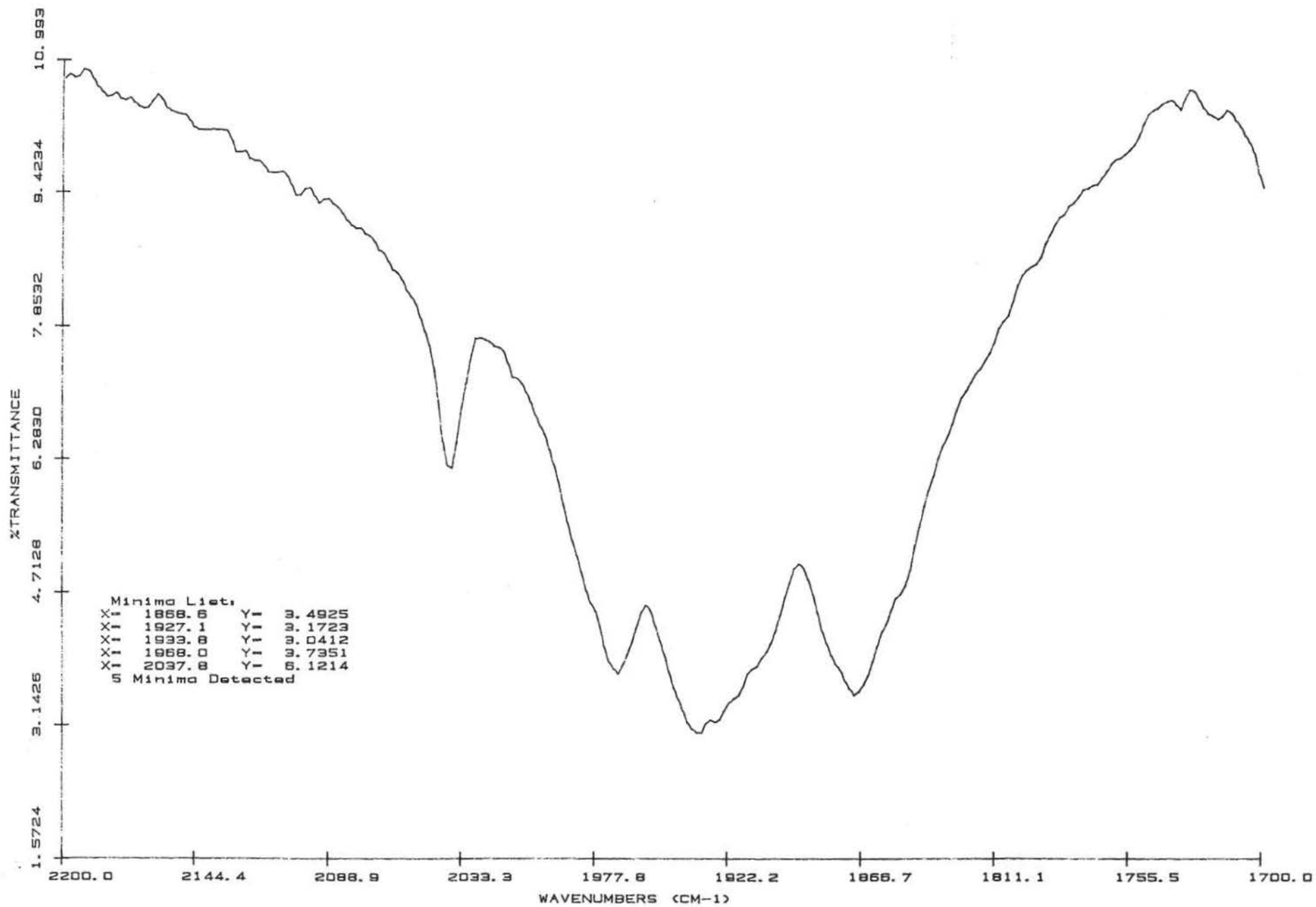
Fig. A31   Solid IR of (Et4N)(HCr2(CO)10)
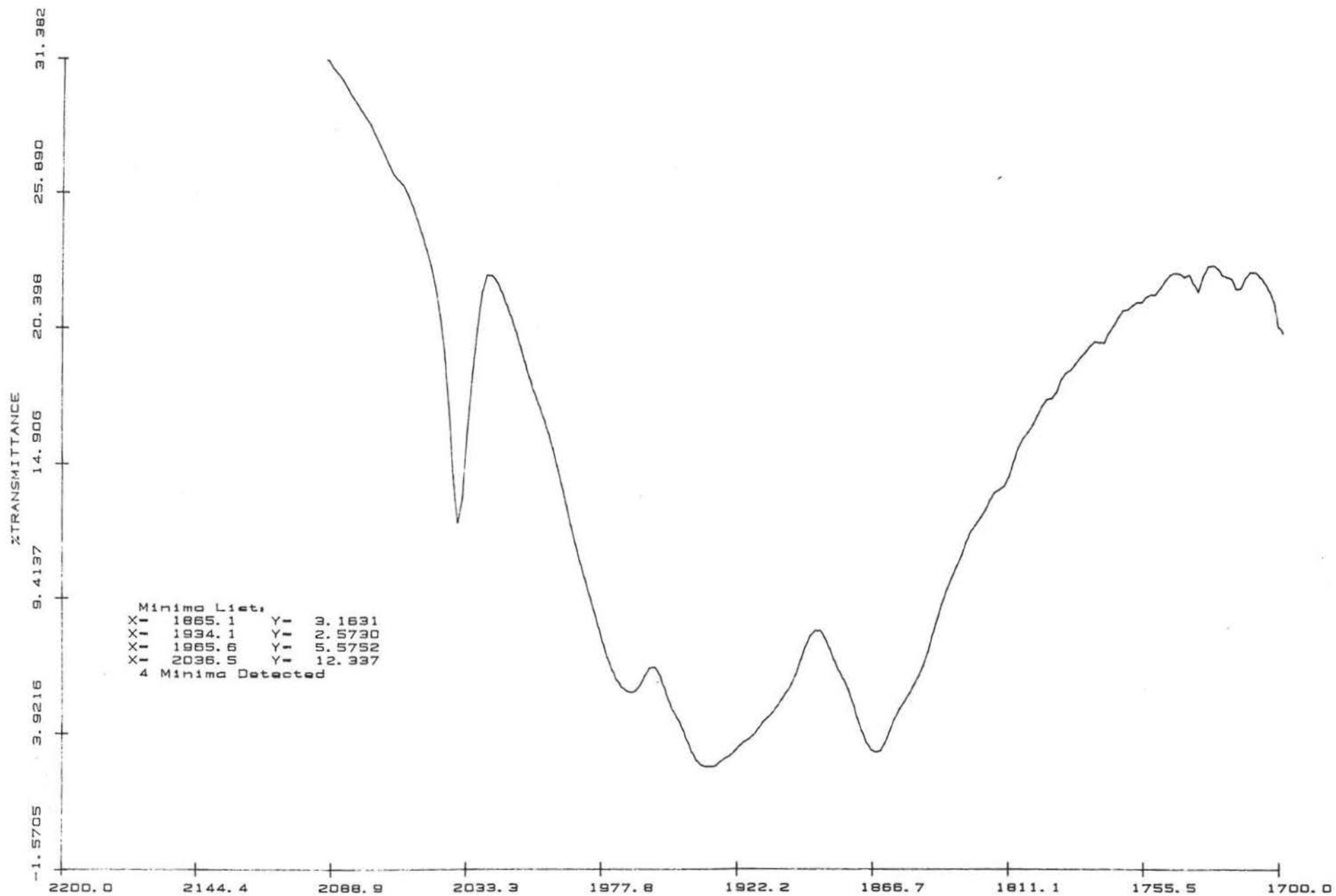
Fig. A32   Solid IR of (Et4N)(DCr2(CO)10)
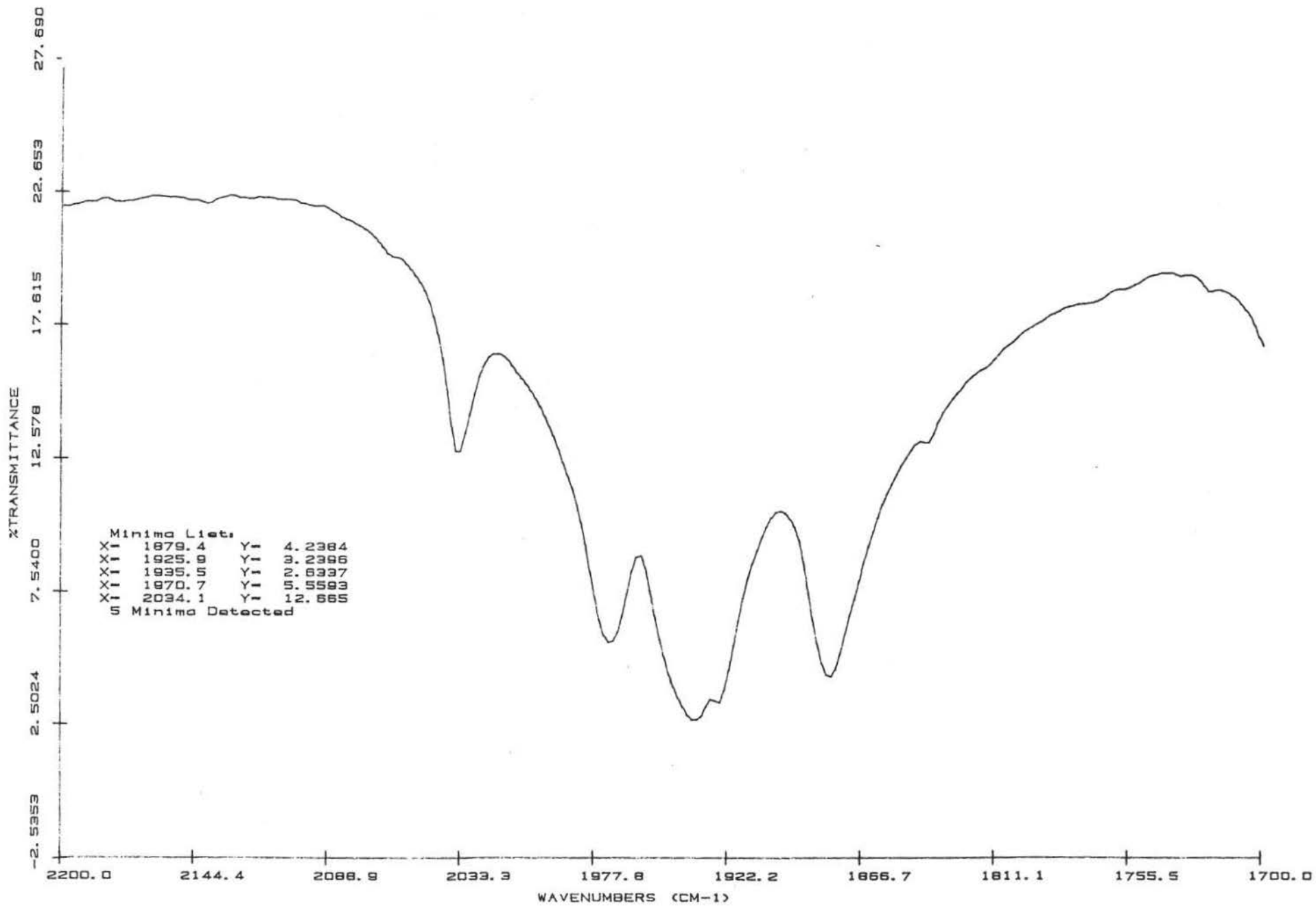
Fig. A33   Solid IR of (PPN)(HCr2(CO)10)
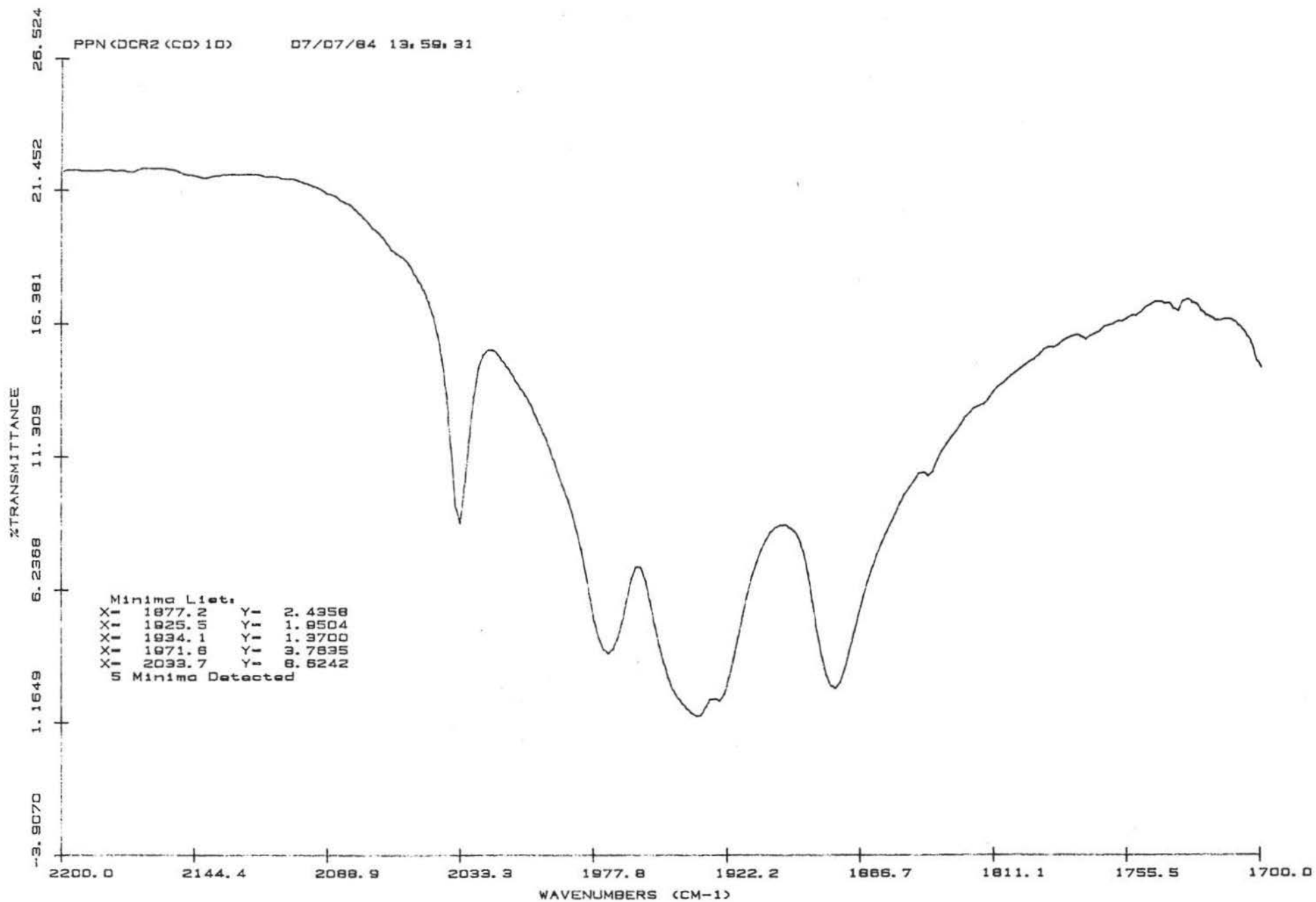
Fig. A34   Solid IR of (PPN)(DCr2(CO)10)
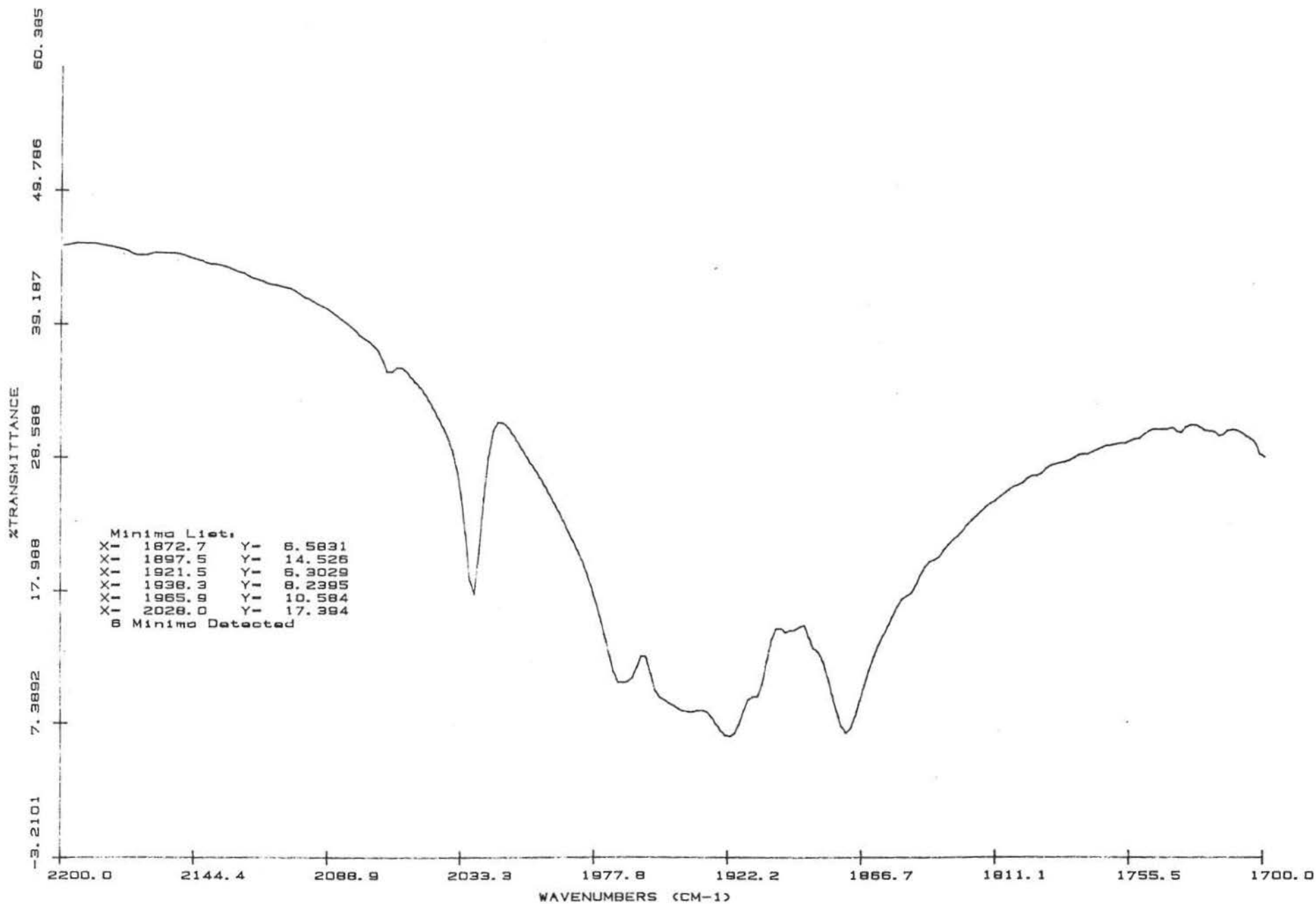
Fig. A35   Solid IR of (Ph4P)(HCr2(CO)10)

Minima List:
X= 1871.4   Y= 7.3841
X= 1885.2   Y= 17.520
X= 1898.6   Y= 17.337
X= 1910.4   Y= 11.012
X= 1921.6   Y= 6.8577
X= 1936.1   Y= 9.1989
X= 1965.1   Y= 12.407
X= 2028.2   Y= 20.081
 8 Minima Detected
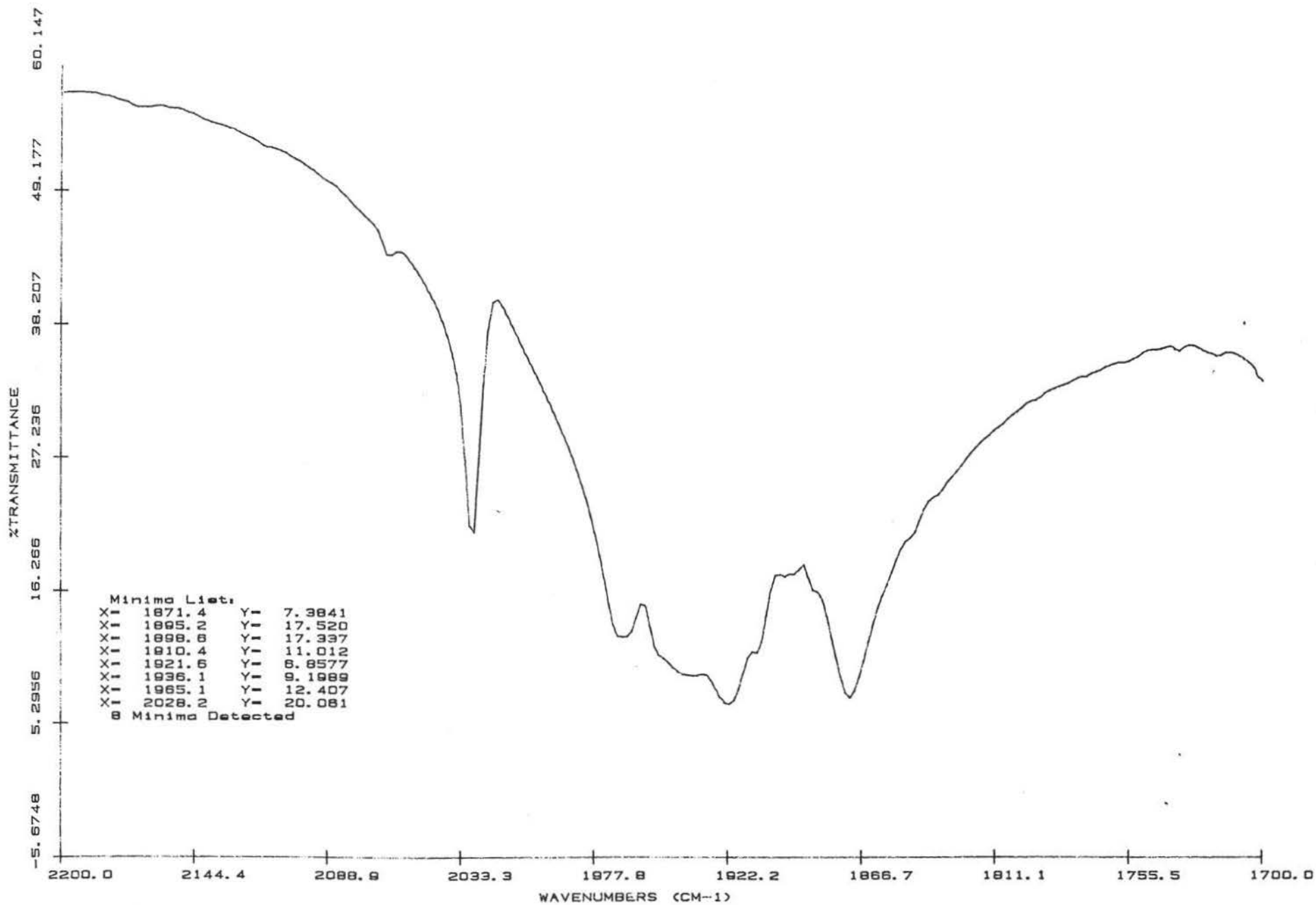
Fig. A36   Solid IR of (Ph4P)(DCr2(CO)10)

APPENDIX II

IR and ^{1}H NMR spectra of mixtures with TPPO

(Fig. A37 - Fig. A64)
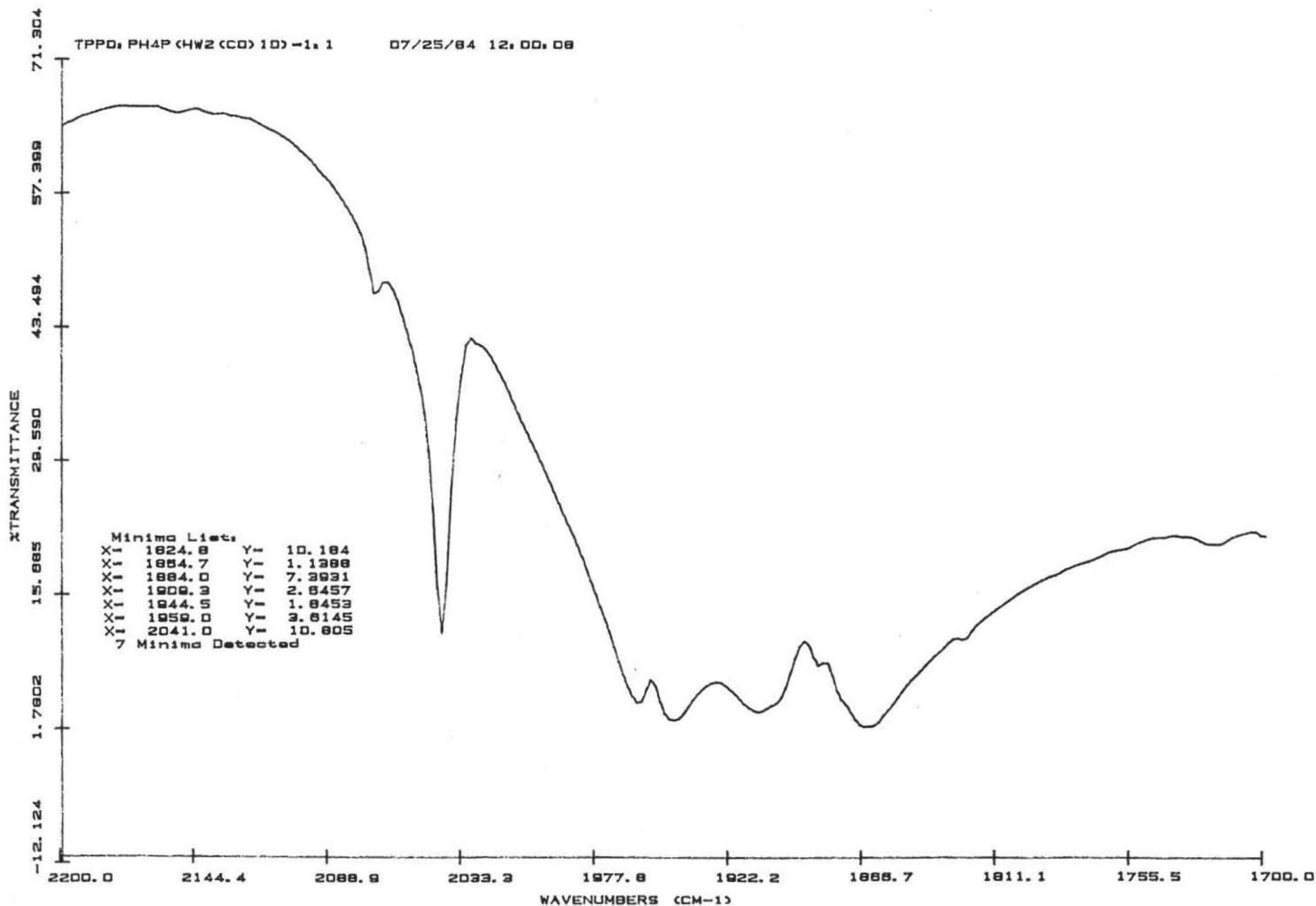
Fig. A37   Solid IR for mixture of TPPO and (Ph4P)(HW2(CO)10)   (1:1) (2200-1700 cm^{-1})
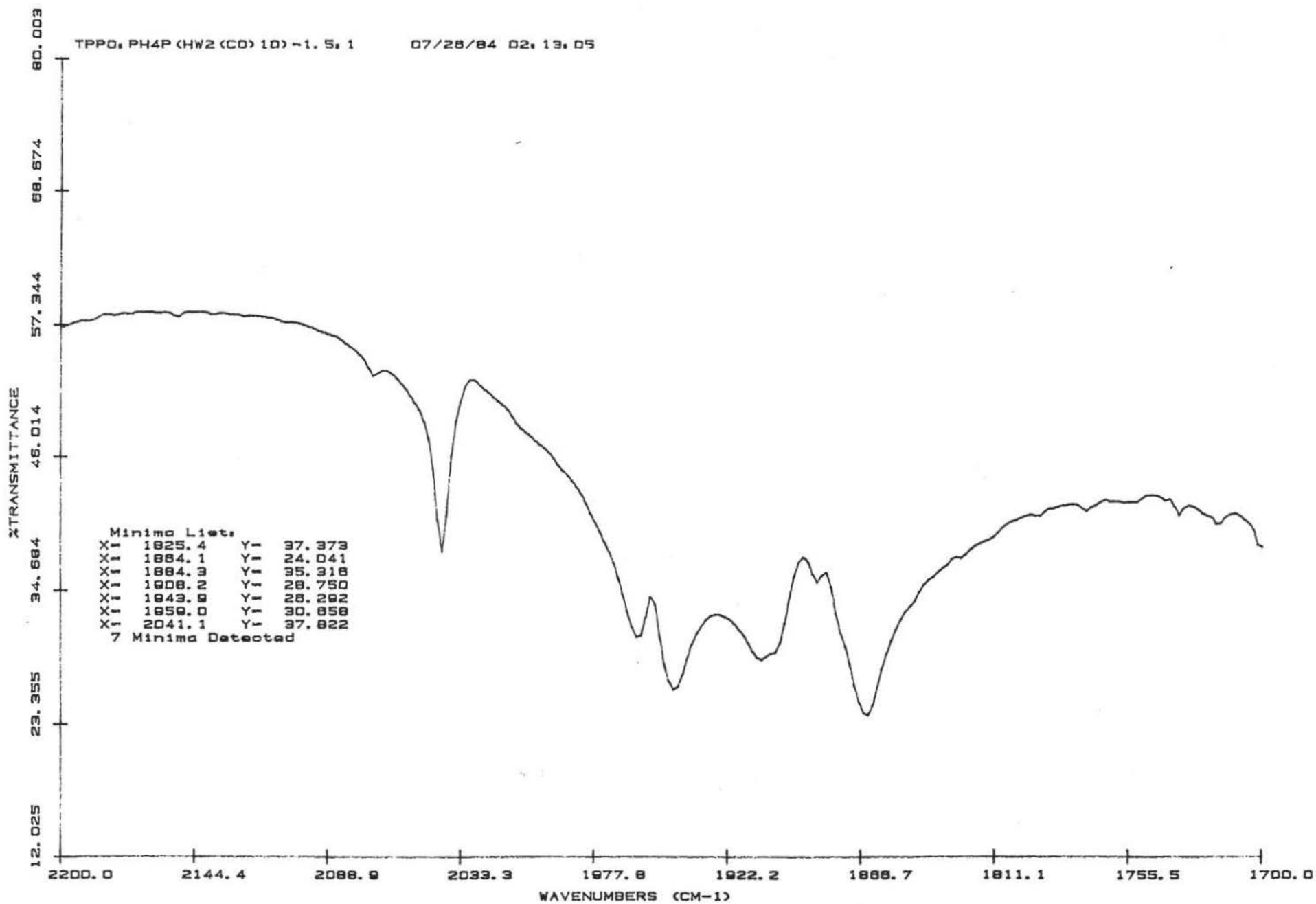
Fig. A38   Solid IR for mixture of TPPO and (Ph4P)(HW2(CO)10)   (1.5:1)(2200-1700 cm^{-1})
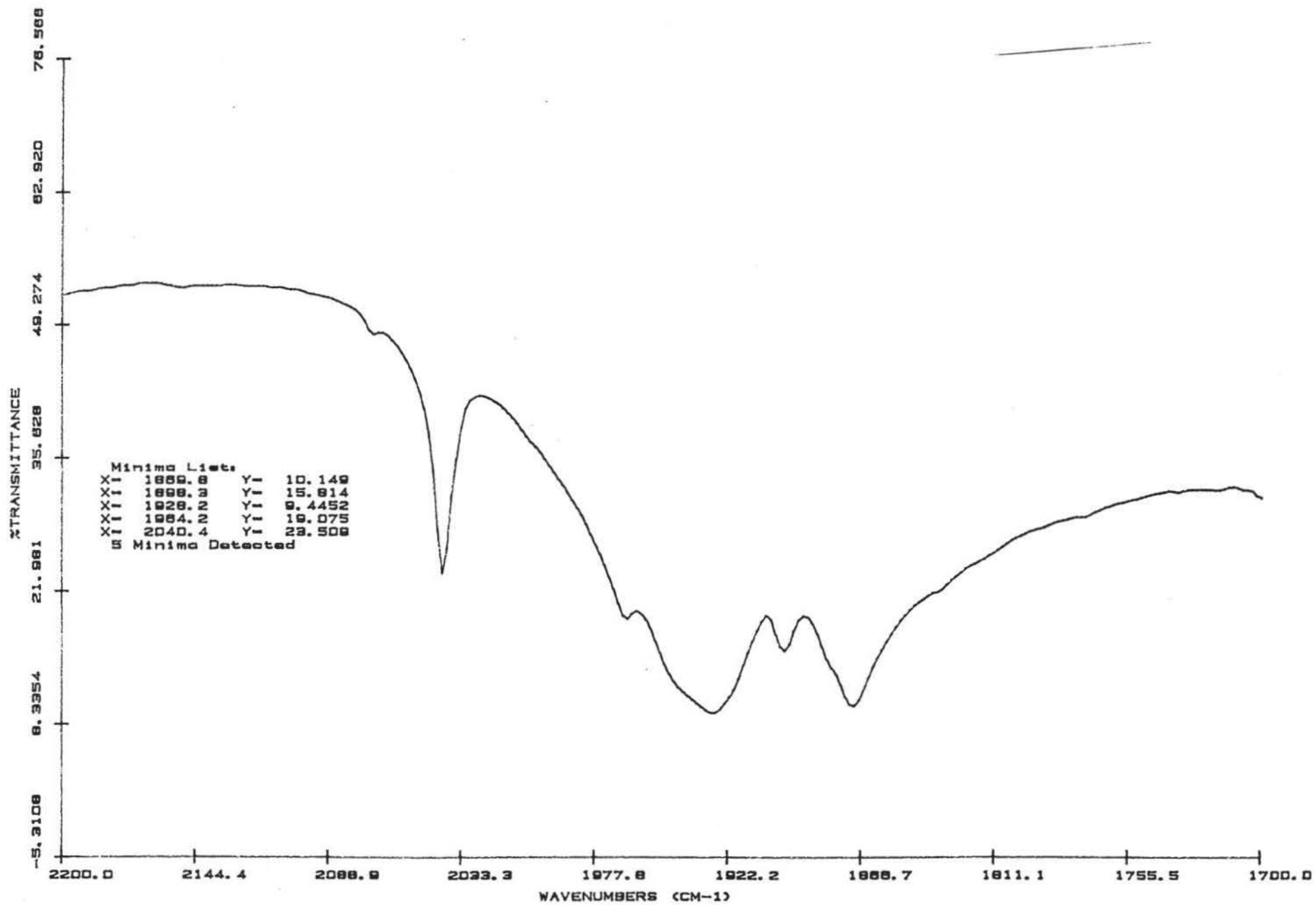
Fig. A39 Solid IR for mixture of TPPO and (PPN)(HW$_2$(CO)$_{10}$) (1:1) (2200-1700 cm^{-1})
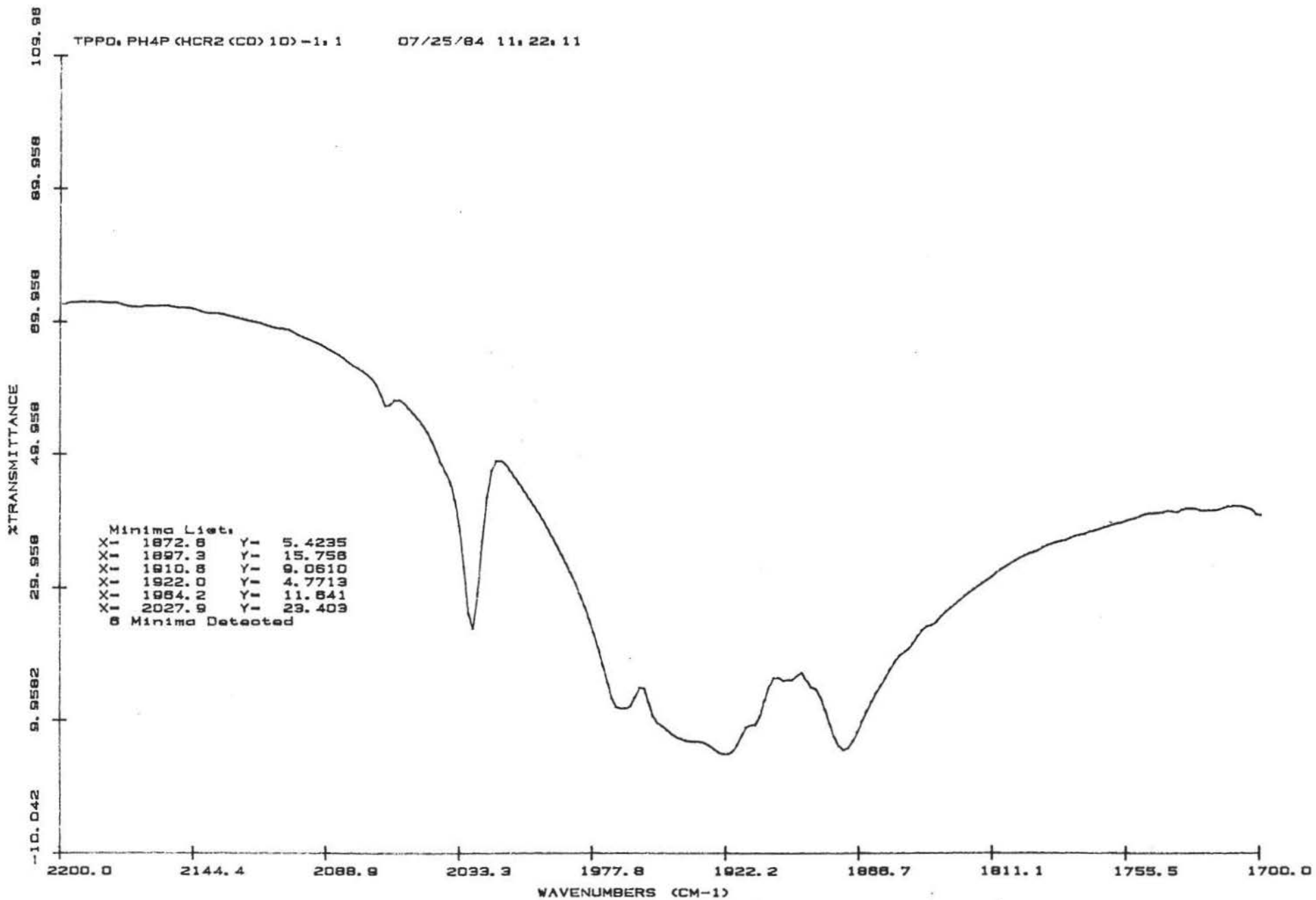
Fig. A40 Solid IR for mixture of TPPO and (Ph4P)(HCr2(CO)10) (1:1) (2200-1700 cm^{-1})
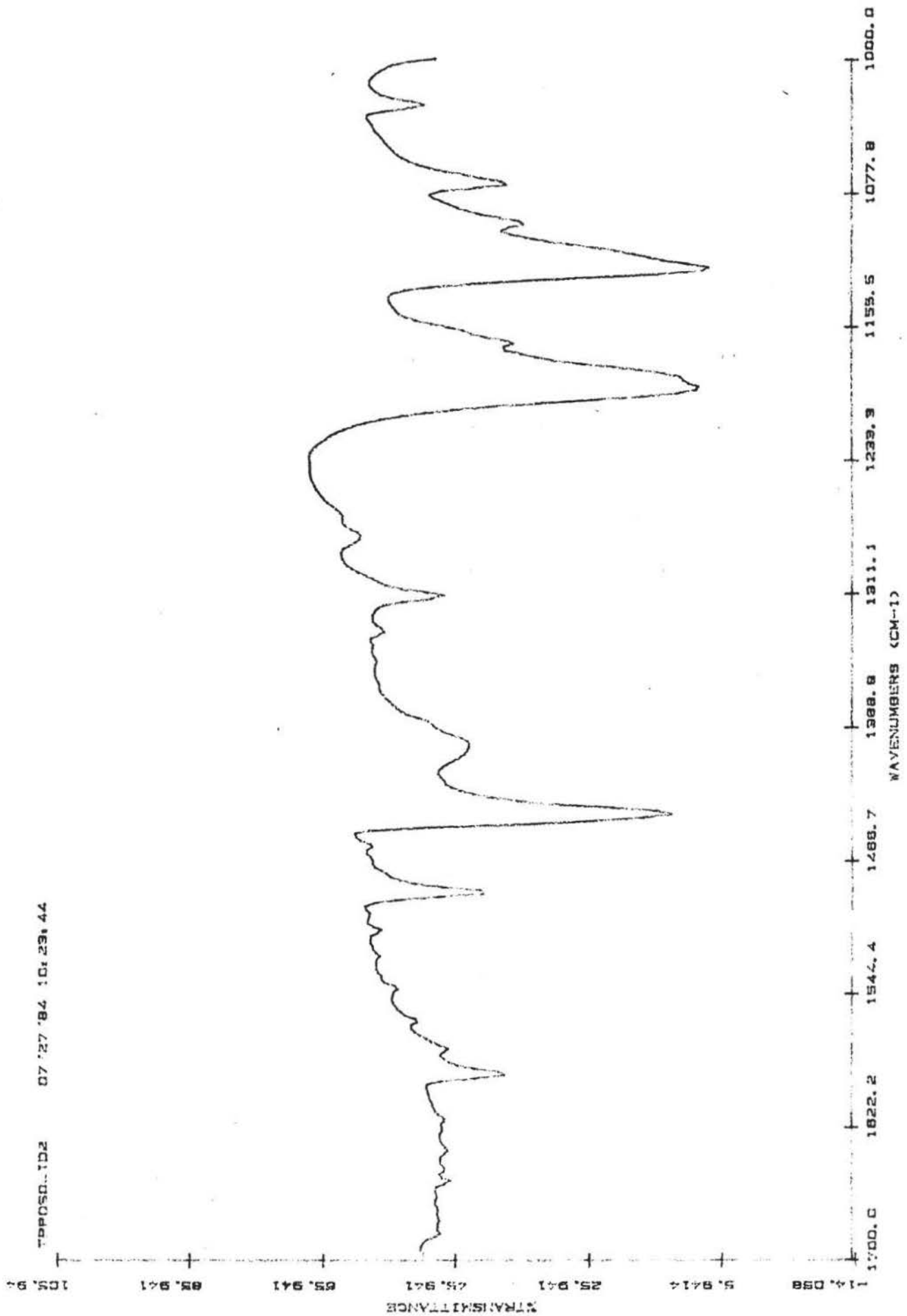
Fig. A41 Solid IR of TPPO (1700-1000 cm⁻¹)
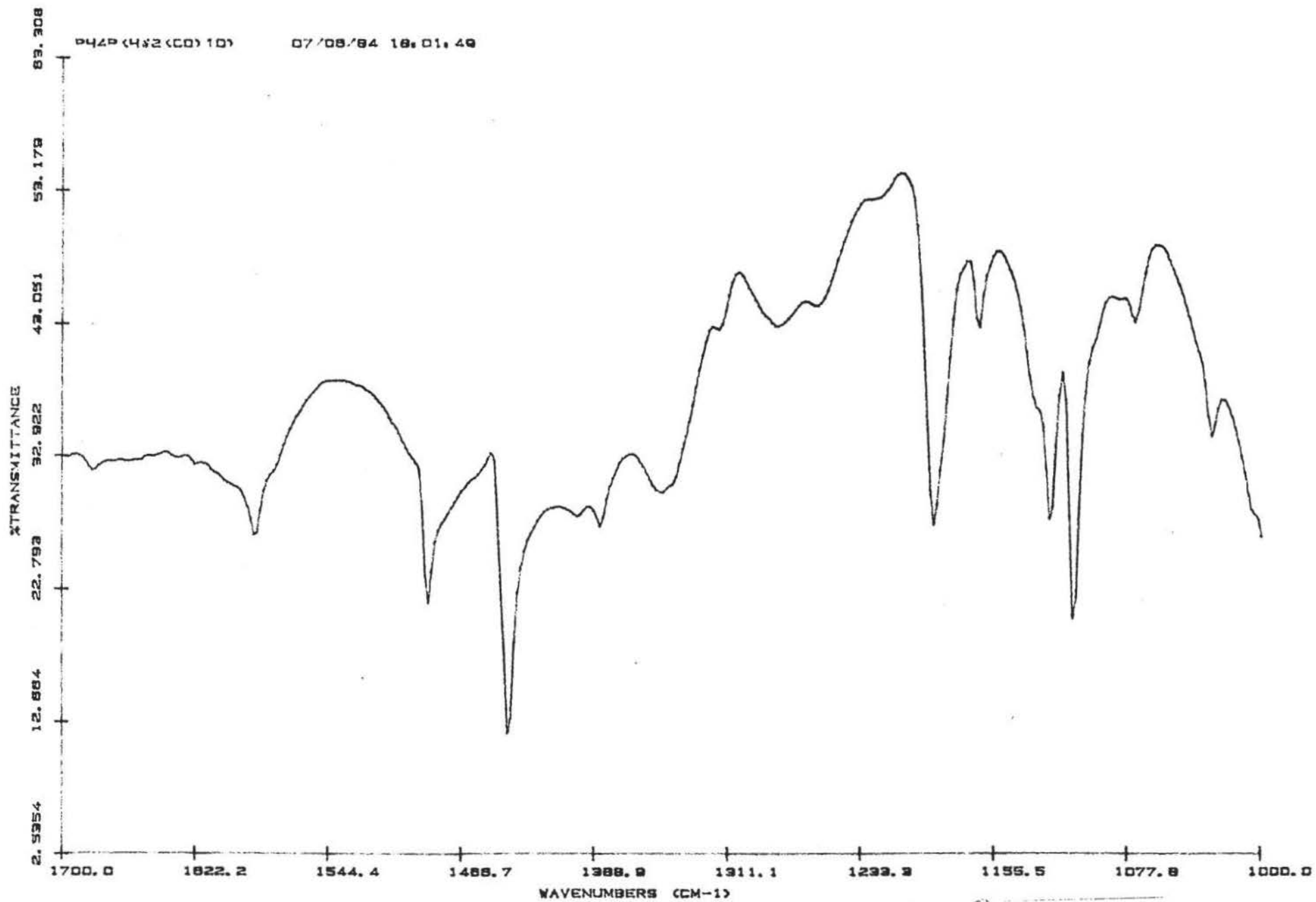
Fig. A42   Solid IR of (Ph4P)(HW$_2$(CO)$_{10}$)   (1700-1000 cm^{-1})
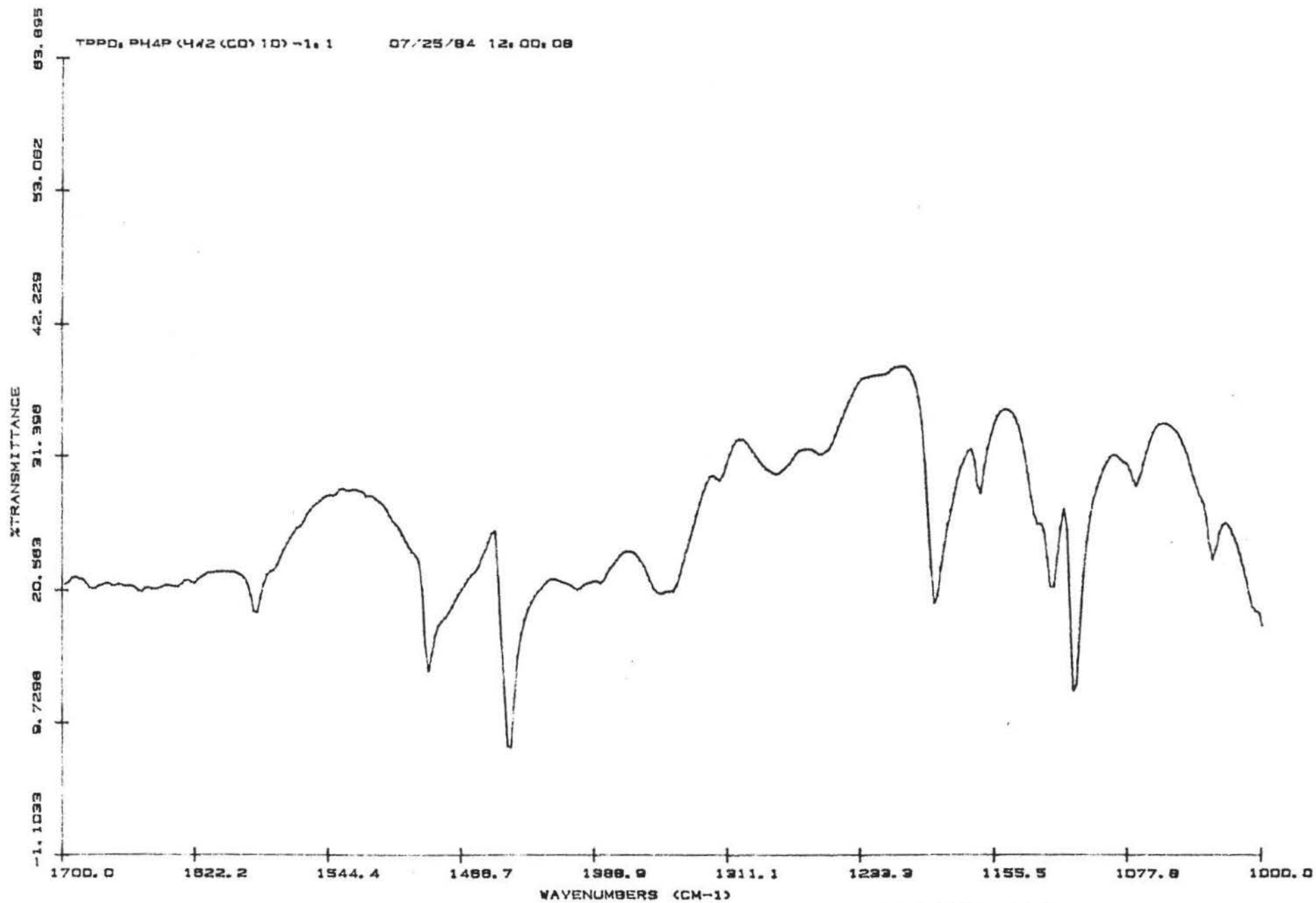
Fig. A43   Solid IR of mixture of TPPO and (Ph4P)(HW2(CO)10) (1:1) (1700-1000 cm-1)
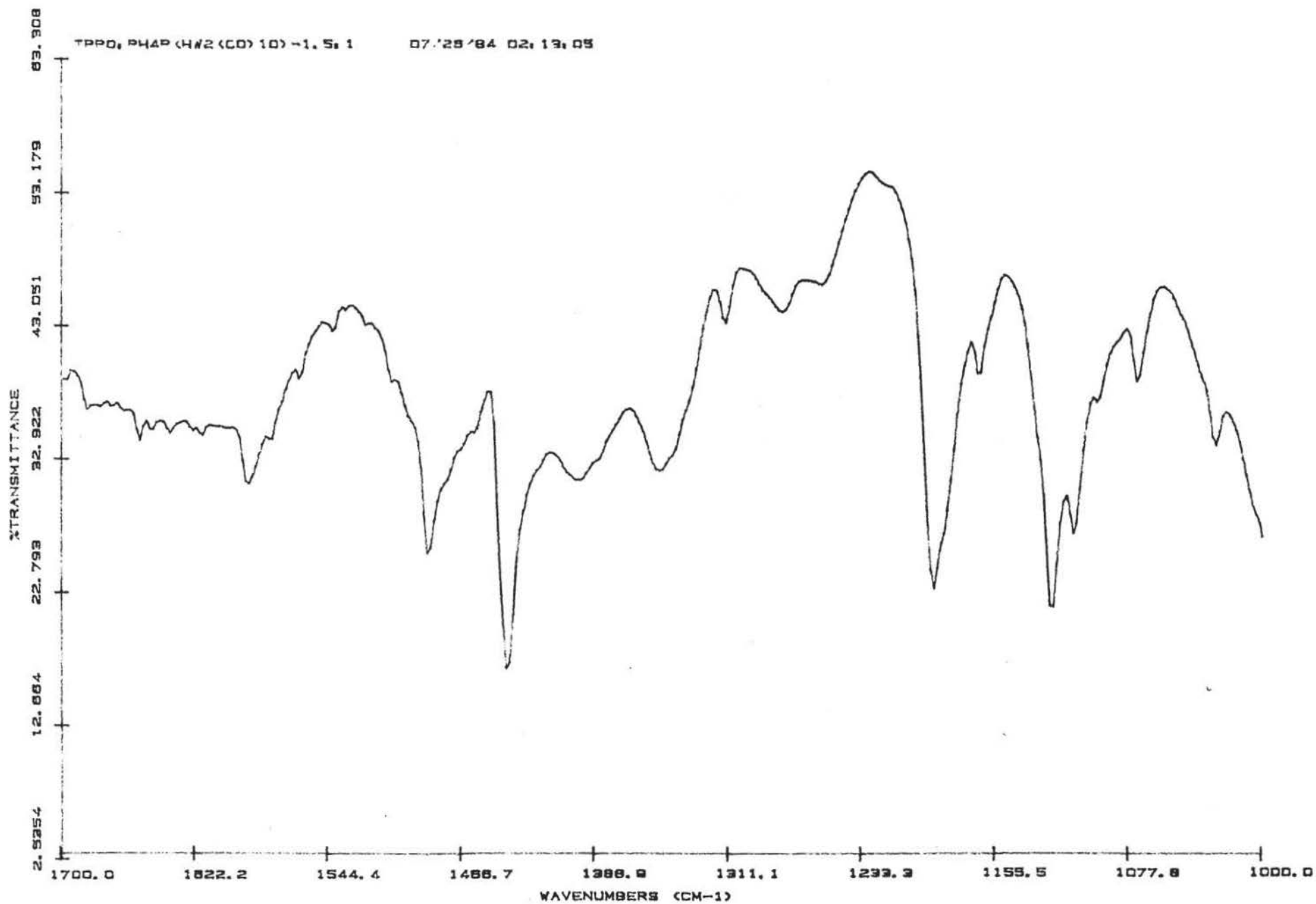
Fig. A44 Solid IR of mixture of TPPO and (Ph4P)(HW2(CO)10) (1.5:1) (1700-1000 cm^{-1})
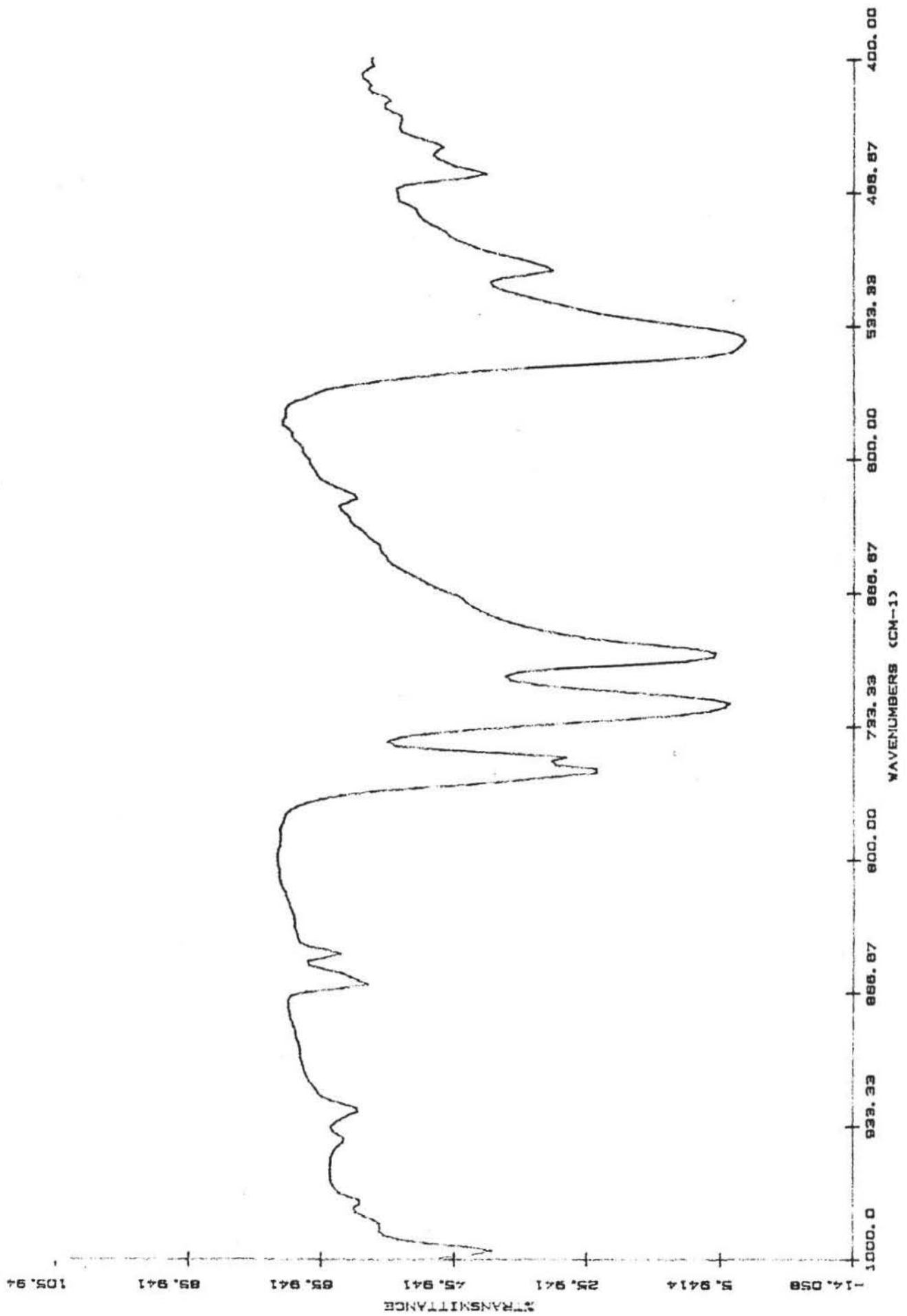
Fig. A45 Solid IR of TPPO (1000-400 cm^{-1})
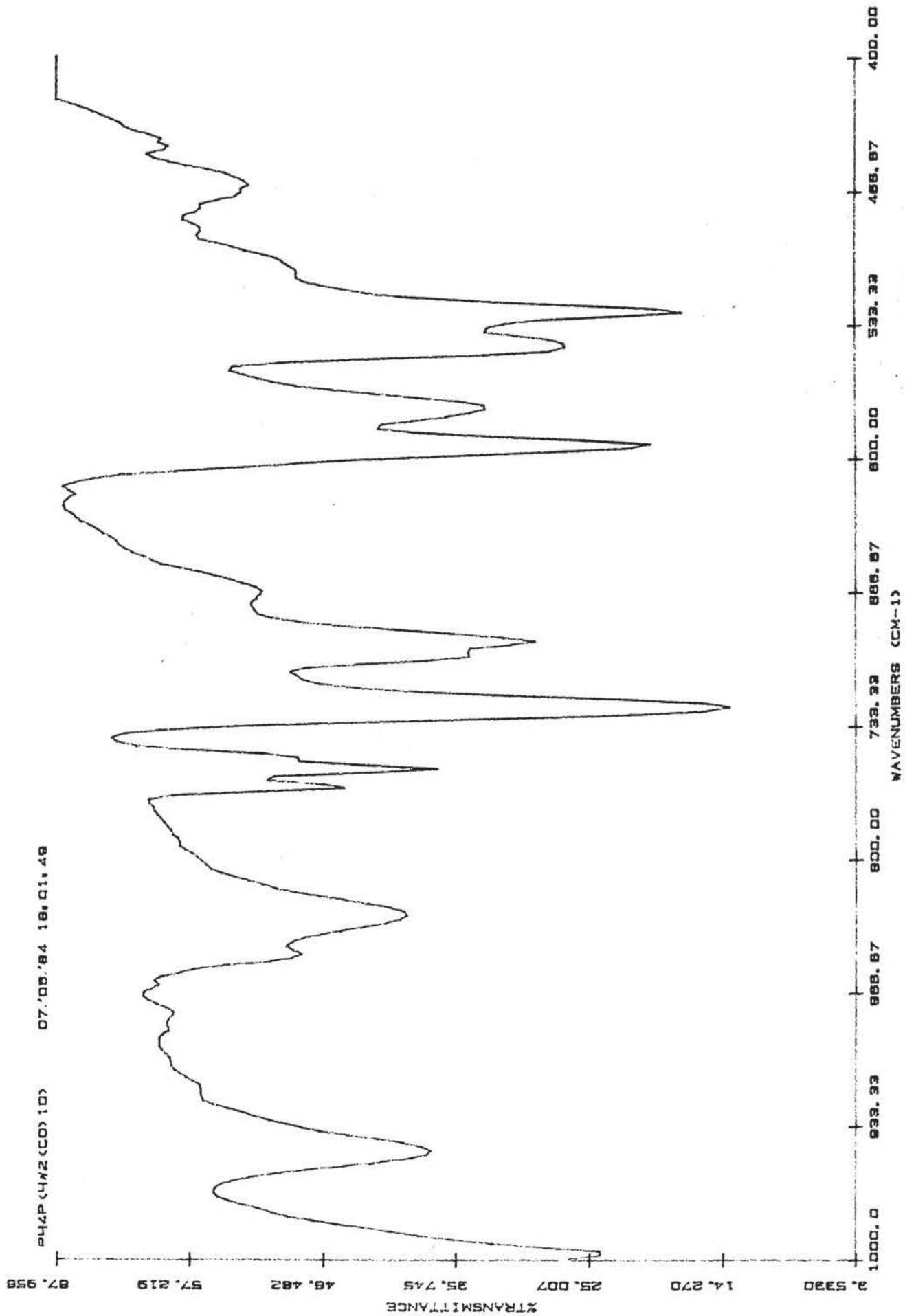
Fig. A46   Solid IR of (Ph4P)(HW2(CO)10)   (1000-400 cm^{-1})
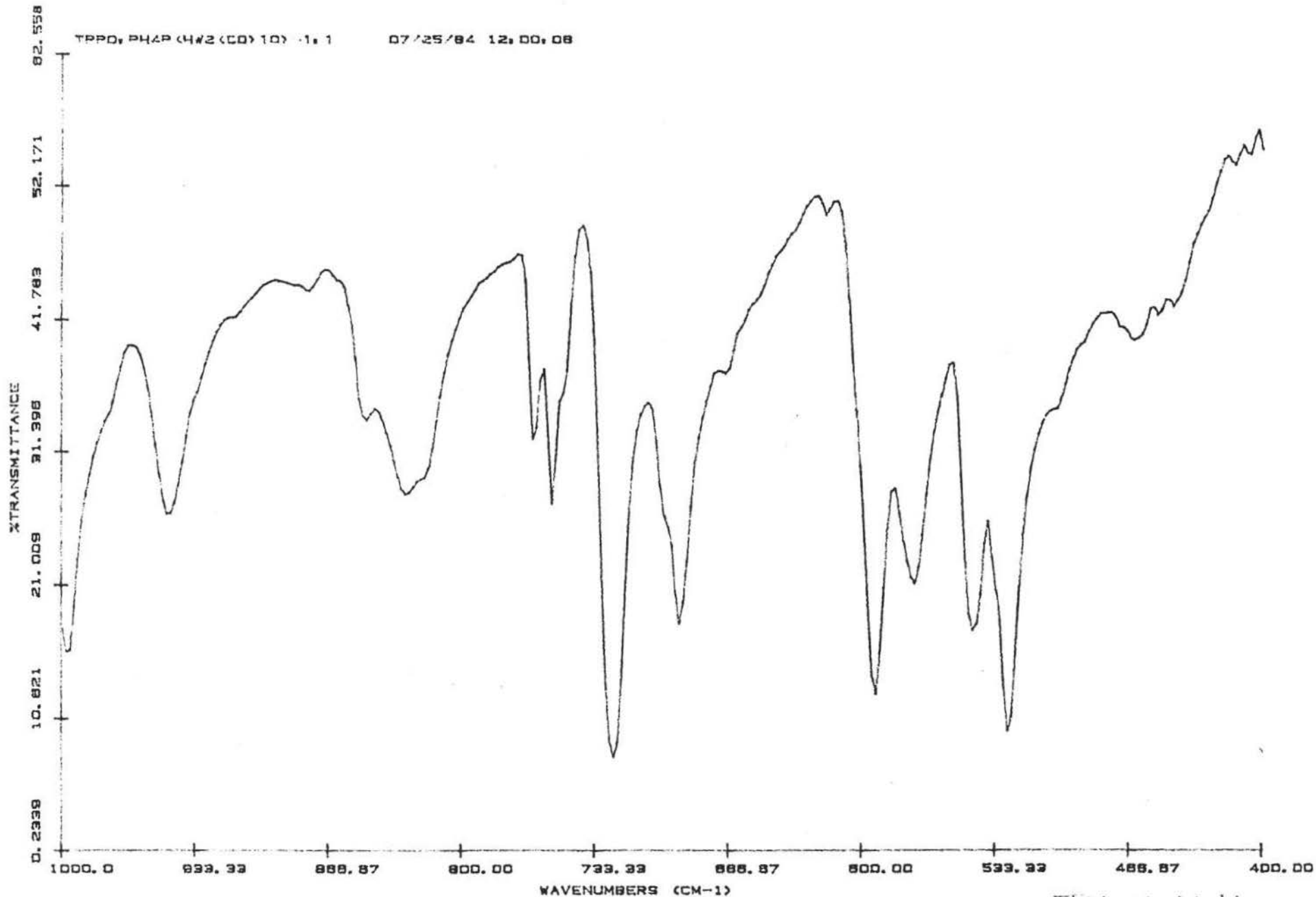
Fig. A47   Solid IR of mixture of TPPO and (Ph4P)(HW2(CO)10) (1:1) (1000-400 cm^{-1})
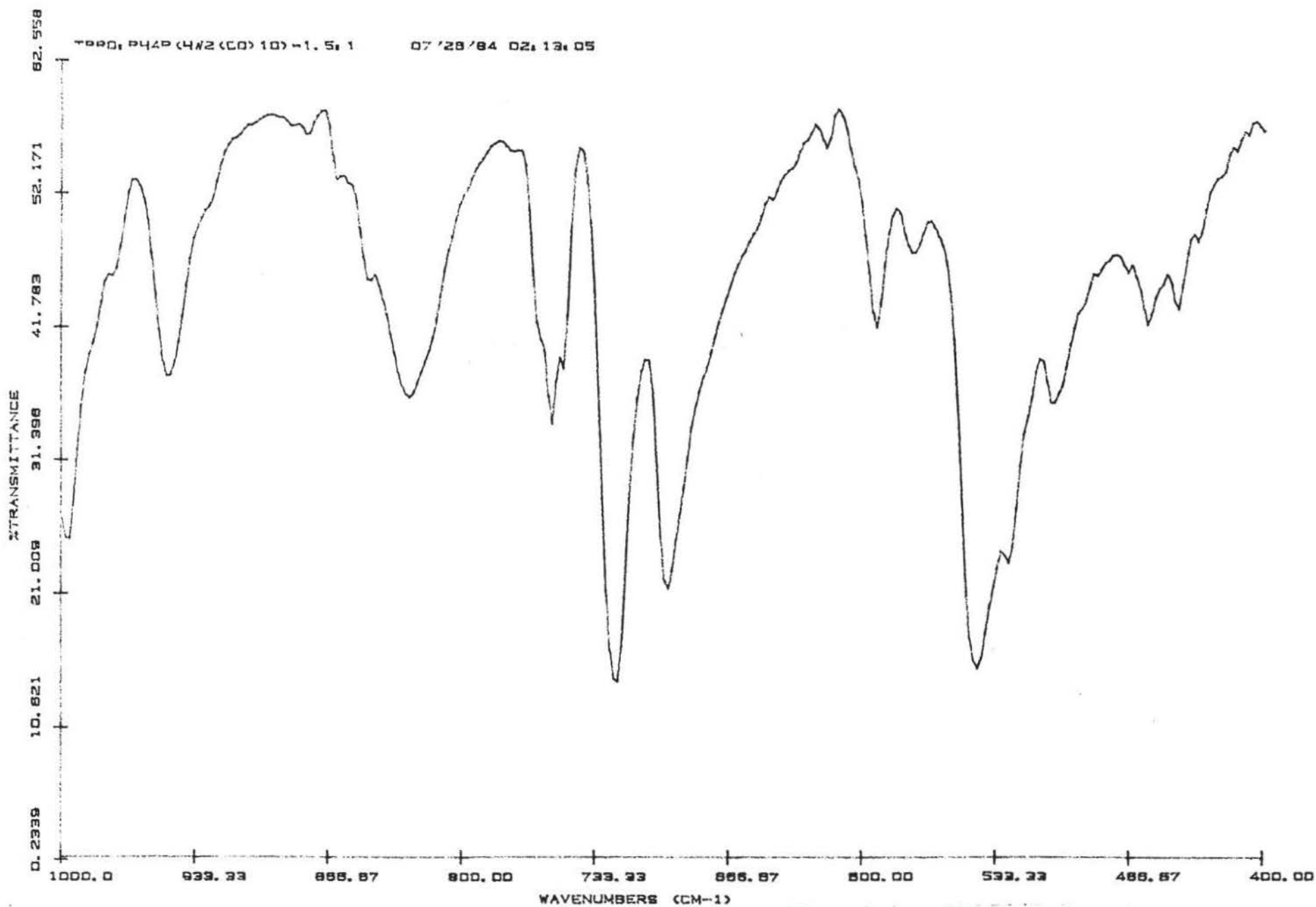
Fig. A48 Solid IR of mixture of TPPO and (Ph4P)(HW2(CO)10) (1.5:1) (1000-400 cm-1)
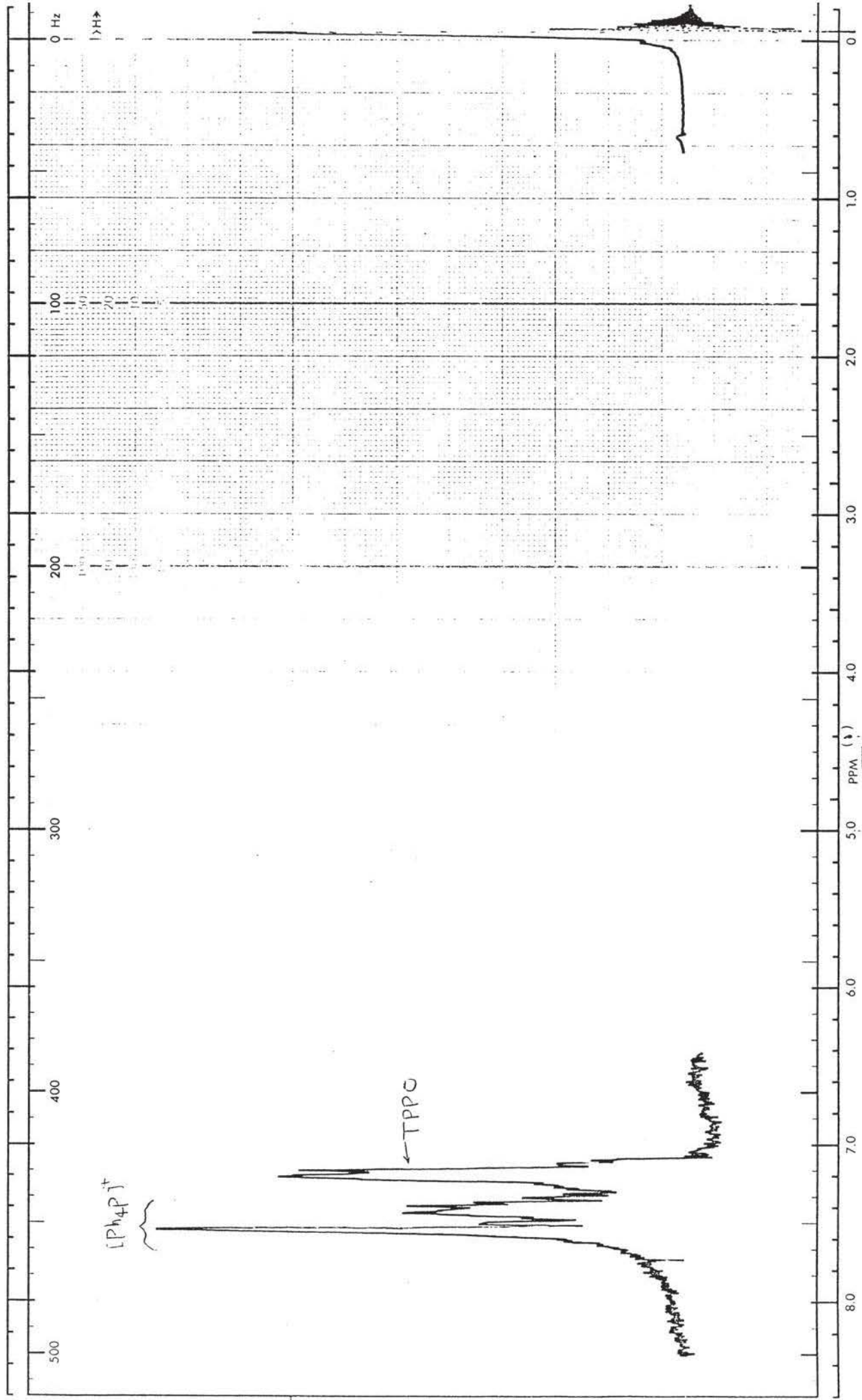
Fig. A49 ^{1}H NMR of mixture of TPPO:(Ph4P)(HW2(CO)10) (1.5:1) in THF
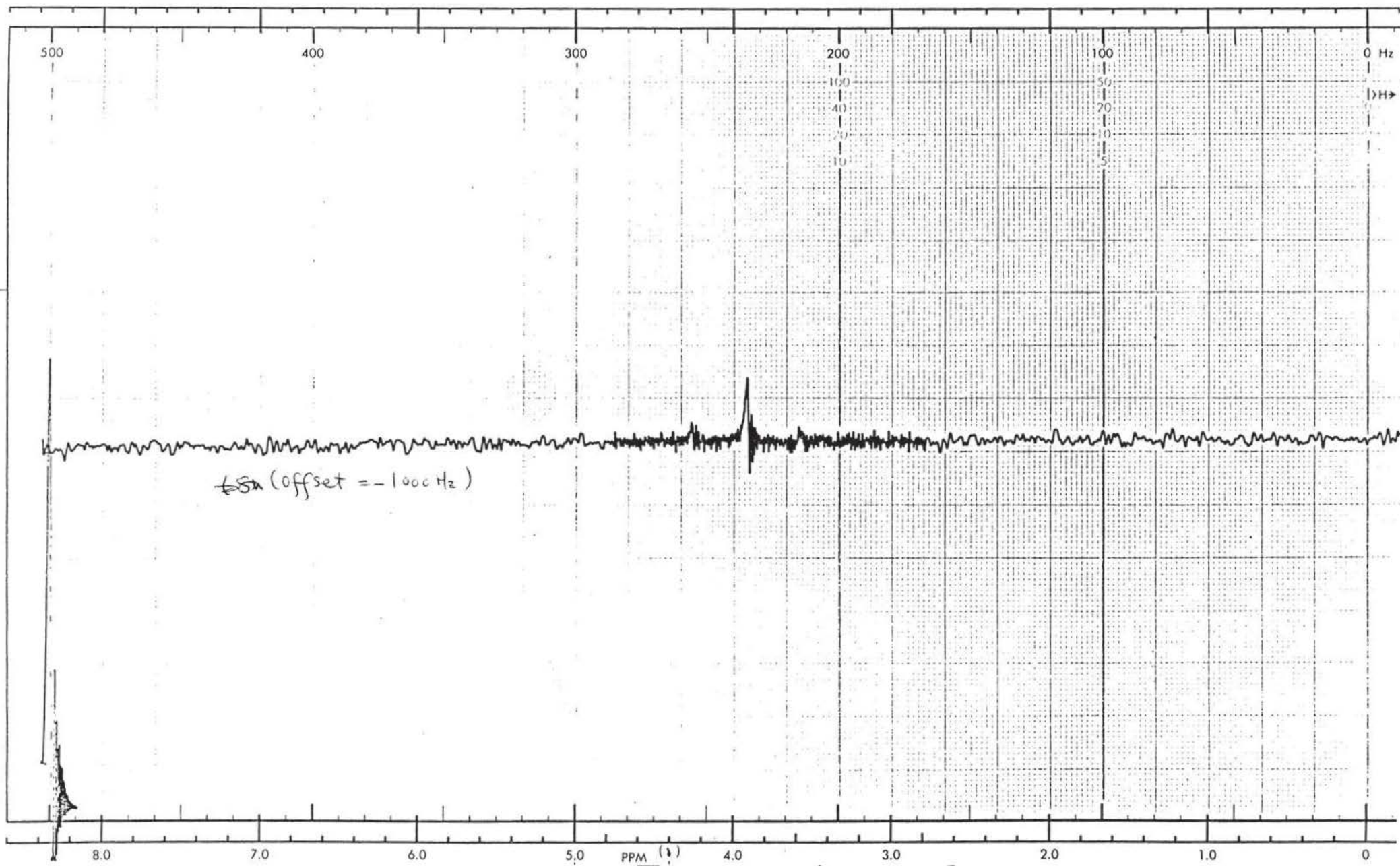
Fig. A49 ^{1}H NMR of mixture of TPPO:(Ph4P)(HW2(CO)10) (1.5:1) in THF
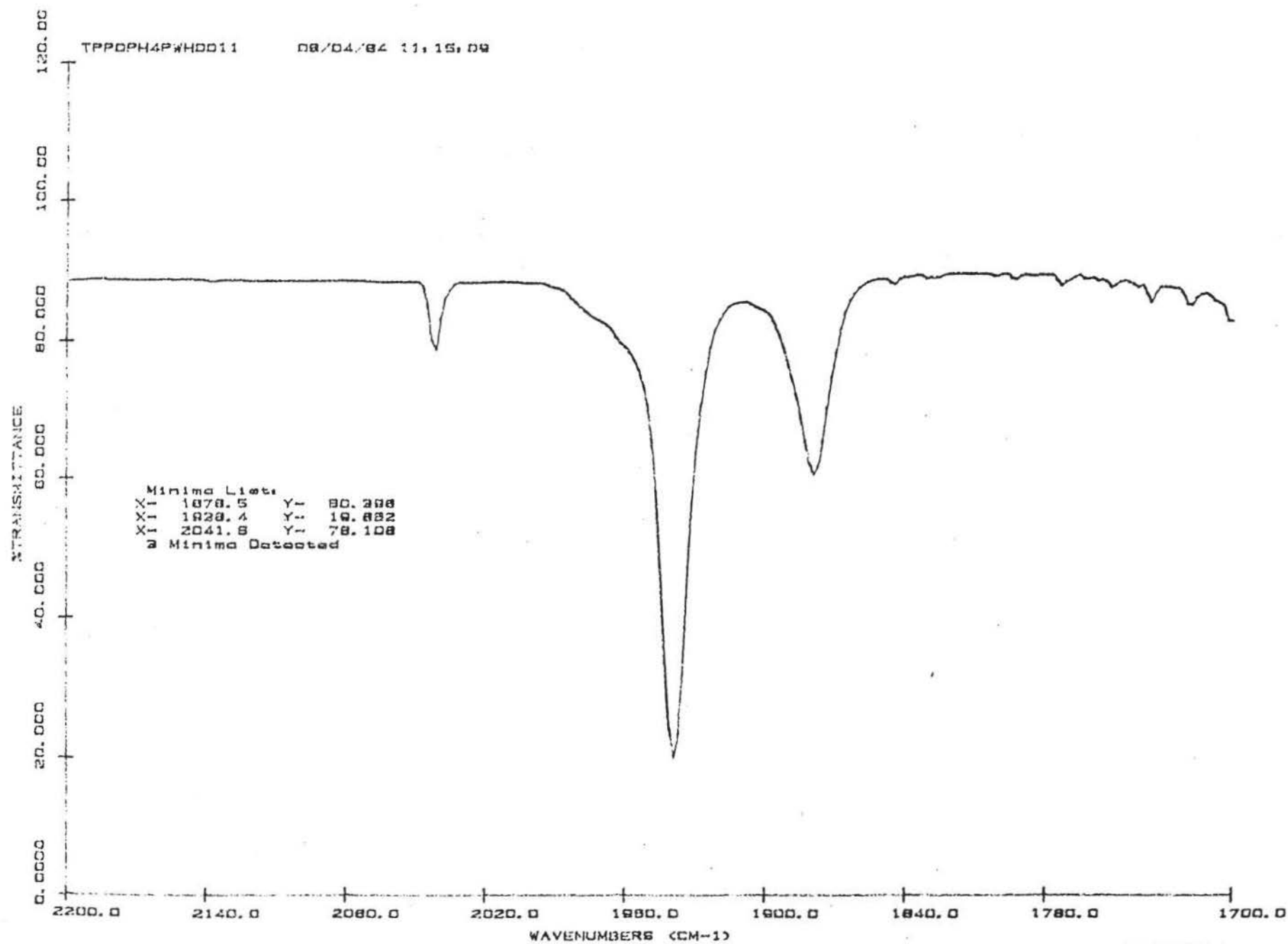
Fig. A50 IR of mixture of TPPO:(Ph4P)(HW$_2$(CO)$_{10}$) (1:1) in THF (2200-1700 cm^{-1})
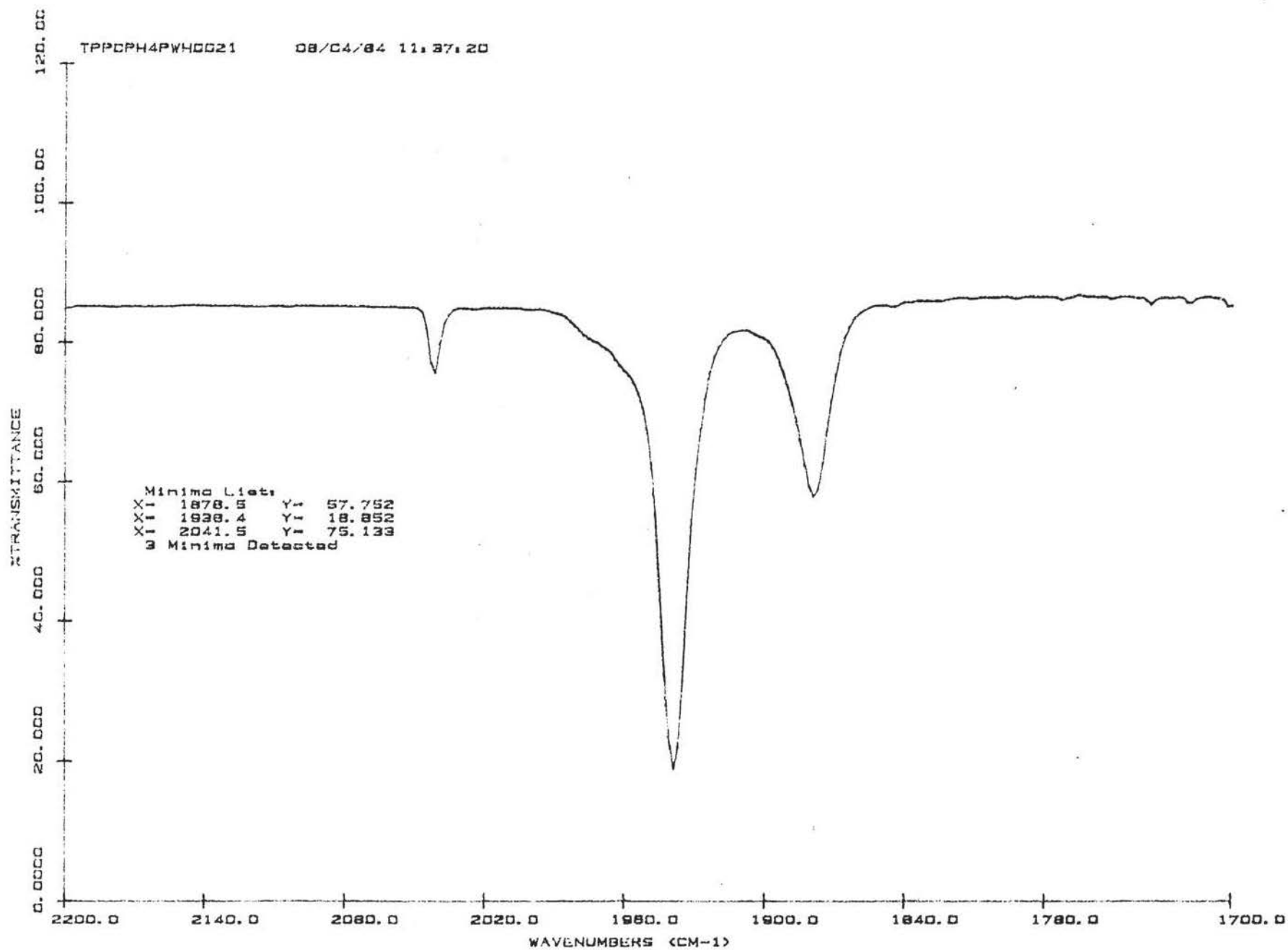
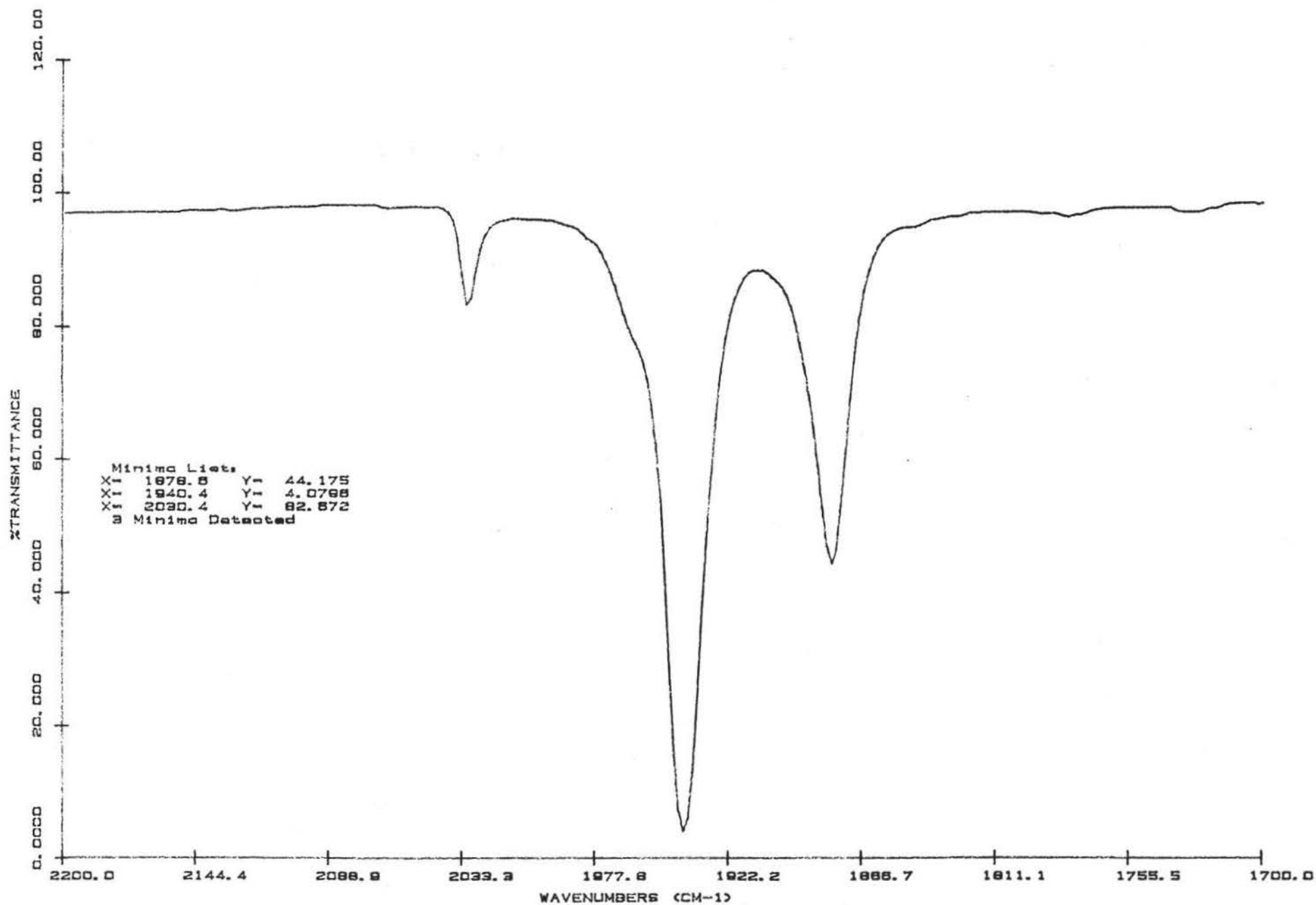Fig. A51   IR of mixture of TPPO:(Ph4P)(HW2(CO)10) (2:1) in THF (2200-1700 cm^{-1})
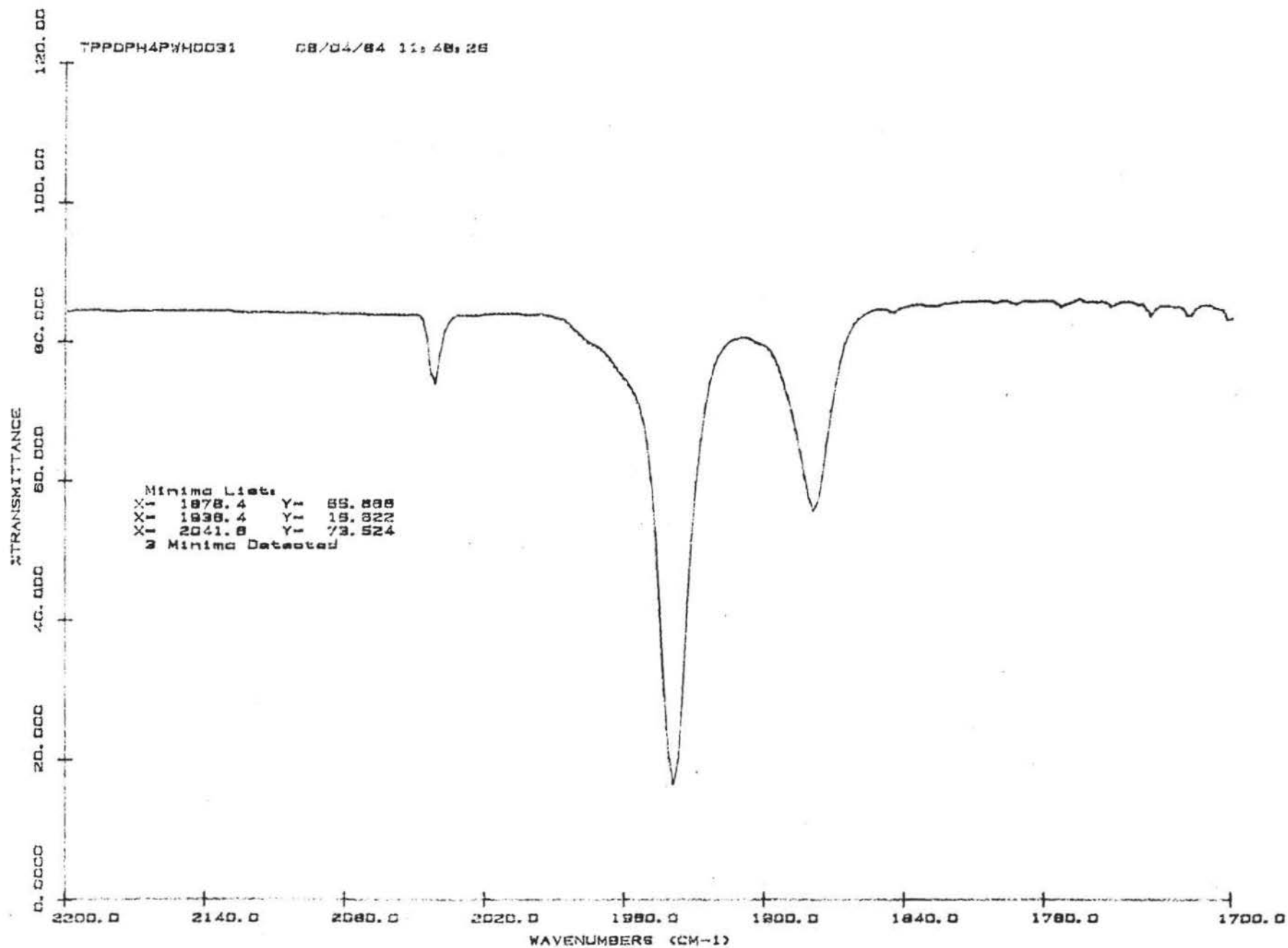
Fig. A52 IR of mixture of TPPO:(Ph4P)(HW$_2$(CO)$_{10}$) (3:1) in THF (2200-1700 cm^{-1})
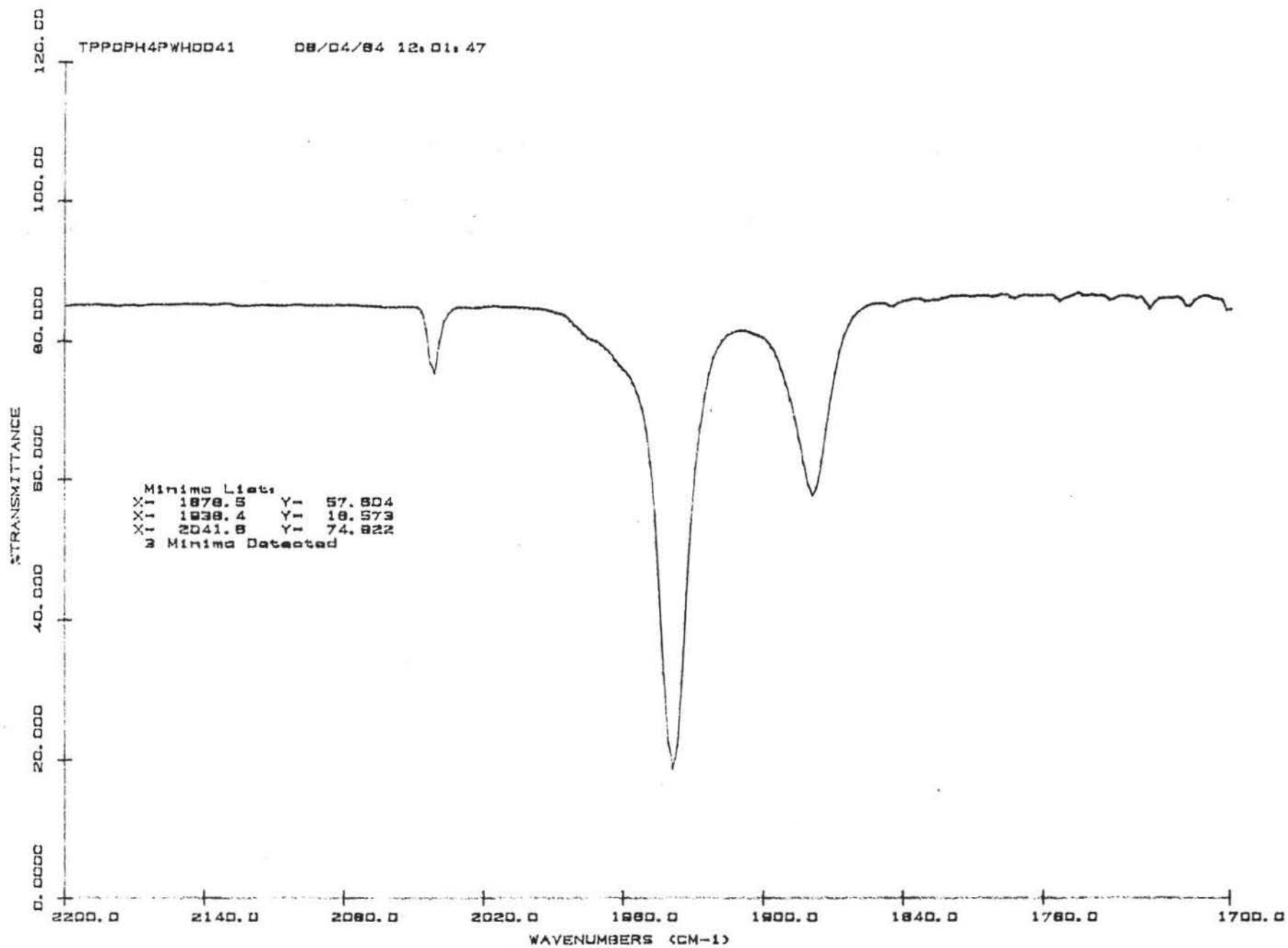
Fig. A53 IR of mixture of TPPO:(Ph4P)(HW$_2$(CO)$_{10}$) (4:1) in THF (2200-1700 cm^{-1})
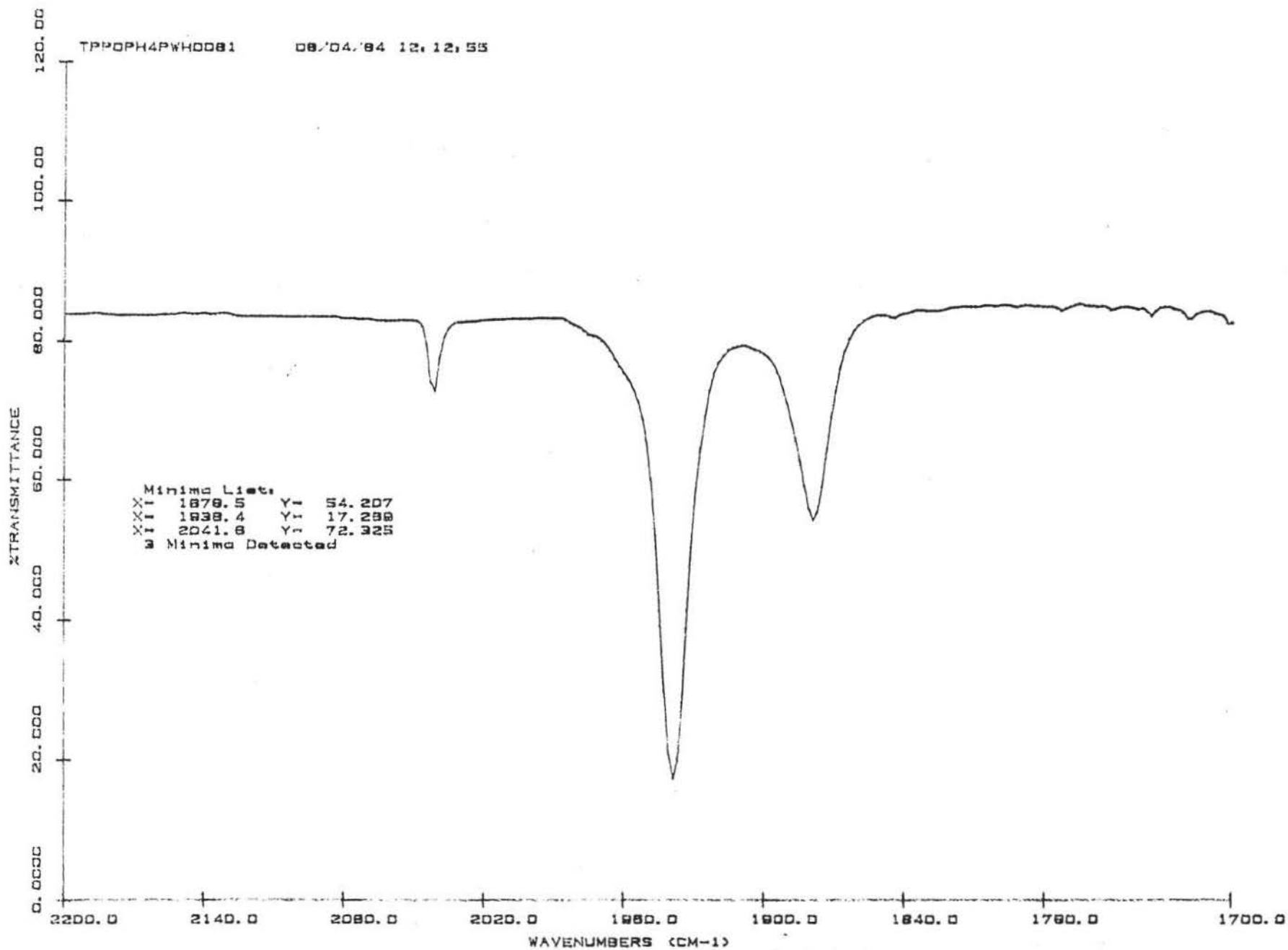
Fig. A54   IR of mixture of TPPO:(Ph4P)(HW2(CO)10) (8:1) in THF (2200-1700 cm^{-1})

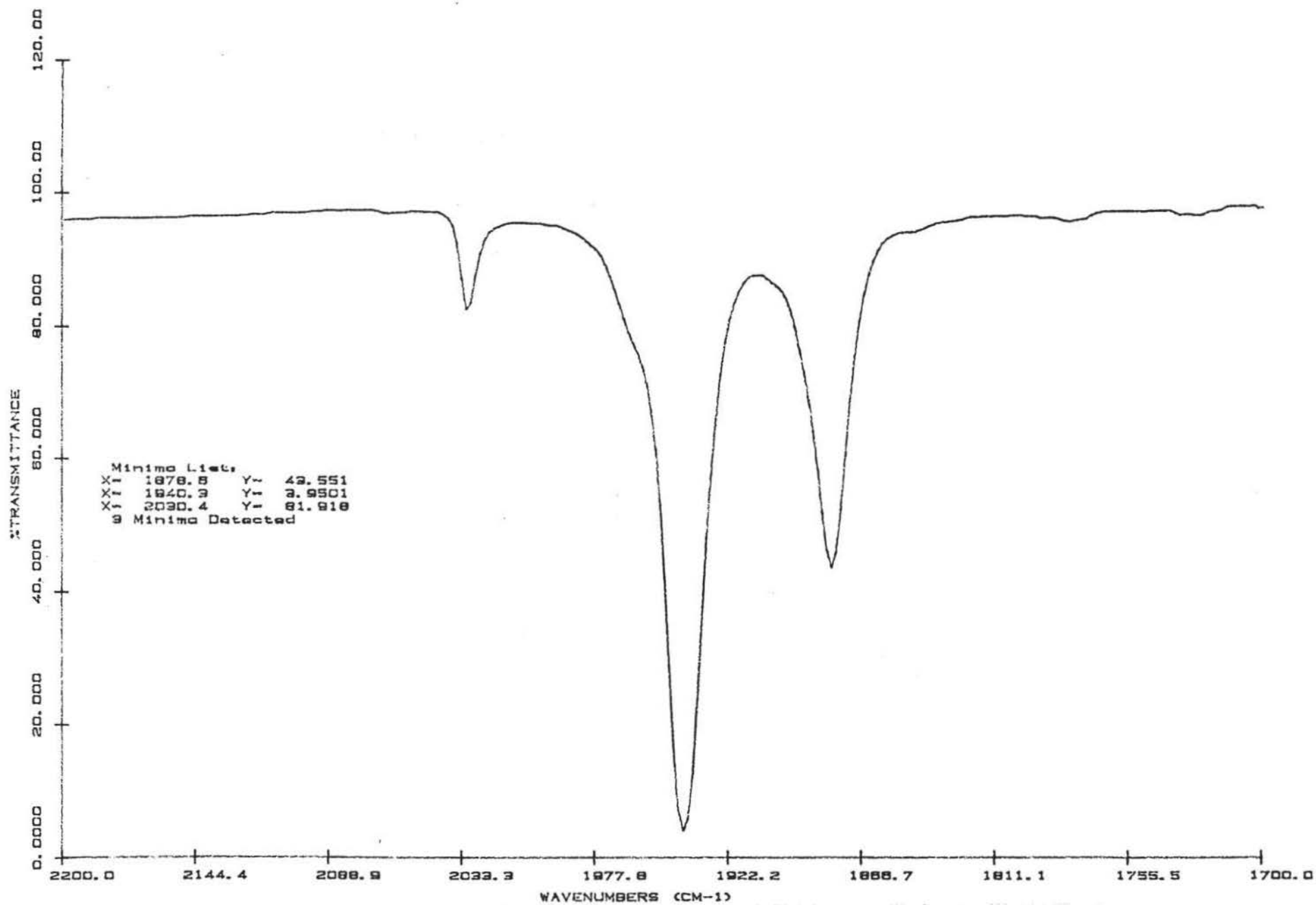Fig. A55 IR of mixture of TPPO:(Ph4P)(HCr2(CO)10) (1:1) in THF (2200-1700 cm-1)

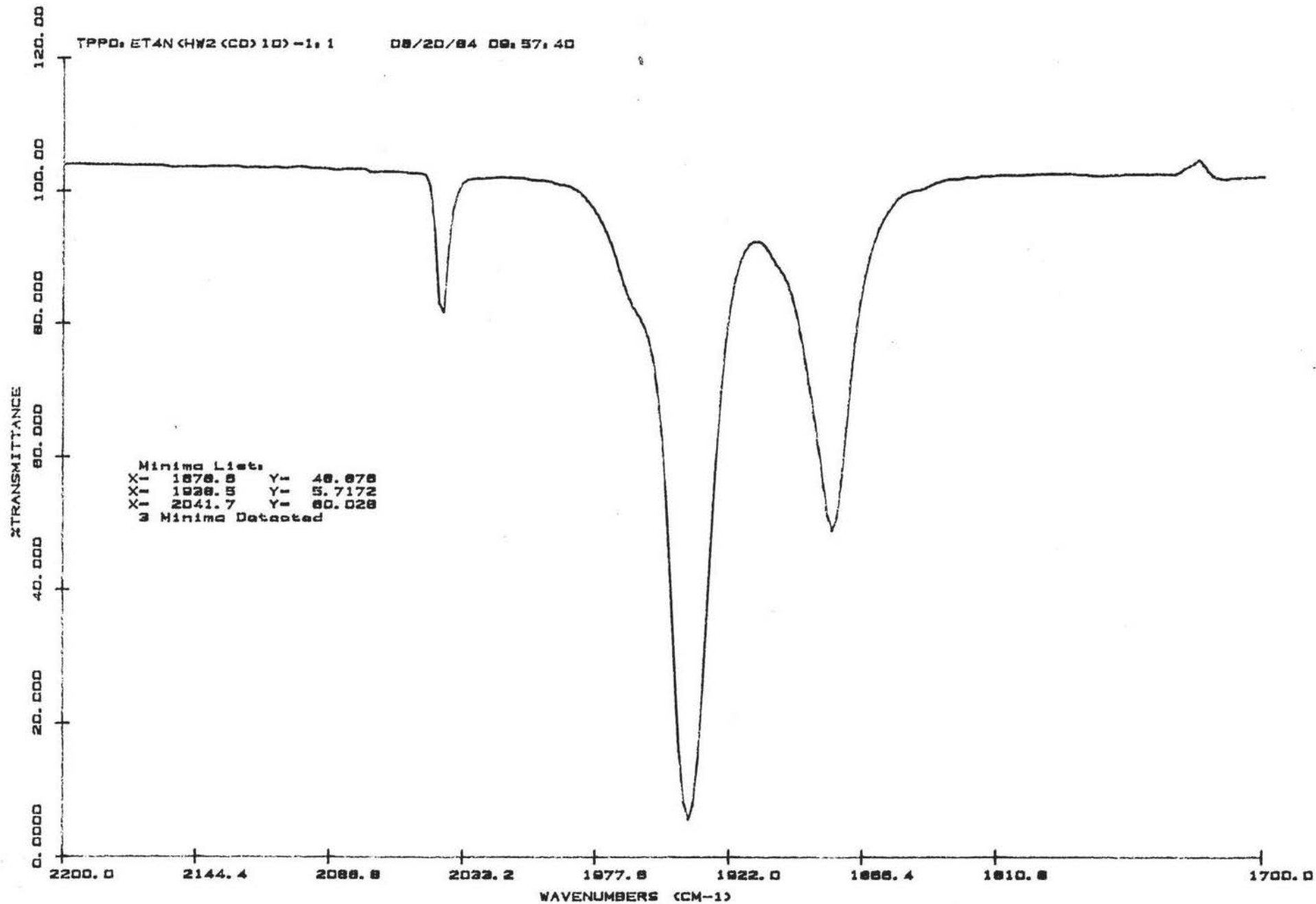Fig. A56 IR of mixture of TPPO:(Ph4P)(HCr2(CO)10) (2:1) in THF (2200-1700 cm^{-1})

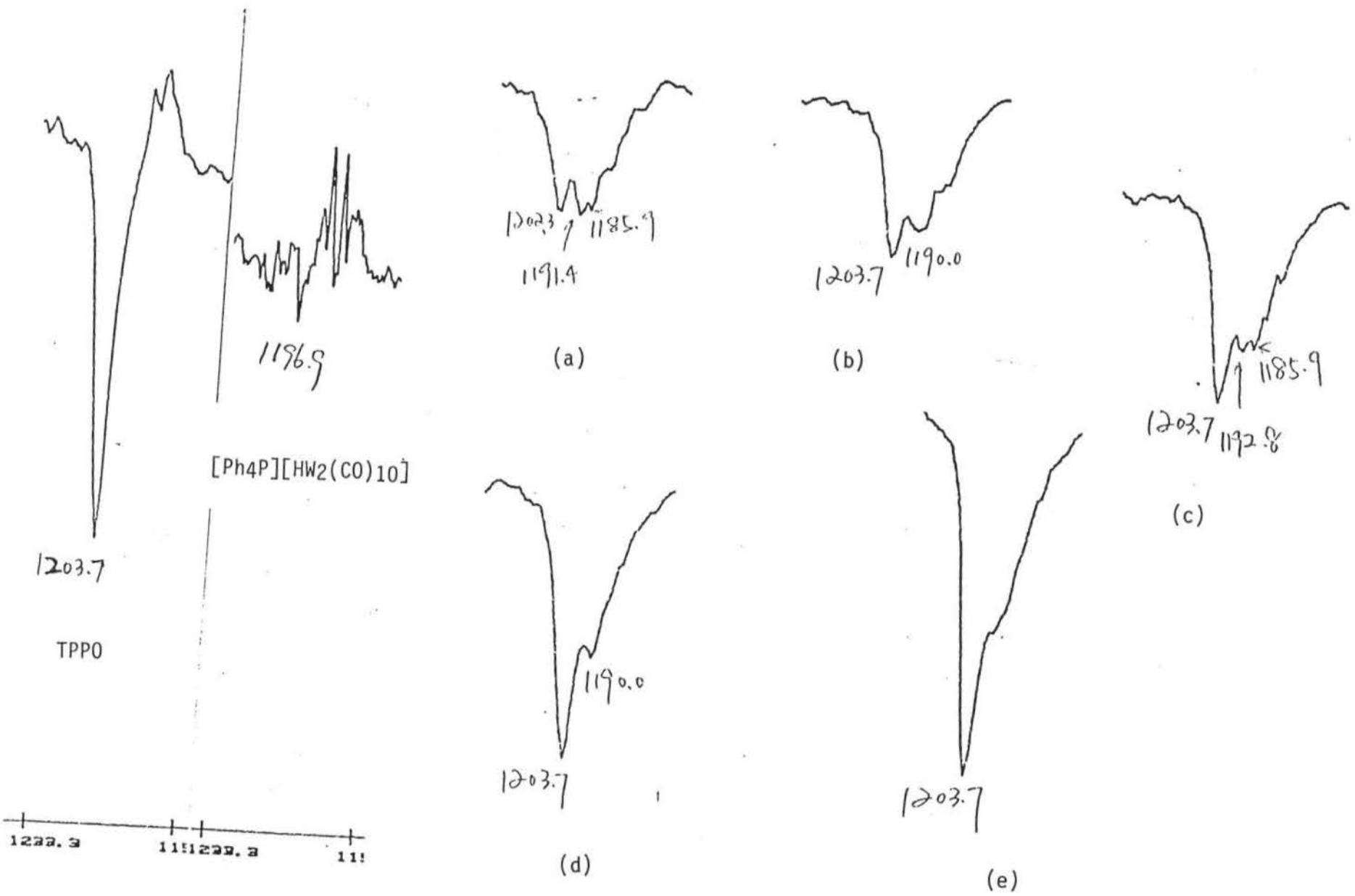Fig. A57 IR of mixture of TPPO:(Et4N)(HW2(CO)10) (1:1) in THF (2200-1700 cm^{-1})
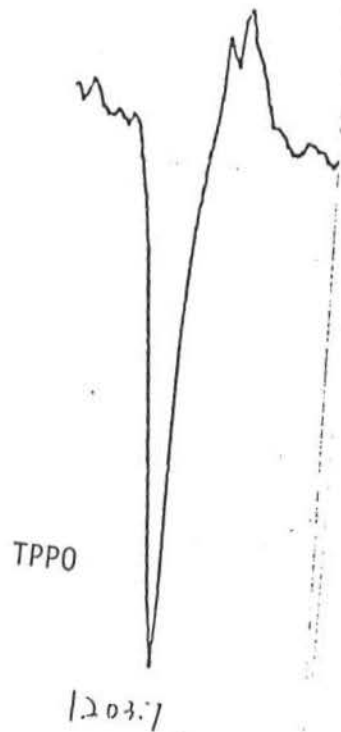
Fig. A58 IR spectra at P=O stretching region of TPPO and (Ph4P)(HW2(CO)10) and their mixtures (1:1(a), 2:1(b), 3:1(c), 4:1(d) and 8:1(e))
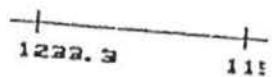
TPPO

1203.7

[Ph4P][HCr2(CO)10]

1181.8

1188.7

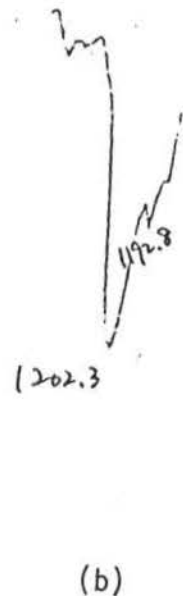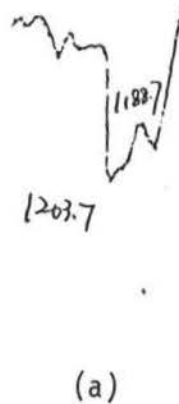1203.7

(a)

1192.8

1202.3

(b)

1222.3   115

Fig. A59 IR spectra at P=O stretching region of TPPO and (Ph4P)(HCr2(CO)10)
and their mixtures (1:1(a), 2:1(b))

TPPO

[Et4N]LHW2(CO)10]

1181.8

1203.7

1203.7

(a)

1233.3   115
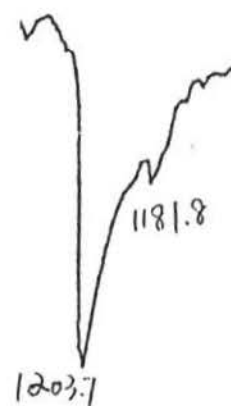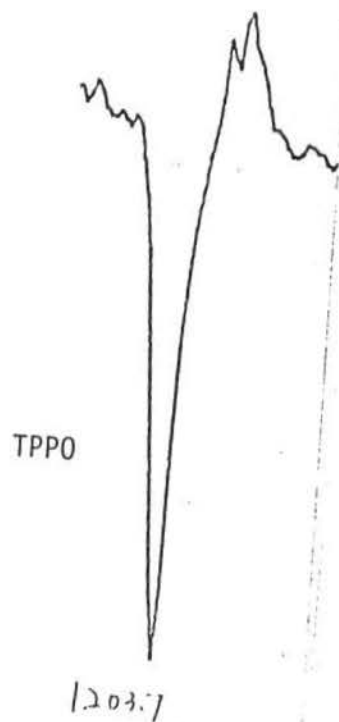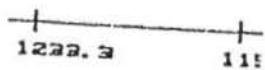
Fig. A60   IR spectra at P=O stretching region of TPPO and (Et4N)(HW2(CO)10)
and mixture at 1:1 ratio (a)

697.66

TPPO

542.37

583.58

594.53

[Ph4P][HW2(CO)10]

(a)

593.36

593.36

(b)

573.36

(c)

593.36

(d)

593.36

(e)

888.87   800.00   533

Fig. A61   IR spectra at M-C-O bending region of TPPO and (Ph4P)(HW2(CO)10)
and their mixtures(1:1(a), 2:1(b), 3:1(c), 4:1(d) and 8:1(e))

697.66

TPPO

888.87   800.00   533

666.01

[Ph4P][HCr2(CO)10]

664.84

(a)

664.84

(b)

888.87

Fig. A62   IR spectra of M-C-O bending region of TPPO and (Ph4P)(HCr2(CO)10) and their mixtures at ratios 1:1 (a) and 2:1 (b)

697.66

594.53

[Et4N]LHW2(CO)10]

594.53

TPPO

594.53

(1:1)

888.87
800.00
533

888.87
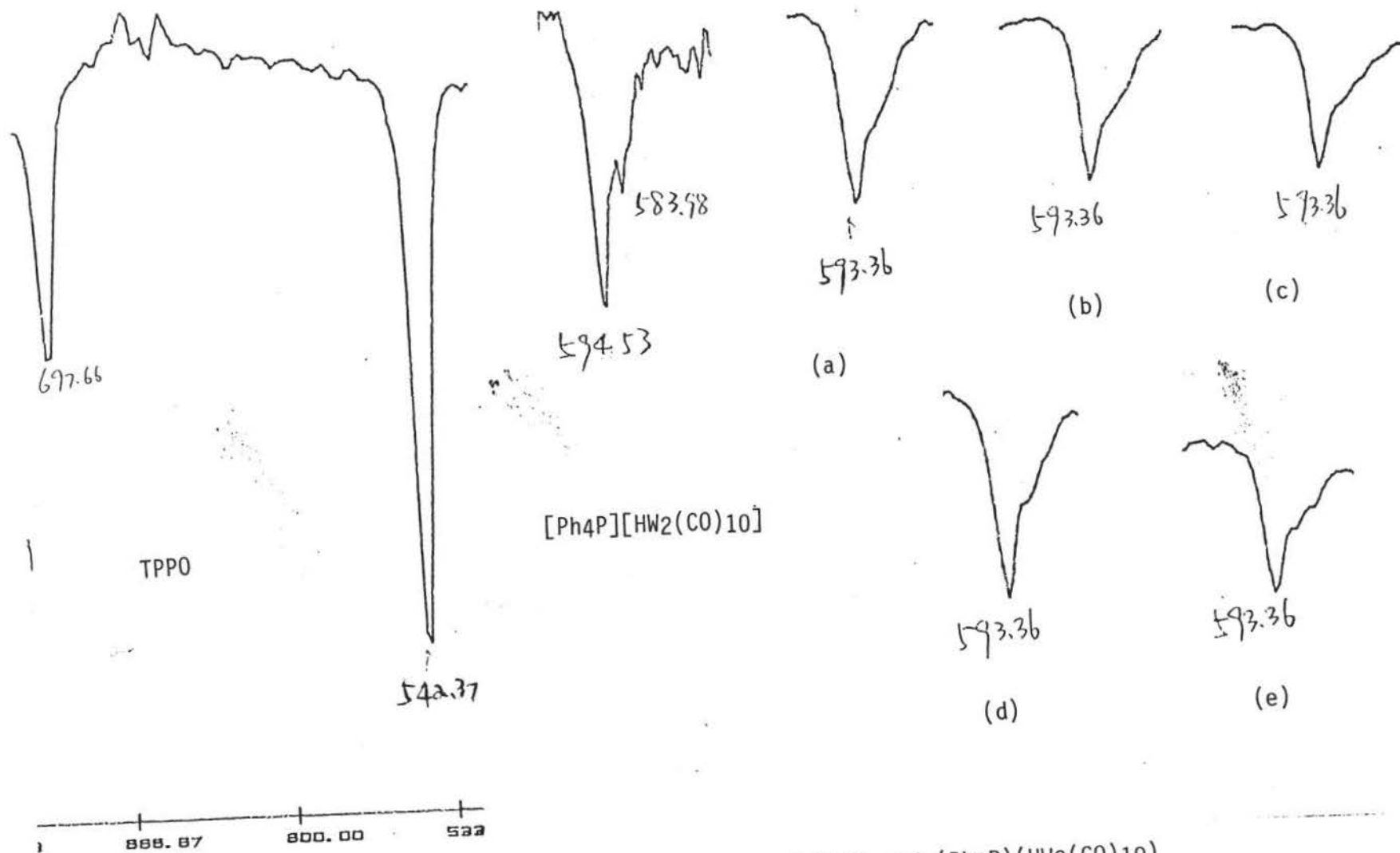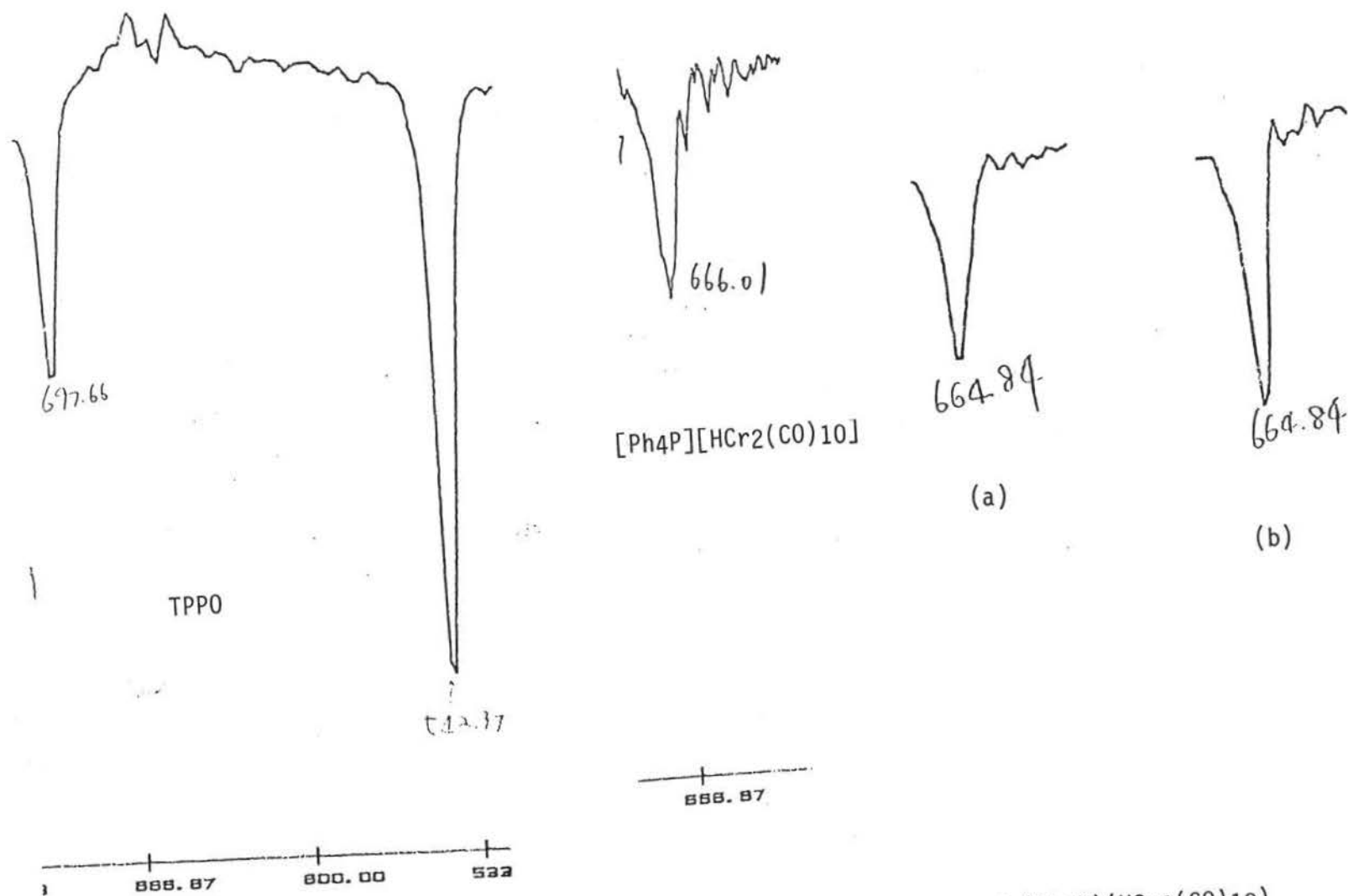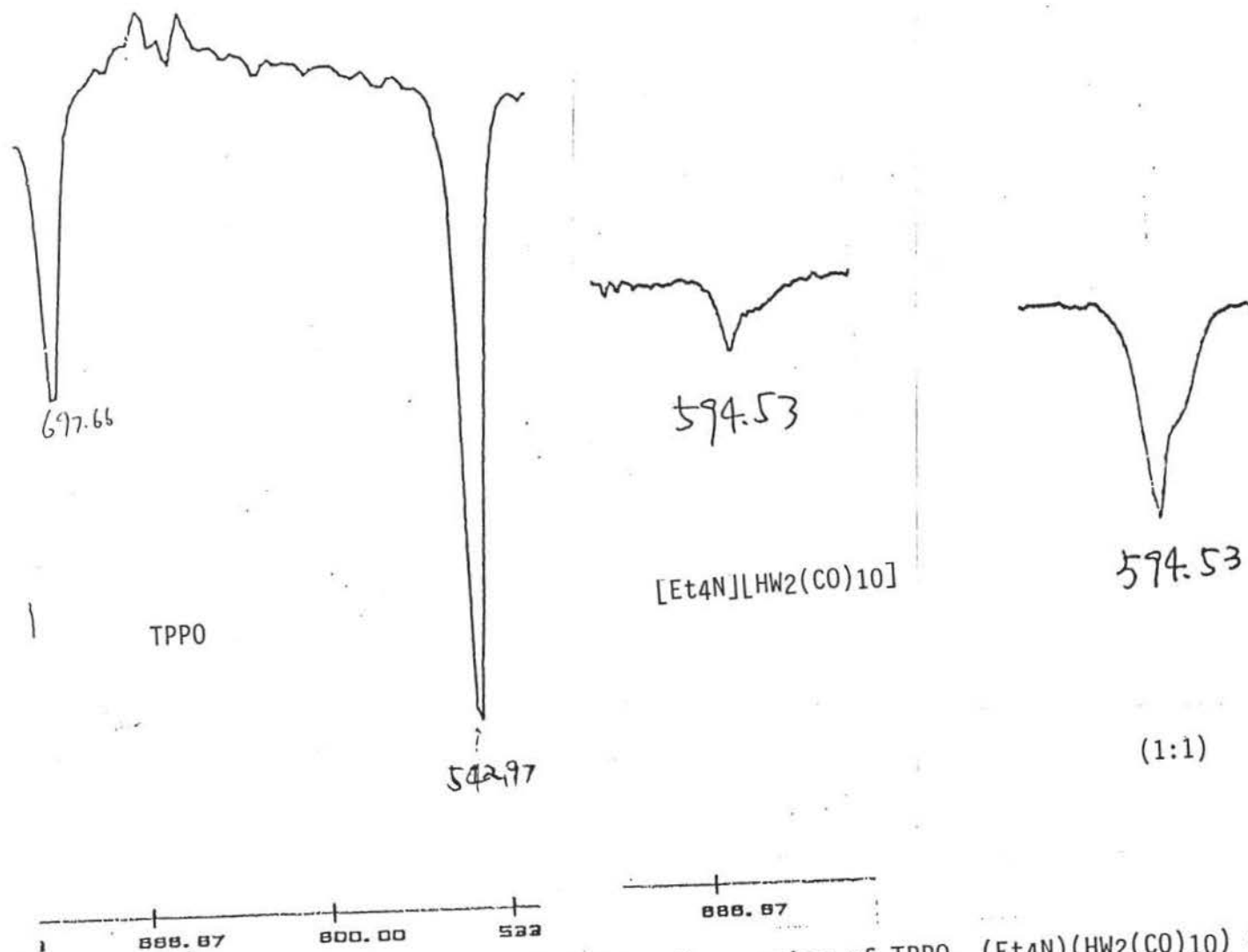
Fig. A63 IR spectra at M-C-O bending region of TPPO, (Et4N)(HW2(CO)10) and their mixture at 1:1 ratio
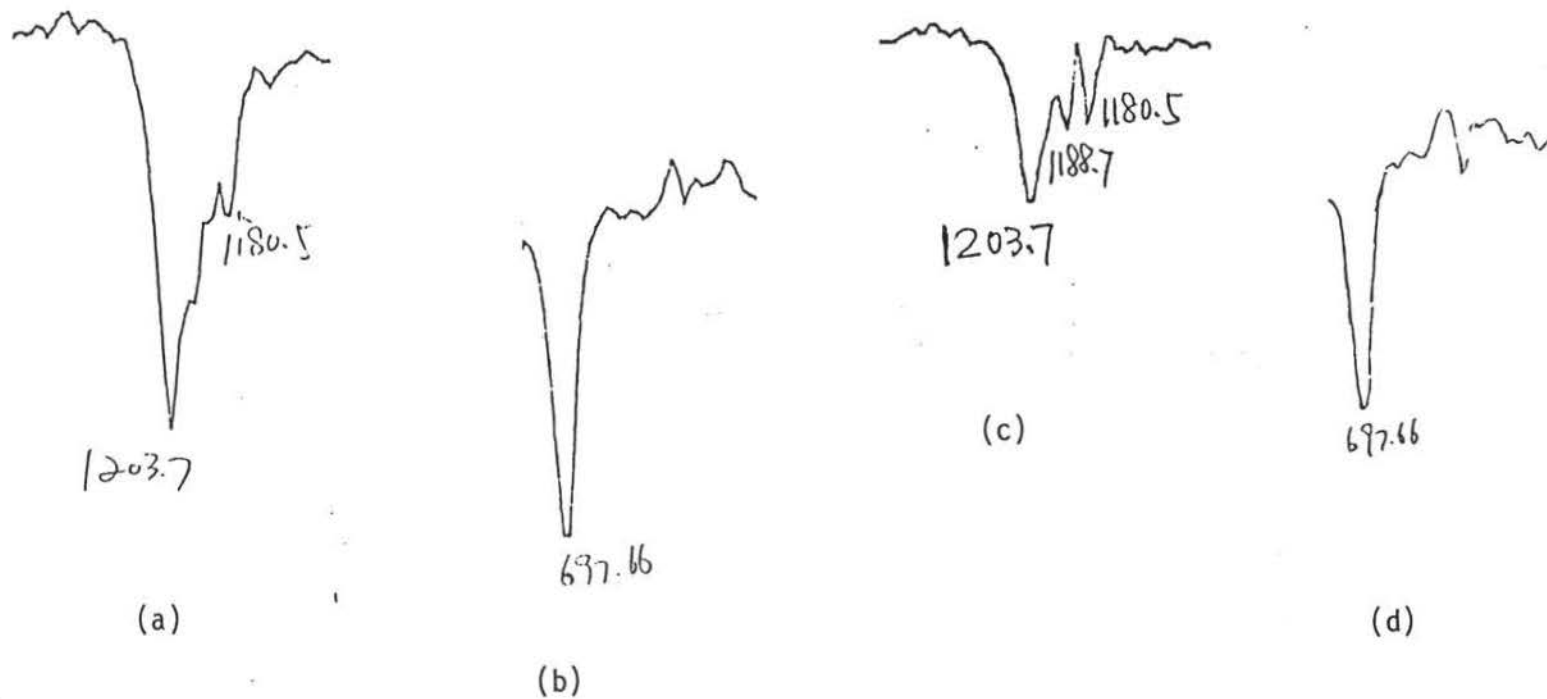
Fig. A64 IR spectra of mixture of TPPO and Ph4PCl at P=O stretching (a) and M-C-O bending (b) regions, and of TPPO and Et4NBr at P=O stretching (c) and at M-C-O bending (d) regions in THF (mixtures in 1:1 ratios)

Appendix III

Determination of infrared active modes of carbonyl stretching in $[HM_2(CO)_{10}]^-$ complexes of D_{4h} and D_{4d} symmetry

The irreducible representation to which CO vibrations belong can be found by taking C-O bond stretching as the basis of the representation. This way is easy because it is not necessary to consider translations or rotations since they are not included in the basis.

A. D_{4h}

See figure AIII on the following page. The ten arrows shown are the basis of the CO stretching representation. The reducible representation table is given below. The number in the reducible representation under a certain operation corresponds to the number of arrows unshifted after this operation. The arrows can never be transformed into minus themselves.

D_{4h}	E	$2C_4$	C_2	$2C_2'$	$2C_2''$	i	$2S_4$	σ_h	$2\sigma_v$	$2\sigma_d$
Γ_i	10	2	2	0	0	0	0	0	6	2

Consult with the character table.

$^{\#}A_{1g} = (1/16)\,[10\text{x}1\text{x}1 + 2\text{x}2\text{x}1 + 1\text{x}2\text{x}1 + 2\text{x}6\text{x}1 + 2\text{x}2\text{x}1] = 2$

$^{\#}A_{2g} = (1/16)\,[10\text{x}1\text{x}1 + 2\text{x}2\text{x}1 + 1\text{x}2\text{x}1 + 2\text{x}6\text{x}(-1) + 2\text{x}2\text{x}(-1)] = 0$

$^{\#}A_{1u} = (1/16)\,[10\text{x}1\text{x}1 + 2\text{x}2\text{x}1 + 1\text{x}2\text{x}1 + 2\text{x}6\text{x}(-1) + 2\text{x}2\text{x}(-1)] = 0$

$^{\#}A_{2u} = (1/16)\,[10\text{x}1\text{x}1 + 2\text{x}2\text{x}1 + 1\text{x}2\text{x}1 + 2\text{x}6\text{x}1 + 2\text{x}2\text{x}1] = 2$

Fig. AⅢ
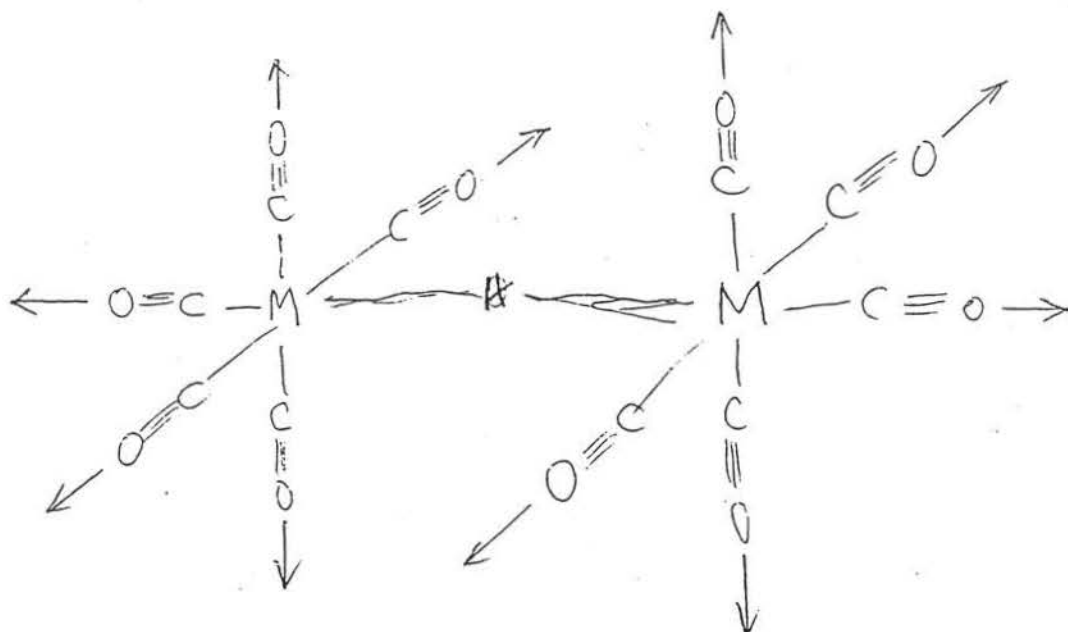
(1) D_{4h}
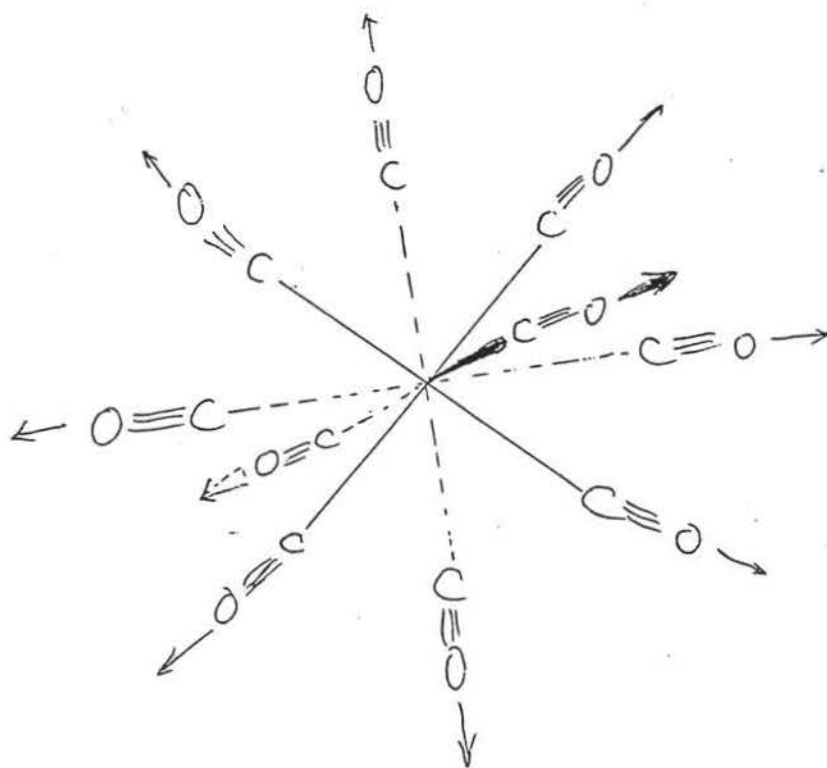
(2) D_{4d}

AⅢ-2   ⟶ is perpendicular to the paper

E_u $= (1/16) [1x10x1 +1x2x(-2) +0] =1$

E_g $= (1/16) [1x10x2 +1x2x(-2) +0] =1$

$B_{1g} = (1/16) [1x10x1 +2x2x(-1) +1x2x1 +2x6x1 +2x2x(-1)] =1$

$B_{2g} = (1/16) [1x10x1 +2x2x(-1) +1x2x1 +2x6x(-1) +2x2x1] = 0$

$B_{1u} = (1/16) [1x10x1 +2x2x(-1) +1x2x1 +2x6x(-1) +2x2x1] = 0$

$B_{2u} = (1/16) [1x10x1 +2x2x(-1) +1x2x1 +2x6x1 +2x2x(-1)] =1$

This reduces to : $2A_{1g} + 2A_{2u} + B_{1g} + B_{2u} + E_g + E_u$

The infrared active modes can be determined by consulting the character table for D_{4h}. Since z belongs to A_{2u} and (x,y) belongs to E_u, the infrared active modes are $2A_{2u} + E_u$. $2A_{2u}$ indicates two different vibrations (nondegenerate) of the same symmetry. E_u indicates one band which consists of two degenerate vibrations. Thus, if the anion has a symmetry of D_{4h}, its IR spectrum should have only three vibration peaks.

B. D_{4d}

See Figure AIII. The ten arrows shown are the basis of the CO stretching representation. The reducible table is shown below.

D_{4d}	E	$2S_8$	$2C_4$	$2S_8$	C_2	$4C_2$	$4\sigma_d$
Γ_2	10	0	2	0	2	0	4

#$A_1 = (1/16) [1x10x1 + 2x2x1 + 1x2x1 + 4x4x1] = 2$

$\#A_2 = (1/16)\,[1x10x1 + 2x2x1 + 1x2x1 + 4x4x(-1)] = 0$

$\#B_1 = (1/16)\,[1x10x1 + 2x2x1 + 1x2x1 + 4x4x(-1)] = 0$

$\#B_2 = (1/16)\,[1x10x1 + 2x2x1 + 1x2x1 + 4x4x1] = 2$

$\#E_1 = (1/16)\,[1x10x2 + 1x2x(-2)] = 1$

$\#E_2 = (1/16)\,[1x10x2 + 2x2x(-2) + 1x2x2] = 1$

$\#E_3 = (1/16)\,[1x10x2 + 1x2x(-2)] = 1$

So, Γ_2 is reduced to $2A_1 + 2B_2 + E_1 + E_2 + E_3$

Since z belongs to B_2 and (x, y) belongs to E_1, the IR active modes are $2B_2 + E_1$. Thus, the observable CO stretching bands in IR are three if $[HM_2(CO)_{10}]^-$ has a symmetry of D_{4d}.

In another words, if the number of the observable CO stretching bands in the IR spectrum of a $[HM_2(CO)_{10}]^-$ complex is not equal to three, the complex does not have the symmetries of either D_{4h} or D_{4d}.